Hilde Enevoldsen
Karoline Boel Johansen

Contribution of Microgrid to the Reliability of Distribution Systems

Master's thesis in Energy and Environmental Engineering
Supervisor: Vijay Venu Vadlamudi
June 2021

Master's thesis

NTNU
Norwegian University of
Science and Technology

Hilde Enevoldsen
Karoline Boel Johansen

Contribution of Microgrid to the Reliability of Distribution Systems

Master's thesis in Energy and Environmental Engineering
Supervisor: Vijay Venu Vadlamudi
June 2021

Norwegian University of Science and Technology
Faculty of Information Technology and Electrical Engineering
Department of Electric Power Engineering

NTNU
Norwegian University of
Science and Technology

Abstract

As the attention around finding sustainable solutions to meet the future power demand has increased together with the requirement for increased power system reliability, implementing microgrids has shown to be a promising solution. This drives the need to evaluate the contribution of microgrids to system reliability.

This thesis presents a foundation for understanding the reliability evaluation procedure of distribution systems, where both analytical and simulation methods are considered for the adequacy part of reliability. Emphasis is placed on presenting the methods in a transparent and detailed manner. The overall objective of the thesis is to evaluate the contribution of a microgrid to the reliability of distribution systems.

A time-sequential Monte Carlo Simulation program for evaluating the reliability of passive distribution systems is developed and verified for Buses 2, 5 and 6 of the Roy Billinton Test System (RBTS). The program is further extended to consider variable loads to account for more realistic scenarios. Furthermore, utilising available Distributed Energy Resources (DER) in the distribution system is assessed to enable microgrid operation. The modelled Distributed Generation (DG) units are based the Renewable Energy Resources (RES) such as wind and solar.

The evaluation of the contribution of incorporating microgrid to the reliability of distribution systems is accomplished by utilising Bus 6, Feeder 4 of the RBTS, where the microgrid is designed in Sub-Feeder 2. The operation strategy of the microgrid is proposed based on a combination of available literature and suggestions tailored to the specific system design. The ability to prioritise loads within the microgrid to enhance the reliability in island mode operation is given due consideration. The impact of intermittent behaviour of the RES is dealt with by considering facilities of an Energy Storage System (ESS), where a Battery Energy Storage System (BESS) is modelled and incorporated in the evaluation.

The main results of the reliability assessment reveal that the load points of the defined microgrid experienced a significant reliability improvement. However, as the microgrid evaluated in the case study only serves 13.27% of the total customers, the impact on the distribution system customer-oriented reliability indices were significantly smaller. Further, by considering the

ability to prioritise load points inside the microgrid, the high priority loads were found to experience a significant reliability improvement, which was reflected in the microgrid reliability indices. Moreover, the implementation of a BESS with the considered DGs showed to have a positive impact on the entire microgrid, where the charging/discharging capacity of the battery is significant. The DER localisation within the microgrid does also impact the analysis, where the optimal placing of the DER facilities was found to be in the feeder end from a conducted sensitivity analysis.

Keywords— Distribution System Reliability, Microgrid, Distributed Energy Resources, Monte Carlo Simulation

Sammendrag

Det elektriske kraftsystemet gjennomgår en kontinuerlig endring. Etterspørselen etter bærekraftig og pålitelig elektrisitet øker i takt med den pågående elektrifiseringen, samtidig som store deler av eksisterende nettkonstruksjoner er i ferd med å bli utdatert. Dette har ført til et økt fokus på hvilke teknologiske løsninger det skal satses på i fremtiden. En aktuell oppfatning er implementering av mikronett, som består av desentralisert kraftproduksjon i kombinasjon med smarte kontrollenheter i distribusjonssystemet. For å rettferdiggjøre satsning på mikronett, må blant annet pålitelighetsbidraget til distribusjonssystemet evalueres.

Denne masteravhandlingen presenterer grunnlaget for å forstå og mestre prosedyrene for pålitelighetsevaluering av distribusjonssystemer, der både analytiske- og simuleringsmetoder er benyttet. Det er lagt vekt på en pedagogisk og detaljert beskrivelse av metodene. Hovedformålet med avhandlingen er å belyse påvirkningen et mikronett har på påliteligheten til et distribusjonssystem.

Et tidssekvensielt Monte Carlo-simuleringsprogram for evaluering av påliteligheten til passive distribusjonssystemer er utviklet og verifisert for "Bus 2", "Bus 5" og "Bus 6" i "Roy Billinton Test System" (RBTS). Programmet er videreutviklet til å omfatte variabel last for å oppnå mer realistiske scenarioer. De fornybare energiressursene vind og sol er modellert og inkludert i analysen som distribuerte energikilder, som muliggjør mikronettdrift.

Evalueringen av pålitelighetsbidraget til mikronettdrift i distribusjonssystemer er oppnådd ved å benytte "Bus 6, Feeder 4" av RBTS, der mikronettet er designet i "Sub-feeder 2". Driftsstrategien til mikronettet er definert basert på en kombinasjon av tilgjengelig litteratur og forslag skreddersydd til system-designet. Resultatet av å prioritere lastene innad i mikronettet er studert som en tilleggsstrategi hos mikronettet for å oppnå mer tilfredsstillende øy-drift. Variasjonene i produksjonen fra de fornybare energikildene er forsøkt stabilisert ved hjelp av et batterisystem som er modellert og inkludert i analysen.

Hovedresultatene fra analysen viser at lastpunktene til det definerte mikronettet opplever en betydelig pålitelighetsforbedring. Ettersom mikronettet som ble evaluert i casestudien kun betjente $13,27\%$ av de totale kundene, var pålitelighetseffekten hos distribusjonssystemet betydelig

mindre. Ved å innføre prioritering av lastpunktene innad i mikronettet, opplevde de prioriterte lastpunktene en betydelig forbedring, noe som ble reflektert i pålitelighetsindeksene innad i mikronettet. Implementering av batterisystemer viste seg å ha en positiv innvirkning på hele mikronettet, der batteriets kapasitet for opplading/utlading har stor innvirkning på resultatet. Lokaliseringene av energikildene i mikronettet påvirket også analysen. Ved å gjennomføre en sensitivitetsanalyse, ble den optimale plasseringen funnet til å være i enden av "feederen".

Acknowledgement

This thesis concludes our Master of Science (MSc) degree in Energy and Environmental Engineering at the Department of Electric Power Engineering at the Norwegian University of Science and Technology (NTNU).

We would like to thank our supervisor, Associate Professor Vijay Venu Vadlamudi at the Department of Electric Power Engineering NTNU, for his continuous guidance and encouragement throughout the semester. We are truly thankful for his suggestions, greatly enhancing the narrative presentation of our thesis. In addition, we would like to express gratitude towards Stine Fleischer Myhre and Sondre Johan Kjellin Berg. Your inputs, availability and guidance have been highly appreciated.

<div align="center">

Trondheim, June 2021

</div>

Karoline Boel Johansen   Hilde Enevoldsen

Contents

Abbreviations

AENS Average Energy Not Supplied

ASAI Average Service Availability Index

ASUI Average Service Unavailability Index

BESS Battery Energy Storage System

CAIDI Customer Average Interruption Duration Index

DER Distributed Energy Resource

DG Distributed Generation

DSM Demand Side Management

EENS Expected Energy Not Supplied

EPS Electrical Power System

ESS Energy Storage System

FMEA Failure Modes and Effect Analysis

ILOLP Island Loss of Load Probability

IOSR Island Operation Successful Rate

LP Load Point

LV Low Voltage

MAIDI Microgrid Average Interruption Duration Index

MCS Monte Carlo Simulation

MG Microgrid

MTBF Mean Time Between Failure

MV Medium Voltage

NO Normally Open

PCC Point of Common Coupling

PSR Power System Reliability

PV PhotoVoltaic

RBTS Roy Billinton Test System

RELRAD RELiability in RAdial Systems

RES Renewable Energy Sources

RTS (IEEE) Reliability Test System

SAIDI System Average Interruption Duration Index

SAIFI System Average Interruption Frequency Index

SoC State of Charge

TTF Time To Failure

TTR Time To Recover

TTR Time To Switch

WT Wind Turbine

Nomenclature

Δt Time increment

ΔT Time segment of interest

η Drive train efficiency

η^{ch} Charging efficiency

η^{dch} Discharging efficiency

γ Lateral feeders of the system

Γ Gamma function

λ Failure rate [f/yr]

λ_C Failure rate for customer C [f/yr]

λ_i Failure rate of load point i [f/yr]

λ_k Failure rate of component k [f/yr]

λ_s Failure rate of the system s [f/yr]

λ_{up} Failure rate for LV network (i.e. Microgrid) [f/yr]

ρ Air density in [kg/m^3]

σ_G Standard deviation of solar radiation

σ_V Standard wind speed deviation

A Area in [m^3]

C_p Rotor power coefficient

c Scale parameter

E^{max} Upper limit of the battery to be charged [MWh]

$E^{reserve}$ Lower limit of the battery to be discharged [MWh]

E_t^{stored} Energy stored at time t [MWh]

$F(V)$ Cumulative distribution function of V

$f(\Delta G)$ Normal distribution of the variation of solar radiation ΔG

$f_T(t)$ Probability density function of an exponential distribution

$f(V)$ Probability density function of V

f Main feeders of the system

G Solar radiation in [W/m^2]

G_d Available solar radiation [W/m^2]

G_{max} Maximum solar radiation during a day [W/m^2]

ΔG Variation of solar radiation [W/m^2]

G_{std} Solar radiation in the standard environment [W/m^2]

k Shape parameter

L_{ai} Average load connected to the load point i

M Number of the total sampled years

$m(k)$ Number of years of the time span with this specified outage rate k

N_i Number of interrupted customer of load point i

P_L The probability of a shut-down due to a failure in the LV Feeder

P_M The probability of unsuccessful isolation

P_t^{sur} Surplus power of the system at time t [MW]

$P_{Li,avg}$ Average load connected to the load point i

$P_{Li,peak}$ Peak load connected to the load point i

P_{Li} Predicted load for load point i [MW]

P_{WT} Mean available wind power [W]

P_{PV} Output power of PV [W]

P_r Rated output power of WT [W]

P_{sn} Equivalent rated capacity of the PV [W]

P_{WT} Output power of WT [W]

$Pr(V' \leq V)$ Probability that the random quantity V' is less or equal the numeric value of V

P_t^{ch} Charging capacity at time t [MW]

$P^{ch,max}$ Rated charging capacity at time t [MW]

P_t^{dch} Discharging capacity at time t [MW]

$P^{dch,max}$ Rated discharging capacity at time t [MW]

$p(k)$ The probability distribution of a load point outage rate k

R_c A certain radiation point in [W/m2]

r_k Repair time of component k [h]

r_s Repair time of the system s [h]

r Repair time in [h]

S State vector

T Total number of time increments

T_a The average time to restore the microgrid [h]

T_d Down-duration time after a modification due to e.g. isolation

T_r Repairing time of a faulted component

T_s Time to transition of system s

T_i Time to transition of component i

T_u Up-duration time

U Outage duration (unavailability) [h/yr]

U_C Outage duration for customer C [h/yr]

U_{up} Outage duration for LV network (i.e. Microgrid) [f/yr]

U_i Average annual outage duration of load point i [h/yr]

U_k Average annual outage duration of component k [h/yr]

U_s Average annual outage duration of the system s [h/yr]

V Wind speed in [m/s]

V_a Lower limit of wind speed [m/s]

V_b Upper limit of wind speed [m/s]

V_{ci} Cut-in speed of WT [m/s]

V_{co} Cut-out speed of WT [m/s]

$\overline{V}$ Mean wind speed [m/s]

V_r Rated speed of WT [m/s]

W_d Daily weight factor

W_h Hourly weight factor

W_w Weekly weight factor

List of Figures

List of Tables

Chapter 1

Introduction

1.1 Background

UNDP's Sustainable Development Goal 7 aims to supply affordable and clean energy to the global population by 2030; today, one out of seven still lacks access to electricity, most concerning people living in rural areas in the developing world [1]. Possible solutions are being investigated for such areas, where researchers claim that building affordable microgrid structures are convenient options contributing to reaching the goal [2, 3]. Another key driver for microgrids is related to the liberalisation of today's electricity sector. For increased security of supply, it is becoming more common to include distributed generation and energy storage system at the customer levels.

As the ongoing digitalisation and electrification of several sectors are speeding up, so is the need for reliable power systems. New digital technologies are affecting the way people live and work. Consequently, society is depending on a reliable power supply to operate functionally [4]. The electrification of large sectors increases the need for adequate and secure power. Constructing large, centralised power plants to serve this need, requires an expansion of the existing transmission grid, which in total accounts for a large investment cost for the society. Implementing small scale decentralised power station constructed as microgrids on a distribution level has shown to be an adequate alternative [5, 6].

Microgrids can provide flexible resources to distribution systems. As a microgrid can operate periodically without being connected to the main system, it can contribute and provide benefits in several aspects [6].

The electric power system operates in an uncertain environment as random outages of gener-

ators, transmission lines and other power devices occur. Reliability analysis has been studied widely for both generation and transmission facilities, however, the focus on addressing reliability analysis of distribution systems until recently has received considerably less attention. A general statement is that approximately 80% of all customer interruptions occur due to failures in the distribution system [7], which justifies the ongoing interest of studying the performance of distribution system reliability.

1.2   Scope of the Project

This thesis is a contribution to the repository of computational tools in the ongoing project of building a comprehensive framework for conducting power system reliability assessment, at the Department of Electric Power Engineering at NTNU. The objectives of this thesis are summarised in the following problem statements:

- Develop in-house software tools (MATLAB-based) as part of the development of a comprehensive framework for conducting adequacy studies for distribution system using the time-sequential Monte Carlo Simulation (MCS) method.

- Evaluate the reliability impact of microgrid operation in distribution systems.

A significant part of the project has been to develop satisfying MATLAB scripts addressing distribution system adequacy studies including Distributed Energy Resources (DERs). To do so, this thesis carries out a procedure of adding elements to the study step by step to illustrate the effect of the different elements which are necessary for pedagogical clarity and for the underlying goal of understanding how implementing microgrids impacts the distribution system reliability. This procedure is illustrated and described by the flow chart in Figure 1.1, which serves as a summarising of the approach conducted in this thesis.

As a basis for comparison, a reliability analysis utilising an analytical method is conducted along with a comprehensive literature review on the state-of-the-art within reliability evaluation of future distribution systems. Further, a time-sequential MCS is developed and verified, through comparison with analytical results, for reliability investigation on the well-established benchmark Roy Billinton Test System (RBTS), specifically on the Buses 2, 5 and 6.
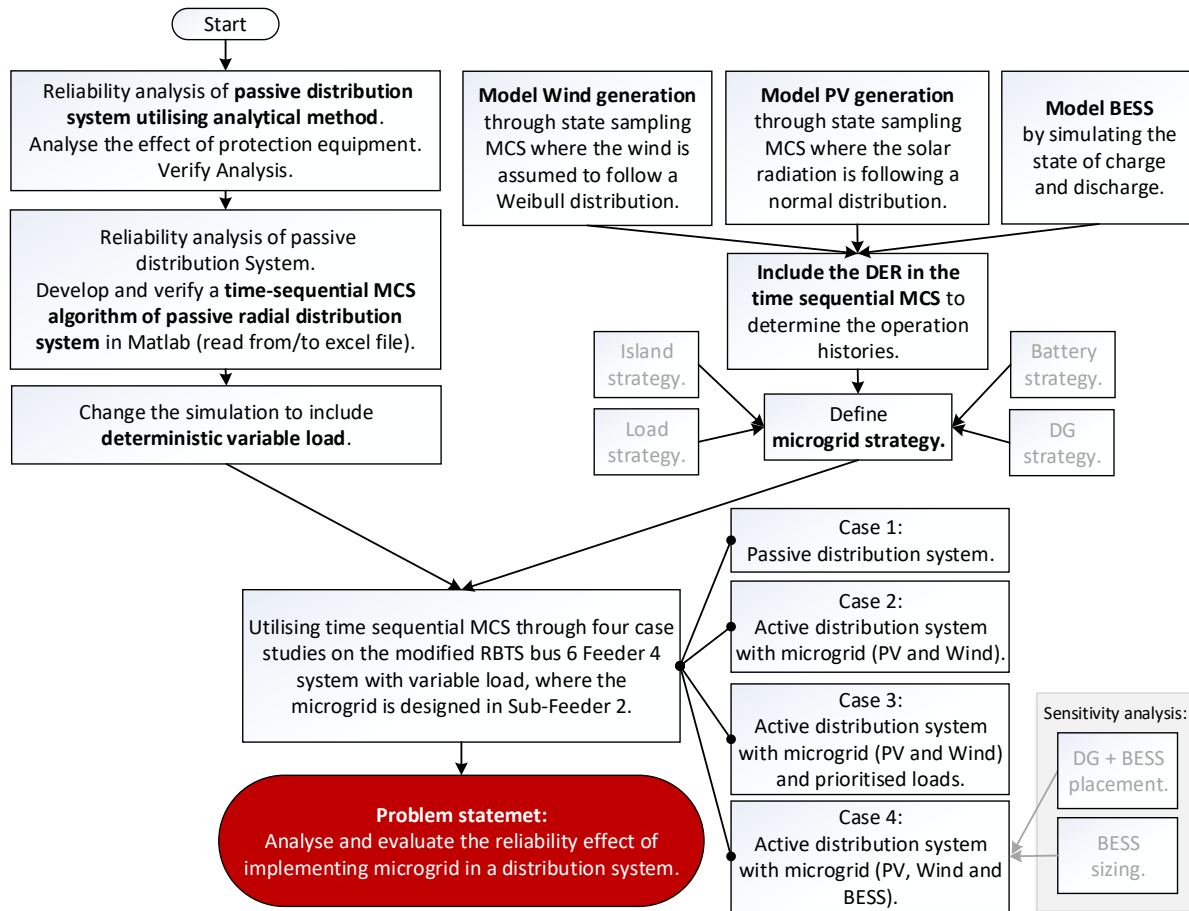
Figure 1.1: Flow chart illustrating the conducted procedure of this thesis.

To include microgrid in the reliability analysis in an appropriate manner, an operation strategy is proposed. The reliability contribution of the microgrid is evaluated in island mode and limited to benefit only local load points inside the microgrid. The operation of the incorporated DERs is modelled based on their respective probability distributions, while their up and down cycles are simulated in the time-sequential MCS program with the other components of the system. Four case studies, presented in Figure 1.1, are defined to address the problem statement by evaluating a variety of load point-, distribution system- and microgrid reliability indices.

The analysis conducted in this thesis is concentrated on power system reliability analysis of distribution systems and does not include cost-related analysis, nor optimal design/operation considerations of distribution systems and microgrids. The scope of the thesis does not include the implementation of distribution system power flow analysis.

1.3   Thesis Contribution

- This thesis, in combination with the specialisation project [8], presents the foundation in the field of power system reliability analysis of distribution systems, where the theory enhances pedagogical dissemination.

- A software program for evaluation of power system reliability of passive distribution system through time-sequential MCS is developed, verified and released for further internal education and research use at the Department of Electric Power Engineering at NTNU.

- A test system for reliability analysis of distribution system including microgrid is constructed through modification of Feeder 4 of the Bus 6 defined in the RBTS. Reliability and system parameters are provided for further research.

- A software program for modelling DERs (Wind, PV and battery) and reliability evaluation of distribution system including microgrid through time-sequential MCS is developed.

- The reliability effect of incorporating microgrid with DGs based on RES in a distribution system is evaluated. In addition, the effects of prioritised loads and BESS are considered in the evaluation.

1.4   Structure of the Report

Chapter 1 - *Introduction*, outlines the background, scope and contributions of this thesis.

Chapter 2 - *Literature Review and Conceptual Background*, gives the essential theory and concepts of microgrids and reliability analysis of distribution systems. In addition, the modelling concepts of considered DERs and a literature review of reliability evaluation of distribution systems are also presented.

Chapter 3 - *Methodological Approach*, provides the proposed methodology addressing the problem statement.

Chapter 4 - *Verification and Description of Simulation Program*, provides a description of the process for verifying the created and applied methodology through comparison of analytical

and simulation approach for systems of the RBTS.

Chapter 5 - *Case Studies and Results*, presents and discusses the results obtained by applying the proposed methodological approaches for reliability evaluation to four cases: (1) passive distribution system; (2) active distribution system with incorporated microgrid by DGs; (3) active distribution system with incorporated microgrid by DGs and prioritised loads, and; (4) active distribution system with incorporated microgrid by DGs and ESS.

Chapter 6 - *Conclusions and Future Work*, presents a summary of the work, results from the main findings from Chapter 5 and remarks on the work conducted in this thesis. Additionally, suggestions for further work are given.

1.4.1 Relation with the Specialisation Project

This thesis is an extension of the Specialisation Project, undertaken during the Autumn of 2020 [8], where the main focus was on achieving a conceptual understanding of the theoretical and algorithmic aspects of power system reliability assessment and the application of MCS in power system adequacy assessment. The significance of distribution system analysis was emphasised, where the effect of protection equipment (disconnectors, fuses, additional supply) on the reliability evaluation was comprehensive studied.

For this thesis to be a complete and independent unit in and of itself, suitable theory and literature studies presented in Chapter 2 overlap with what is presented in the specialisation project; however, all detailed examples are originals from this thesis work.

Chapter 2

Literature Review and Conceptual Background

This chapter presents a review of distribution systems and microgrids, as well as an introduction to the basic concepts of power system reliability studies, with emphasised focus on distribution system reliability. Definitions and classifications of distribution system reliability are provided, along with a clarification of reliability indices. Two methods for performing reliability evaluation on distribution system are described - analytical method and simulation with Monte Carlo. The modelling of DERs are explained in detail for the RES wind and solar and for battery systems in terms of energy storage. Finally, the chapter is completed with a literature review addressing a state-of-the-art within the field of distribution system reliability and microgrid reliability.

2.1   Introduction to Modern Distribution Systems

In a traditional power system, the electricity is produced and delivered to customers through three levels: (i) generation facilities responsible for producing the required power to meet the demand; (ii) transmission facilities responsible for transporting bulk power over long distances and; (iii) distribution facilities which are responsible for delivering electricity to the end-users. However, in modern power systems, it is becoming more common to include distributed generation, energy storage systems and microgrids in distribution systems, allowing a bi-directional power flow at the distribution level. Consequently, distribution systems are evolving from passive to active networks by implementing generation units to support voltage, reduce losses, provide ancillary services or defer upgrading of the transmission lines [9].

Incorporating microgrids into distribution systems can contribute and provide benefits in several aspects. Economic potential benefits may be the reduction of transmission and distribution costs and energy losses, higher energy efficiency and the impact of low capital cost into a competitive market as it can potentially enable low-cost entry [6]. Furthermore, the advantages of improved reliability of distribution systems are essential aspects, and are in this thesis, assessed further.

2.2 Review of Microgrids

A microgrid is defined by IEEE 2030-2011 [10] as "*a group of interconnected loads and distributed energy resources with clearly defined electrical boundaries that act as a single controllable entity with respect to the grid and can connect and disconnect from the grid to enable it to operate in both grid-connected or island modes.*" Accordingly, microgrids should not be confused with the backup generation, which has existed for ages to prevent power cuts of important loads in an area. Microgrids provide a wider range of benefits regarding reliability, resiliency and power quality [5]. A typical microgrid as illustrated in Figure 2.1, is composed of several components such as loads, Distributed Energy Resources (DERs), controls, smart switches, protective devices, communication, and automation systems.
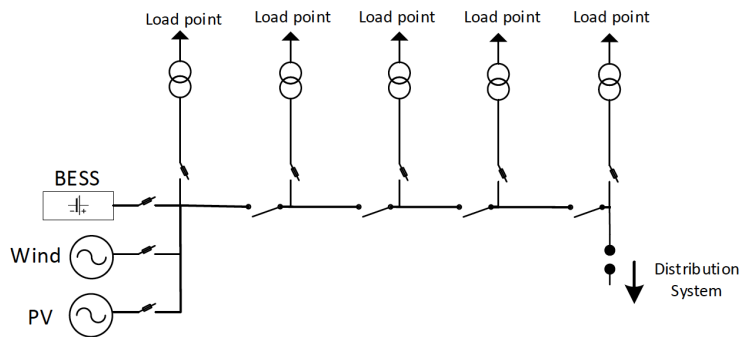
Figure 2.1: Schematic illustration of Microgrid structure.

When designing and planning a microgrid, it has to be tailored to the specific location and operation objective. As such, economic benefit, system reliability and environmental impact are to be considered. In [11] from 2019, IEEE recommends how to proceed when planning and designing a microgrid.

2.2.1 Distributed Energy Resources

DERs are defined as small scale energy resources consisting of both Distributed Generation (DG) and Energy Storage System (ESS). These are constructed and developed within a time frame significantly shorter than large power plants and transmission systems [5]. Research states that the largest increase in penetration of DER will be of renewable sources and battery storage [12], which is often integrated together to ensure stable and reliable power delivered to the customers.

There is no complete agreement on the definition of DG [13]. However, by considering the different proposals, the main features of DGs are locally generation in the distribution system, generally small scale, i.e., a low installed capacity related to conventional power plants, and connected at substations, distribution feeders or the customer load levels.

In theory, DGs can be sourced from many forms of primary energy. Generally, these can be grouped into two main types: intermittent energy sources (e.g. wind, solar), and dispatchable energy sources (e.g. hydro, gas, diesel). The latter type can be modelled using conventional generation approached as either available or unavailable, while the former is more challenging to model as they operate in derated states depending on the available source.

Due to the increased focus on reducing and minimising emissions, DG units based on Renewable Energy Sources (RES) are emphasised. The resources solar and wind are the most frequently implemented RES in microgrids [5], at which is emphasised.

2.2.2 Microgrid Control System

To be able to provide the benefiting aspects of a microgrid, the system needs to be controlled in an optimal manner for each operation mode concerning the characteristics such as the bi-directional power transfer, presence of DGs, Demand-Side Management (DSM) and the considerable presence of power electronics [5].

A microgrid control system is defined by IEEE 2020-2011 [10] as "*a system that includes the control functions that define the microgrid as a system that can manage itself, operate autonomously, and connect to and disconnect from the main distribution grid for the exchange of power and the*

supply of ancillary services; it includes the functions of the microgrid Energy Management System; it is the microgrid controller if implemented in the form of a centralised system.". Hence, the microgrid controller must be able to handle the control in island mode and the transition to island mode.

When controlling a microgrid, the control is structured in three different layers [14]: (i) primary control consisting of frequency and voltage control; (ii) secondary control compensating for deviations in steady-state voltage and frequency due to the primary control; (iii) tertiary control which considers the economic aspect when deciding the power flow between the microgrid and the utility grid. The control architecture is designed as either centralised or decentralised. A centralised architecture obeys a standardised procedure which makes it easy to implement. By using a decentralised architecture, the number of messages transferred between the assets is decreased, and the tasks are divided into sub-problems and solved locally [15].

2.2.3 Different Types of Distributed Resource Island Systems

A microgrid can appear in different sizes and structures. The motivation for this section is to present an overview of different occurrences of microgrids in the distribution network. There are seven main island configurations in an Electrical Power System (EPS) [16], these are shortly described below and illustrated in Figure 2.2.

Facility Island

In a local EPS island also known as facility island, there is only one Point of Common Coupling (PCC) (i.e., the connection between the microgrid and the utility grid). The island is normally served within the customer facility which explains the name. The island system operates with a DG to serve the local loads in case of failure in the upstream EPS. The aim is for the distributed resource island system to parallel the EPS, without the need to shut down the DG. This benefit is achieved by the use of a "tie-breaker" (i.e., a circuit breaker) to isolate the system from the utility grid. The method of operation for paralleling the intentional island and the required interlocks need to be discussed by the EPS and the local EPS operators.
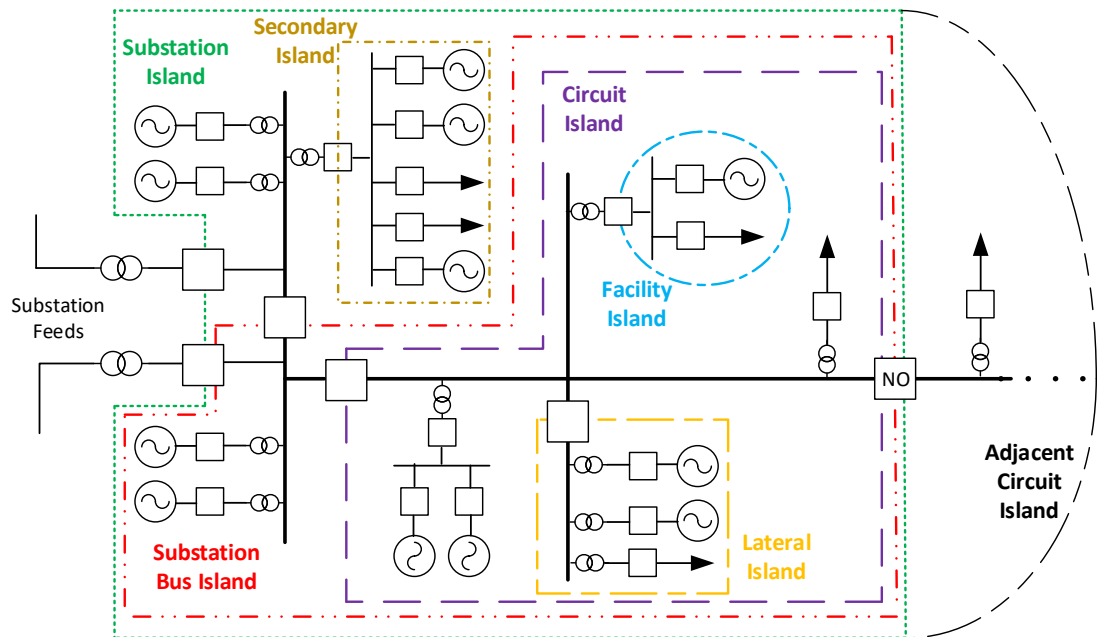
Figure 2.2: Distributed Island Systems, as adapted from [16].

Secondary Island

In the case of multiple loads and one or more DGs connected to the secondary side of a distribution transformer, and the system being able to disconnect from the external grid through PCC, it is known as a secondary island. Several secondary islands may be connected to the same lateral distribution.

Lateral Island

Lateral islanding is when the entire lateral can be disconnected from the external grid and operate in island mode. This is performed by opening the lateral switching device. Note which side of the transformer the island is conducted.

Circuit Island

A circuit island is created when a single distribution circuit is able to disconnect itself from the external grid and operate with its own DGs to serve its loads. A circuit island may contain possi-

bilities to divide into smaller islands such as the three mentioned above.

Substation Bus Island

A substation bus island is created by disconnecting a part of a bus within the substation. When operating in island mode, the system is disconnected from the substation.

Substation Island

In a substation island, the entire network below a substation is disconnected to operate in island mode. This is beneficial if there occurs a failure in the distribution substation or in one of the transformers.

Adjacent Circuit Island

For this type of island operation, the island portion of the circuit serves the adjacent load.

2.2.4 Functionality of the Distributed Island System

A Microgrid system can operate in four different modes as stated in [16]: (i) normal parallel operation with the area EPS; (ii) the transition to island mode; (iii) island mode and; (iv) reconnecting mode.

When the planned island system is operating in grid-connected mode, every DER should be operating in accordance with IEEE 1547-2003 [16]. The monitoring, information exchange, and control equipment needed for island operation are further required to be operating during the parallel mode. This is for the system to be prepared with the necessary information available for a smooth transition to island mode. Following this, the system needs information about the generation and load levels, the protective device status and the system voltages.

During scheduled or unscheduled events, the mode is changed from grid-connected mode to transition-to-island mode. The system is required to react fast due to the protection equipment, and thereby, automatically sectionalise from the EPS system, which is where the knowledge of the prior conditions comes into place. This information will facilitate a smooth transfer. To assist the system voltage and frequency during the transition-to-island mode, available support

from sufficient DERs or additional equipment needs to be available. This needs to be accounted for the entire transition time, which relies on the island interconnection device and the protective relays. It is of importance that the system is sufficiently equipped to dampen any transients produced to avoid tripping off protection relays of the DERs when operating in this mode. If the system is not provided with sufficient DER, then the system needs to be provided with black start capability. Black start is the process of restoring the operation after a total or partly shut down, without the facility from the external electric power transmission network.

During operating in island mode, the system is required to provide enough of both active and reactive power and thus actively regulate voltage and frequency within the ranges, specified in ANSI/NEMA C84.1-2006 [17], for DER island systems including the area EPS. To ensure voltage and frequency stability, some participating DER must operate outside the IEEE 1547-2003 [18] voltage requirements. Additionally, there should be a reserve margin to assure the reliability requirements of the loads. Compared with normal parallel operating, the system now needs additional requirements such as providing a dynamic response from the DER. There exist various techniques to balance the load and generation in an islanded system, such as load shedding and load managing. When the system is operating in island mode, it should be able to maintain transient stability for DER unit outages, island failure and load steps. This is assured by having sufficient protective devices which are maintained in both EPS-connected- and island-mode.

Furthermore, when reconnecting the islanded system to the EPS, monitoring makes sure that the voltage, frequency and phase angles of the two systems are within acceptable limits to initiate a re-connection as specified in IEEE 1547-2003 [18]. The system can be reconnected to the EPS in three different ways: (i) active synchronisation; (ii) passive synchronisation; (iii) open-transition transfer of the island system to the area EPS. As the system is successfully connected to the EPS, it returns to operate in parallel connected mode and returns to the IEEE 1547 compliance within area EPS time requirements [16].

2.3 Distribution System Reliability

Since the 1930s, there has been a recognised need for evaluation of behaviour and performance of power systems [19]. Power systems can be described with the function to satisfy the load requirements economically with a guarantee of continuity and quality. Power system reliability can be employed to evaluate the ability of the power system to maintain its function of supplying its consumers.

Traditionally, power system reliability studies are divided into two aspects: system adequacy and system security [20]. System adequacy is related to the presence of sufficient facilities in the system to fulfil the demand for a consumer at any given time. Thus, it is related to the static conditions, not including system disturbances. On the other hand, system security is related to the potential to respond to disturbances occurring and is accordingly, associated with the system's response [19]. In this thesis work, only adequacy aspects of power system reliability studies are evaluated.

2.3.1 Functional Zones and Hierarchical Levels

Power system reliability studies differ with respect to what segment of the power system it is addressing. The power system is divided into three functional zones, each concerning its hierarchical level as shown in Figure 2.3. The levels are assembled in such a way that HLI consists of the Generation zone, HLII consists of both HLI and the Transmission facilities, and finally, HLIII consists of the HLII combined with the Distribution facilities.

As the HLIII evaluation begins at the generation station and terminates at the individual load points, the assessment of the overall problem becomes complex. The distribution zone is usually evaluated separately as a separate entity to avoid this complexity issue. However, the HLIII evaluation can be more manageable by using the HLII load-point indices as input values of the evaluation of the distribution zone [7].

Today's defined boundaries of the hierarchical levels HLIII and HLII are challenged by modern distribution systems, as explained in Section 2.1, which introduces DERs allowing bi-directional power flow and decentralised control operators.
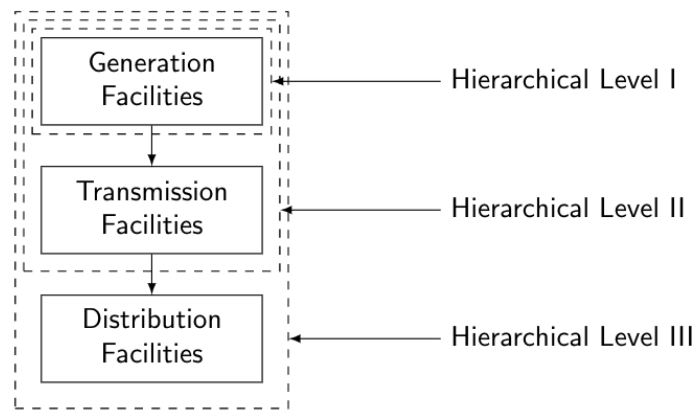
Figure 2.3: Hierarchical levels of a power system, adopted from [19].

The HLIII indices reflect the individual customer adequacy on behalf of the overall system. The HLI and HLII indices have a solid severity as failures in these zones would affect large sections of the power system. The outcome of failures in these levels could have widespread consequences, whereas failures in the distribution system have localised effects.

2.3.2 Distribution Facilities

Concerning reliability modelling and evaluation, distribution systems have received considerably less attention than generating and transmission systems, mainly due to the capital intensiveness of power plants [20, 21]. Another reason is the challenge in terms of large-scale models at the distribution level.

As reported by IEEE 1366-2012 [22], a distribution system is defined as "*that portion of an electric system that delivers electric energy from transformation points on the transmission system to the customer*". The contribution of the distribution functional zone is of primary importance for the overall customer reliability. In fact, the distribution system may be considered as a crucial link between the bulk power system and its customers. The main components of a distribution system are submission circuits, distribution substations, primary and lateral feeders, distribution transformers and consumer connections.

The distribution system is mainly structured with a radial, meshed or weakly-meshed config-uration. As such, different system configurations require specified techniques to analyse the reliability [20]. The reliability evaluation for meshed configurations is conceptually the same as for composite systems, while for radial systems, the technique is based generally on Fail-ure Modes and Effect Analysis (FMEA) [7]. The latter technique involves consideration of the restoration and failure process of each component. This thesis concerns distribution networks of radial behaviour which allows the use of basic evaluation techniques based on FMEA [20], which is addressed further in the following chapters.

Compared to generation and transmission levels that are system-oriented, the application of reliability concepts to distribution level is more customer load point-oriented. A customer is defined by IEEE 1366-2012 [22] as *"a metered electrical service point for which an active bill ac-count is established at a specific location."*.

Radial distribution systems can be designed and constructed as a combination of single radial feeder systems, at which the components are connected in series on the single feeder. These components are generally the main feeder breaker (i.e., circuit breaker), lines or cables, discon-nectors, busbars, fuses, transformers and, finally, load points/customers. In practice, the failure rate of lines and cables are dependent on voltage level and normally found approximately pro-portional to their length [20].

Protection equipment is frequently used in distribution systems, to reconfigure the system in case of a failure or similar. The most common devices in distribution systems are circuit break-ers, disconnectors and fuse gears. These are assumed located as illustrated in Figure 2.4, based on the description presented in "Chapter 7" in [20] which is essential for the evaluation con-ducted in this thesis.

Fuse-gears are installed at the tee-point in the lateral distributor as lateral protection. If a failure occurs downstream of the fuse (i.e., on the lateral line or the local transformer), the fuse is op-erated to immediately trip creating a disconnection of its load point until the failure is cleared. Since the fuse is located at the tee-point in the lateral distributor, it would not affect the other load points.
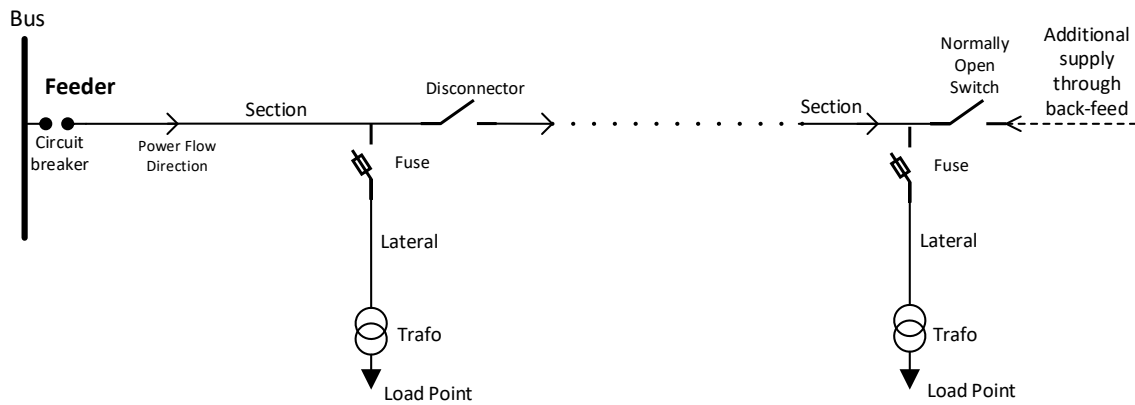
Figure 2.4: Schematic design of section, lateral and load point including disconnector, fuse and transformer in a distribution system; inspired by [20].

In addition to the installation of fuses in the lateral distributors, disconnector switches are normally installed at judicious points along the main feeder. A failure along the main feeder will cause the main breaker to operate by isolating the feeder from the bus. Then, when the failure is located, the appropriate disconnectors will open to isolate the failure and, as such, allowing the main breaker to re-close. The motivation for investing in disconnectors is to restore and re-energise the load points between the supply and the isolated part of the system before the repair process is completed and, thereby, decrease the outage time for the respective load points.

Furthermore, a single radial feeder can be constructed as a weakly meshed system but operated as a radial system by including a switch called "normally open point" (noted as *NO* in Figure 2.4), offering an additional supply and contributing to bi-directional power flow. This incorporation may contribute to reducing the amount of equipment exposed to a failure; done by closing the NO switch when the failure on the main feeder is isolated, which further minimise the amount and duration of unsupplied load points [20]. The back-feed is implemented combined with the disconnectors, as it would be of no interest without the ability to isolate failed parts of the system.

An essential step in improving reliability is by defining what measure to optimise, as the possible solutions change with the goal. For this, system reliability parameters need to be defined.

2.4 Reliability Indices

Reliability indices are used for quantifying the reliability of a system. This section describes some of the most common indices used to evaluate the reliability of distribution systems. It should be noted that these indices only represent average values in the long run.

2.4.1 Basic Reliability Parameters

In the context of reliability, the basic parameters are defined as the failure rate λ, the outage duration (i.e., unavailability) U and the repair time r [20]. Depending on the system of interest, the techniques on how to calculate the basic system reliability parameters depends on the structure, i.e., if the system consists of series or parallel connections. For systems of radial structure, the basic reliability parameters are developed based on the principle of series connections as explained below and discussed in [20].

The average failure rate of a single radial feeder λ_s consisting of k components can be calculated as the sum of the individual failure rates of load points i, shown in Equation 2.1. The annual outage time of the system U_s is defined as the sum of the individual failure rates multiplied by the individual outage duration of load points i, expressed in Equation 2.2. Following, the average repair time of the system r_s is given by the average annual outage duration divided by the average failure rate of the system, as given by Equation 2.3.

$$\lambda_s = \sum_{i=1}^{k} \lambda_i \ [\text{f/yr}] \tag{2.1}$$

$$U_s = \sum_{i=1}^{k} \lambda_i \cdot r_i \ [\text{h/yr}] \tag{2.2}$$

$$r_s = \frac{U_s}{\lambda_s} \ [\text{h}] \tag{2.3}$$

These basic parameters do not present a sufficient evaluation of the system reliability. However, the indices play a crucial role in calculating more specified reliability indices such as customer-

oriented and load- and energy-oriented indices as addressed in the following sections.

2.4.2 Customer-Oriented Indices

The performance of system reliability at the distribution level is assessed by indices describing the interruption statistics of customers, usually based on a well-defined average [23]. The customer-oriented indices are calculated based on the three basic indices, as described in 2.4.1, combined with the number of customers connected to each load, to give an appreciation of the system performance [7]. In this thesis, the definitions of the reliability indices represented by IEEE 1366-2012 [22] and by [23] are employed.

System Average Interruption Frequency Index (SAIFI) is defined as the ratio between the total interruptions of the customer and the total served customers, as expressed in Equation 2.4, where N_i is the number of interrupted customers during the reported period. More simply, SAIFI represents the average number of interruptions a system of customer experiences during a set period.

$$\text{SAIFI} = \frac{\text{Total number of customers interrupted}}{\text{Total number of customers served}} = \frac{\sum \lambda_i N_i}{\sum N_i} \; [\text{int/cust}] \tag{2.4}$$

Additionally, the Mean Time Between Failure (MTBF), known as the reciprocal value of the failure rate, can be used to measure SAIFI [24].

System Average Interruption Duration Index (SAIDI) includes the duration of the interruptions in the calculations, as presented in Equation 2.5. SAIDI is an indication of the total duration of interruption experienced by the average customer during a specified period.

$$\text{SAIDI} = \frac{\text{Total customer hours of interruptions}}{\text{Total number of customers served}} = \frac{\sum U_i N_i}{\sum N_i} \; [\text{h/cust}] \tag{2.5}$$

Customer Average Interruption Duration Index (CAIDI) is a measure of the utility response time to the system contingencies and measures how long an average interruption lasts, i.e., the aver-

age required time for the service to restore. CAIDI is calculated as expressed by Equation 2.6.

$$\text{CAIDI} = \frac{\text{Total customer hours of interruptions}}{\text{Total customers interruptions}} = \frac{\sum U_i N_i}{\sum \lambda_i N_i} \ [\text{h/int}] \tag{2.6}$$

Alternatively, CAIDI can be calculated as the ratio between SAIDI and SAIFI.

There are several more indices presented in the literature [22, 23], such as ASAI, ASUI, CTAIDI, CAIFI, CEMI, NIEPI, ASIDI, AID, AIF and so on. However, the ones presented and addressed in this thesis are the most popular among utilised, according to a survey IEEE conducted in 1996 [25].

Example for Calculating Customer-Oriented Indices

To illustrate the calculation and measurements of the different presented indices, an example of a system is adopted from [24]. The example consists of four outage incidents for a system of 10,000 customers, with the information given in Table 2.1.

Table 2.1: Support data for example calculation of reliability indices

Outage identification	Number of customers	Duration [min]	Customer-hours [h]
1	10	30	5.00
2	100	10	16.67
3	1	75	1.25
4	2	60	2.00
Total	113		24.92

SAIFI is calculated as the sum of the number of customers experiencing outage divided by the sum of the number of customers in the system, as follows:

$$\text{SAIFI} = \frac{113}{10,000} = 0.0113$$

This result implies that the customers at this system had a probability of 0.0113 (1.13%) of experiencing a power outage. During the first outage, 10 customers were affected for 30 min. The customer-hours are obtained by multiplying these: 10 customers · 0.5 hours equal to 5

customer-hours, as seen in Table 2.1. The sum of the customers-hours for all the outages are calculated to be 24h 55min. Further on, the calculation of SAIDI is simple:

$$\text{SAIDI} = \frac{24.92}{10,000} = 0.002492 \text{ hours} = 8.97 \text{ sec}$$

This implies that the average customer was out for approximately 9 sec. Following, CAIDI can be calculated as the ratio between SAIFI and SAIDI:

$$\text{CAIDI} = \frac{0.002492}{0.0113} = 0.2053 \text{ hours} = 13 \text{ min } 13.8 \text{sec}$$

On average, any customer who experienced an outage was out of service for 13 min 13.8 sec.

2.4.3 Load- and Energy-Oriented Indices

In addition to the customer-oriented indices, the load- and energy-orientated indices are essential in the evaluation at the distribution level. The Expected Energy Not Supplied (EENS) index is similar to the customer-oriented indices defined by the basic load point reliability indices. Equation 2.7 presents the EENS, where L_{ai} is the average load connected to the load point i [23].

$$\text{EENS} = \text{Total energy not supplied} = \sum L_{ai} U_i \tag{2.7}$$

Following, the Average Energy Not Supplied (AENS) can be calculated by Equation 2.8.

$$\text{AENS} = \frac{\text{Total energy not supplied}}{\text{Total number of customers served}} = \frac{\sum L_{ai} U_i}{\sum N_i} \tag{2.8}$$

2.4.4 Additional Microgrid Reliability Indices

As there does not exist a standard for evaluating the reliability of a microgrid or a system including microgrids, a sample of indices suggested in the literature [11, 26, 27] are presented in this

thesis.

In [26], the failure rate (λ_C) and outage duration (U_c) for a customer C connected to any main feeder f and lateral feeder γ of a microgrid network, are given by:

$$\lambda_C = \sum_{i \in f} \lambda_i + \sum_{i \in \gamma} \lambda_i P_L + \lambda_{up} P_M \tag{2.9}$$

$$U_C = \sum_{i \in f} \lambda_i r_i + \sum_{i \in \gamma} \lambda_i P_L T_a + U_{up} P_M T_a \tag{2.10}$$

These load point reliability indices take into account the probability of unsuccessful isolation P_M, the probability of a shut-down due to a failure in the LV feeder P_L and the average time to restore the microgrids T_a. According to [26], the isolation process of a microgrid from the MV upstream network is assumed to have a high success rate. Thus, in the event of a failure occurring outside a microgrid, the process of isolating a microgrid from the MV upstream network is assumed to have a high probability of success so the microgrid may remain energised [28, 29].

Specified microgrid reliability indices are presented in [11, 27]. Microgrid Average Interruption Frequency Index (MAIFI), Microgrid Average Interruption Duration Index (MAIDI) and Microgrid Customer Average Interruption Duration Index (MCAIDI) refers to the average interruption frequency and duration experiences by a customer on each year within the microgrid. MAIFI, MAIDI and MCAIDI are calculated in the same way as for SAIFI, SAIDI and CAIDI, respectively, as given in Equations 2.4 to 2.6, wherein this case, i denotes the load points inside the microgrid.

The Island Operation Successful Rate (IOSR) is defined as the probability of switching successfully from grid-connected mode to island mode operation. This index is mathematically expressed as in Equation 2.11.

$$\text{IOSR} = \frac{\text{Total number of forming island successfully}}{\text{Total numbers of outages on PCC}} \text{ [pu]} \tag{2.11}$$

Island Loss of Load Probability (ILOLP) is defined as the fraction of time the load demand is unsatisfied during island mode, as expressed in Equation 2.12.

$$\text{ILOLP} = \frac{\text{Islanded hours with demand unsatisfied}}{\text{Total microgrid islanded hours}} \text{ [pu]} \qquad (2.12)$$

The Microgrid Islanded Operation Probability (MIOP) is defined as the probability of the Microgrid to operate in island mode as described in Equation 2.13.

$$\text{MIOP} = \frac{\text{Microgrid hours in island mode}}{\text{Total microgrid operation hours}} \text{ [pu]} \qquad (2.13)$$

2.5 Analytical Approach

Distribution system reliability can be assessed by several analytical methods, where the most used tools include FMEA, state-space diagrams, event trees, minimal cut sets, and fault trees [30]. These analytical approaches all evaluate the reliability indices based on mathematical equations, which are suggested for reliability analysis of basic systems, when average values of the system indices are sufficient [31]. One of the main advantages of utilising an analytical approach is the fast and accurate computation time compared to simulation-based methods [31]. Further, the use of analytical methods on a simplified distribution system is an often-used procedure to compare and evaluate simulation algorithms [7, 31].

In this thesis work, techniques based on an inductive (i.e., what if) analysis are considered to identify the failure mode of the components and the load points in the system. The well-established classical technique is based on FMEA that systematically evaluates component-by-component and how their failures affect the load points. The FMEA technique is suited for simple radial networks, as complex systems will result in a wide range of failure modes and, thereby, increase the length of the failure events which makes the FMEA evaluation difficult [31].

In [32], an approach called RELRAD (RELiability in RADial systems) is presented as a specific analytical simulation method for reliability calculation in a radially operated distribution system. The procedure of the RELRAD approach is illustrated in Figure 2.5b. Compared to the

(a) Minimal cut set for load point L_1

(b) RELRAD approach
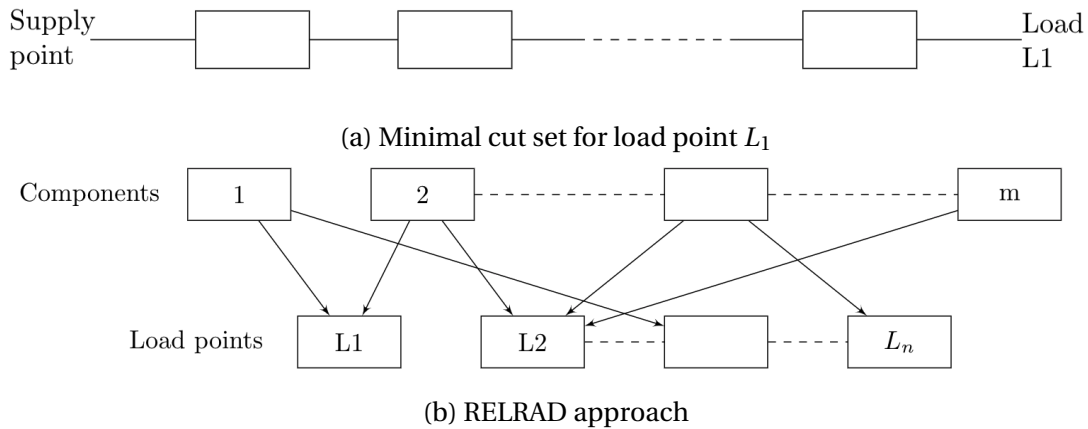
Figure 2.5: Analytical techniques for radial distribution systems, adopted from [32].

well-established classical technique which uses the minimal cut set to assess the individual load point reliability as illustrated in Figure 2.5a, RELRAD identifies which load points will have an outage caused by the failure of a particular component through a topology-based analysis. In other words, RELRAD focuses on analysing the individual components of the network contribution to the load points reliability, while the minimum cut set considering which component gives outage at the respective load point.

2.5.1 Example of Utilising Analytical Approach

To illustrate the main features of the analytical approach RELRAD, two examples are presented. In the first example, the system is simplified where all components are series-connected without the ability to isolate any failures, while the second example evaluates a system containing disconnectors and fuses in the main sections and laterals, respectively. Due to the operating policy assumed, the first example is not very realistic in today's distribution systems; the second example is included to illustrate the impact of additional protection in a more realistic system. It is of great importance to understand how the different protection equipment affects the analysis and, thus, the load point reliability indices. Note that the protection devices are located as discussed in Section 2.3.2 and illustrated by Figure 2.4.

In these examples, Feeder 1 of Bus 5 of the benchmark RBTS is used [33]. This is a feeder composed of four sections, seven laterals, seven transformers and seven load points. The reliability

and system data for RBTS Bus 5 are listed in Appendix C, where all the relevant data for this respective example is extracted and listed in the Tables 2.2 and 2.3.

The upstream network, bus, circuit breaker and protection equipment are assumed fully reliable. The supply is assumed re-energised to the possible load points by using appropriate disconnectors and back-feed supply if available, with the same switching time for the NO switch as for the other section components. The capacity of the individual lines is not considered in this example. Furthermore, the capacity of the alternative supply is assumed sufficiently large. It is assumed that any failure, single-phase or otherwise, will trip all three phases.

Table 2.2: Reliability and system parameters for Feeder 1 of Bus 5 [34].

Component	Failure rate, λ [f/yr]	Repair time, r [h]	Switching time, r_s [h]
Section	0.04 /km	30	3
Lateral	0.04 /km	20	3
Transformer	0.015	200	3

Table 2.3: Line parameters for Feeder 1 of Bus 5 [33].

Length [km]	Feeder section number
0.50	1, 6, 9
0.65	4, 7, 8
0.80	2, 3, 5, 10, 11

Example 1: Simplified system

When operating a radial system in its most basic mode and least capital intensive with no protective equipment, it is fairly simplified [20]. Since all the components are short-circuited, a customer connected to any load point requires all components to operate to be supplied. The single line representation of such distribution feeder is illustrated in Figure 2.6.

The load point reliability indices are calculated straight forward by applying the Equations 2.1, 2.3 and 2.2. The failure rate, outage duration, and annual outage duration for load points LP1, LP5 and LP7 are listed in Table 2.4. A failure located anywhere in the system will trip the main feeder breaker and disconnect the supply until the failure is cleared.
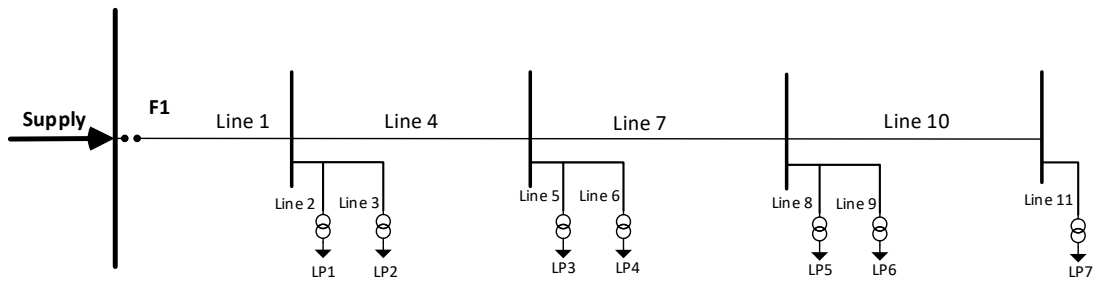
Figure 2.6: Single distribution of Feeder 1, Simplified.

Since there are no occasions where a failure can be isolated, all failures will affect all load points in the feeder and, thus, the failed component must be repaired before the main breaker can be re-closed. This results in identical reliability indices of all customer load points.

Table 2.4: Load point reliability indices of Feeder 1, without any protection devices.

Components		Load Point 1			Load Point 5			Load Point 7		
		λ [f/yr]	r [h]	U [h/yr]	λ [f/yr]	r [h]	U [h/yr]	λ [f/yr]	r [h]	U [h/yr]
Sections	L1	0.020	30	0.60	0.020	30	0.60	0.020	30	0.60
	L4	0.026	30	0.78	0.026	30	0.78	0.026	30	0.78
	L7	0.026	30	0.78	0.026	30	0.78	0.026	30	0.78
	L10	0.032	30	0.96	0.032	30	0.96	0.032	30	0.96
Transformers	T1	0.015	200	3.00	0.015	200	3.00	0.015	200	3.00
	T2	0.015	200	3.00	0.015	200	3.00	0.015	200	3.00
	T3	0.015	200	3.00	0.015	200	3.00	0.015	200	3.00
	T4	0.015	200	3.00	0.015	200	3.00	0.015	200	3.00
	T5	0.015	200	3.00	0.015	200	3.00	0.015	200	3.00
	T6	0.015	200	3.00	0.015	200	3.00	0.015	200	3.00
	T7	0.015	200	3.00	0.015	200	3.00	0.015	200	3.00
Laterals	L2	0.032	30	0.96	0.032	30	0.96	0.032	30	0.96
	L3	0.032	30	0.96	0.032	30	0.96	0.032	30	0.96
	L5	0.032	30	0.96	0.032	30	0.96	0.032	30	0.96
	L6	0.020	30	0.60	0.020	30	0.60	0.020	30	0.60
	L8	0.026	30	0.78	0.026	30	0.78	0.026	30	0.78
	L9	0.020	30	0.60	0.020	30	0.60	0.020	30	0.60
	L11	0.032	30	0.96	0.032	30	0.96	0.032	30	0.96
Total		0.403	74.29	29.94	0.403	74.29	29.94	0.403	74.29	29.94

Example 2: Protection equipment: disconnectors, fuses and alternative supply

Additional facilities are installed to improve the load point reliability and, thereby, the system reliability indices. Subsequently, the single-line diagram is modified by incorporating disconnectors, fuses and alternative supply as illustrated in Figure 2.7.
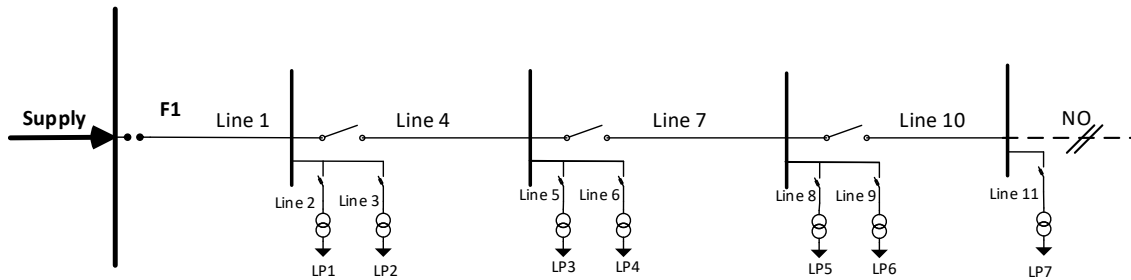
Figure 2.7: Single distribution of Feeder 1 with protection equipment.

The effect of installing fuse-gears in the laterals are shown in Table 2.5. As a result, the failure rate and outage duration become zero for the transformers and lateral feeders not directly connected to the respective load point.

By considering disconnectors, the outage duration of the components located further away on the main feeder through the disconnector of the respective load point will be equal to the switching time of the individual disconnector. The decrease in outage duration (from repair time to switching time) has an impact on the annual outage duration due to the definition described by Equation 2.2.

An additional supply (i.e., back-feed) is suggested by closing the NO-switches which makes the system operate as a meshed system. The additional supply aims to serve load points that otherwise would have been left disconnected from the supply during the fault clearing time.

If a failure occurs on a section between two disconnectors, the outage duration of the components in the failed section experiences an outage duration equal to its respective repair time, while the remaining parts of the system experience an outage duration equal to the time to isolate the failed component (i.e., switching time of the disconnector). The resulting outage duration is listed in column *r* in Table 2.5.

The load point reliability indices have experienced a remarkable improvement when comparing the failure rate, outage time and annual outage time listed in the Tables 2.4 and 2.5.

Table 2.5: Load point reliability indices of Feeder 1 with protection equipment.

Components		Load Point 1			Load Point 5			Load Point 7		
		λ [f/yr]	r [h]	U [h/yr]	λ [f/yr]	r [h]	U [h/yr]	λ [f/yr]	r [h]	U [h/yr]
Sections	L1	0.020	30	0.600	0.020	3	0.060	0.020	3	0.060
	L4	0.026	3	0.078	0.026	3	0.078	0.026	3	0.078
	L7	0.026	3	0.078	0.026	30	0.780	0.026	3	0.078
	L10	0.032	3	0.096	0.032	3	0.096	0.032	30	0.960
Transformers	T1	0.015	200	3.000	0	0	0	0	0	0
	T2	0	0	0	0	0	0	0	0	0
	T3	0	0	0	0	0	0	0	0	0
	T4	0	0	0	0	0	0	0	0	0
	T5	0	0	0	0.015	200	3.000	0	0	0
	T6	0	0	0	0	0	0	0	0	0
	T7	0	0	0	0	0	0	0.015	200	3.000
Laterals	L2	0.032	30	0.960	0	0	0	0	0	0
	L3	0	0	0	0	0	0	0	0	0
	L5	0	0	0	0	0	0	0	0	0
	L6	0	0	0	0	0	0	0	0	0
	L8	0	0	0	0.026	30	0.780	0	0	0
	L9	0	0	0	0	0	0	0	0	0
	L11	0	0	0	0	0	0	0.032	30	0.960
Total		0.151	31.867	4.812	0.145	33.062	4.794	0.151	34.0132	5.136

2.6   Monte Carlo Simulation Basics

For a high number of system states and re-configurable systems, MCS is a necessary method for reliability analysis as analytical approaches become impractical for such complex systems. While analytical techniques representing the system by a mathematical model may be infeasible and time-consuming for complex systems, simulation techniques overcome these limitations and have the capability of achieving a closer adherence to reality [7].

MCS may be defined as a process for obtaining estimates (numeric values) for a given system, guided by a prescribed set of goals, by means of random numbers from a probability distribution. The random numbers are used to classify the state of the components in the system, and the transition to other states. The system state is given by the combination of the individual components' states. Thus, a system state can be expressed by a state vector, **S**, where each component is represented by a state value, S_i, as follows:

$$\mathbf{S} = \{S_1 \quad S_2 \quad ... \quad S_i\} \tag{2.14}$$

The available MCS methods are mainly divided into two classifications depending on the time: non-sequential and sequential methods. Whereas the first method samples the system states randomly, the latter method obtains a sequence of the system states depending on the previous state [20].

In MCS, it is important to define stopping criteria. This is normally either a predefined number of trials or a defined maximum error [7]. In many cases, where the desired result is the expected value, a set number of trials are performed until the mean of all results converges to a stable value. This number is dependently on the rareness of the events, as the number of simulations should be large enough to give the rare event a high probability of occurring. For example, if a component is expected to fail once per 100 years, 5,000 simulations will have a high probability of simulating several failures while 50 simulations will not.

2.6.1 Sequential Monte Carlo Simulation

Sequential MCS attempts to model system behaviours precisely as it occurs in reality - as a sequence of random events that build upon each other as the system progresses through time. In reality, some system contingencies can randomly occur at any point, while other contingencies depend upon prior events and the present state of the system [7]. By taking this into consideration and by implementing the probabilistic model with a high level of detail, a sequential MCS can produce a highly realistic simulation, almost comparable to a physical experiment.

In a time-sequential simulation, the essential requirement is to generate realistic artificial histories showing the state sequence of the components. To do so, random number generation and the respective probability distribution of the component failure and restoration parameter are used. These artificial histories depend on the system states and the reliability parameters of the components. In distribution systems, basic transmission equipment such as main and lateral lines and transformers can generally be represented by the two-state model shown in Figure 2.8.
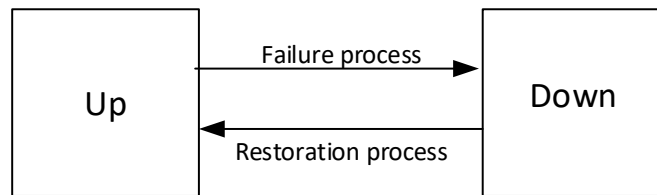
Figure 2.8: State space diagram of component, as adopted from [35].

In this context, "Up" implies the state when the component is operating and "Down" implies the state when the component is inoperable due to a failure. The time duration of the component in up state is referred to as Time To Failure (TTF), while Time To Repair (TTR) is referred to as the time duration of the component in the down state. Further, "failure process" is the designation for the process of transiting from the up to the down state and the "restoration process" is the designation for the opposite transition. Figure 2.9 shows the simulated operating/restoration history of a component.
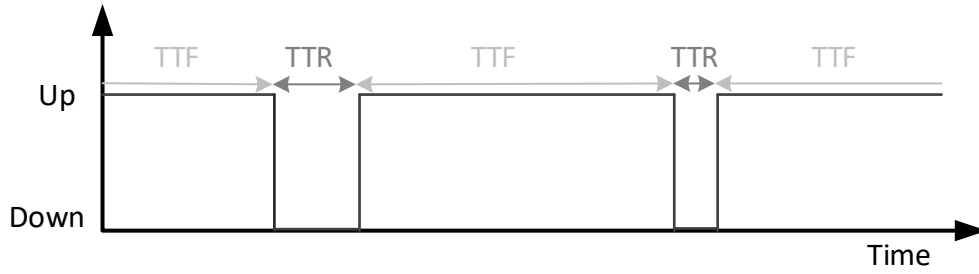
Figure 2.9: Simulated history of an artificial load point.

The parameters TTF and TTR are random and depend on the probability distribution of the component. The most useful distributions in distribution system reliability evaluation are exponential, gamma, normal, lognormal and Poisson distributions. According to [31], many studies indicate that the TTF is reasonably described by an exponential distribution at which is applied in this thesis work; its probability density function is given in Equation 2.15.

$$f_T(t) = \begin{cases} \lambda e^{-\lambda t}, & \text{for } 0 < t < \infty \\ 0, & \text{otherwise} \end{cases} \tag{2.15}$$

The cumulative probability distribution function for the exponential distribution is given in Equation 2.16, where U is a uniformly distribution random number in the range [0,1].

$$U = F(t) = 1 - e^{-\lambda t} \tag{2.16}$$

By solving this equation with respect to the time t, the following expression may be obtained:

$$T = -\frac{1}{\lambda} \ln(1 - U) \tag{2.17}$$

Accordingly, as U is a uniformly distributed random variable, $(1 - U)$ is distributed in the same way as U. By recognising this, and that the time T is exponentially distributed, the expression given in Equation 2.18 can be used to describe the transition time based on the exponential

distribution and the inverse transform method.

$$T = -\frac{1}{\lambda}\ln(U) \tag{2.18}$$

In reliability assessment of distribution systems, the Time to Transition (T) is calculated for all components i in the system using Equation 2.18. Further, the time to transition of the system T_S can then be calculated using Equation 2.19, which states that the time to transition of the system equal the smallest T of all the components.

$$T_S = \min\{T_1 \quad T_2 \quad \dots \quad T_i\} \tag{2.19}$$

As such, T_S is evaluated as long as it is within the respective year or, in some cases, the defined simulation period. Accordingly, in distribution system reliability, the procedure is performed for the number of simulations to evaluate reliability indices. To do so, analytical methods are usually applied in this part of the simulation to evaluate and locate which load point(s) will be affected by a component failure. This procedure depends on the system configuration, the system protection and the maintenance philosophy [31].

2.6.2 Non-sequential Monte Carlo Simulation

The non-sequential MCS assumes that the contingencies occurring in a system are mutually exclusive and that the system behaviours does not depend on past events [7]. A non-sequential MCS determines all contingencies that will occur prior to the simulation start. Contingencies are randomly selected from a pool of possible contingencies based on contingency probability. The selected contingencies are then simulated in any order, assuming that all the contingencies are mutually exclusive.

2.7 Modelling of Distributed Generation

There are different methodologies presented in the literature on how to evaluate DG units. For conventional generating units, a two-state model has been suitable. However, to represent intermittent energy sources such as Wind Turbine (WT) generation and PhotoVoltaics (PV) modules, a two-state model is not sufficient to describe the operating model as the stochastic variables cannot be maintained at a specified stable level.

In general, wind and solar modelling depend on the available historical data for each site. The stochastic nature of the renewable resource and its influence on the reliability of the system can be modelled and studied by the adequacy transition rate. To develop an adequacy model, three factors need to be considered [36]:

1. The random nature of the site resource. For WT, this is the wind speed at a certain height depending on the tower length. For PV, this is the solar radiation at a certain orientation depending on the angle and tilt of the PV module. These variables must be included in an appropriate model to reflect the characteristics of the source.

2. The relationship between the power output and the site resource. The site resource and output power correlation are applied to determine the ability of the generating units. Thus, to consider several output levels, the power curve of the generating unit and the variable site resource is combined.

3. The unavailability of the generation unit. In this thesis, both the WT and PV system are modelled with a failure rate and a repair time, as described in Section 2.4.1.

2.7.1 Wind Turbine Generation

The available power output of a WT is given in Equation 2.20, where ρ is the density of air, A the swept area, V the wind speed, C_p the rotor power coefficient and η the drive train efficiency (generation power/rotor power) [37].

$$P_{WT} = \frac{1}{2}\rho A V^3 C_p \eta \tag{2.20}$$

As shown in the expression above, the available power produced by a wind turbine is proportional to the cube of the wind speed. In other words, the generation is heavily dependent on wind speed. Consequently, to estimate the potential of wind energy for a given site, statistical methods and analysis can be applied for modelling wind speed [37].

In this thesis, the methods for wind speed modelling and WT generation modelling are addressed for evaluating WT systems. It should be noted that when referring to WT systems, this thesis considers the system consisting of WT generation, boost converter and inverter.

2.7.1.1 Modelling of Wind Speed

As the wind speed may be categorised as somewhat random, probability theory is commonly applied to assess its behaviour [38]. A probability distribution is generally characterised by a cumulative density function or probability density function. By considering the wind speed V as the stochastic variable, its cumulative distribution function defined in Equation 2.21 states the probability that the random quantity V' is less or equal to the numeric value of V [37].

$$F(V) = Pr(V' \leq V) \tag{2.21}$$

The probability density function $f(V)$ states the probability of a wind speed occurring between a lower (V_a) and upper limit (V_b), as follows

$$Pr(V_a \leq V \leq V_b) = \int_{V_a}^{V_b} f(V) dV \tag{2.22}$$

As such, the total area under the probability density curve is 1. Hence, if $f(V)$ is known, the mean wind speed $\overline{V}$ and the mean available wind power density $\overline{P}/A$ can be calculated by applying the power expression in Equation 2.20 and is calculated as

$$\overline{V} = \int_0^\infty V f(V) dV \tag{2.23}$$

Whereas the power density is calculated as follows

$$\frac{\overline{P}}{A} = \frac{1}{2}\rho \int_0^\infty V^3 f(V) dV = \frac{1}{2}\rho \overline{V^3} \tag{2.24}$$

Additionally, the probability density function can be defined as the derivative of the cumulative distribution function such as in Equation 2.25.

$$f(V) = \frac{d}{dV} F(V) \tag{2.25}$$

These probability functions can be defined by different probability distributions. The most widely used is the Weibull distribution, named after the developer and Swedish professor Waloddi Weibull (1987-1979) [39]. The Weibull distribution is known for being flexible and is commonly used in reliability analysis. The literature [37, 40, 41] states that it is reasonable to assume that the wind speeds obey the two-parameter Weibull distribution and, hence, is assumed in this thesis. The wind speed is said to be Weibull distributed if the cumulative distribution function is given by the Equation 2.26 [37, 39].

$$F(V) = 1 - e^{\left(\frac{V}{c}\right)^2} \tag{2.26}$$

The corresponding probability density is as follows

$$f(V) = k\left(\frac{1}{c}\right)^k V^{k-1} e^{\left(\frac{V}{c}\right)^2} \tag{2.27}$$

Where k and c denotes the shape and the scale parameters of Weibull distribution, which are functions of $\overline{V}$ and the standard wind speed deviation σ_V. The average velocity can be determined by using Equation 2.27, and is given in Equation 2.28. In this expression, Γ presents the Gamma function defined as $\Gamma(n) = (n-1)!$ for integer n.

$$\overline{V} = c\Gamma\left(1 + \frac{1}{k}\right) \tag{2.28}$$

Additionally, for Weibull distribution, it can be shown that the standard deviation for wind speed is given as

$$\sigma_V = \overline{V}^2 \left[\frac{\Gamma\left(1 + \frac{2}{k}\right)}{\Gamma^2\left(1 + \frac{1}{k}\right)} - 1 \right] \tag{2.29}$$

From this, it is not straightforward on how to obtain c and k in terms of $\overline{V}$ and σ_V. To simplify, analytical approximations can be used. In [42], the approximation given in Equation 2.30 was established and is applied in this project.

$$k = \left(\frac{\sigma_V}{\overline{V}}\right)^{-1.086} \tag{2.30}$$

By utilising this estimation, Equation 2.28 can be used to solve for c. Note that when $k = 1$, the Weibull distribution is equal to the exponential distribution and when $k = 2$, the resulting distribution is known as the Rayleigh distribution [39]. This is also a common distribution used to model wind speed. However, it only requires one parameter; the mean wind speed. Thus, as the Weibull distribution is based on two parameters, it can represent a wider variety of wind regimes [37].

Further, to use the cumulative probability function to determine the wind speed, the inverse transformation method can be applied. By considering U as a stochastic variable that submits uniform distribution in [0,1] and setting the cumulative distribution function in Equation 2.26 equal to U, samples of wind speed can be generated as given in Equation 2.31 [43].

$$V = c \cdot [-ln(1 - U)]^{\frac{1}{k}} \tag{2.31}$$

As U submit uniform distribution, the term $(1 - U)$ can be replaced by U. As such, the Weibull distribution stochastic variable generation can be expressed as

$$V = c \cdot [-ln(U)]^{\frac{1}{k}} \tag{2.32}$$

2.7.1.2 Modelling of WT Generation

A typical power curve of a WT is illustrated in Figure 2.10. From this, is it clear the power output of the WT is heavily dependent on the wind speed, which can be divided into three different ranges: (i) the cut-in speed V_{ci}; (ii) the rated speed V_r; (iii) the cut-out speed V_{co} [8]. The WT starts producing power at V_{ci} and reaches its rated production at V_r. For the interval between V_r and V_{co}, the output is maintained constant at the rated electrical output (i.e., non-linear relationship between the production and wind speed) appropriate black pitch control. At V_{co} and beyond, the unit is shut down for safety reasons and to prevent excessive stress and damage. Due to constant variations in the wind, the power output of the WT lies between zero and rated value for nearly half of the time or even longer for poor wind regime months [44]. To estimate the power extracted by the WT, Equation 2.33 is applied in this thesis work [45].

$$P_{WT}(V) = \begin{cases} 0, & \text{for } 0 \leq V < V_{ci} \\ (A + B \cdot V + C \cdot V^2) \cdot P_r, & \text{for } V_{ci} \leq V < V_r \\ P_r, & \text{for } V_r \leq V < V_{co} \\ 0, & \text{for } V \geq V_{co} \end{cases} \tag{2.33}$$

Here, P_r is the rated power output and A, B and C are defined by the Equations 2.34, 2.35 and 2.36, respectively. These constants depend only on V_{ci} and V_r.

$$A = \frac{1}{(V_{ci} - V_r)^2} \left[V_{ci} \cdot (V_{ci} + V_r) - 4 \cdot V_{ci} \cdot V_r \cdot \left(\frac{V_{ci} + V_r}{2V_r} \right)^3 \right] \tag{2.34}$$

$$B = \frac{1}{(V_{ci} - V_r)^2} \left[4 \cdot (V_{ci} + V_r) \cdot \left(\frac{V_{ci} + V_r}{2V_r} \right)^3 - 3 \cdot (V_{ci} + V_r) \right] \tag{2.35}$$

$$C = \frac{1}{(V_{ci} - V_r)^2} \left[2 - 4 \left(\frac{V_{ci} + V_r}{2V_r} \right)^3 \right] \tag{2.36}$$
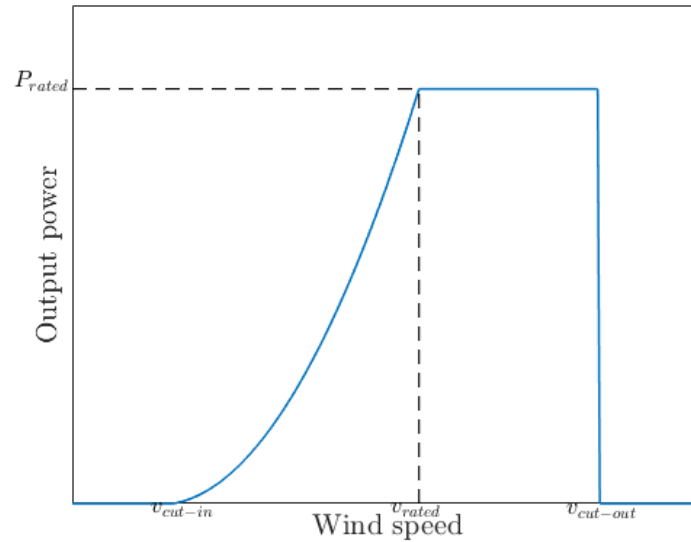
Figure 2.10: A typical power curve of a wind turbine.

2.7.2 PhotoVoltaics Generation

Solar energy is a fast-growing energy source worldwide regarding the installed capacity. The available power output of the PV modules depends upon several factors, among which the most dominant ones are solar radiation and temperature [36, 46]. Thus, to be able to estimate the potential of power production of the PV system, accurate estimates of solar radiation are of interest. Solar radiation mainly depends on atmospheric conditions, such as the attenuation effect of clouds and shadowing, and the altitude angle which varies with geographical position, time of day and time of year [47].

Solar radiation modelling and PV generation modelling are further addressed for evaluating PV systems. This thesis, when referring to PV systems, it considers the system consisting of a PV module, converter and inverter.

2.7.2.1 Modelling of Solar Radiation

Solar radiation is heavily dependent on the location of the site. Unlike wind speed, solar radiation varies randomly with location due to the intermittency inherent to sunlight. Thus, several distribution functions can be used to model radiation, depending on the availability on-site. The authors in [48] expressed a quadratic function, given Equation 2.37, to represent a simpli-

fied hourly variation of solar radiation during a typical day. Here, G_{max} is the maximum sunlight intensity during a day, which is assumed at midday (12 noon). This expression assumes that the solar radiation is accessible in the time range 6 am to 6 pm, as illustrated in Figure 2.11. In reality, this will vary with on-site conditions.

$$G_d(t) = \begin{cases} G_{max} \cdot \left(-\frac{1}{36} \cdot t^2 + \frac{2}{3} \cdot t - 3\right), & \text{for } 6 \le t \le 18 \\ 0, & \text{for } 0 \le t \le 6 \text{ and } 18 \le t \le 24 \end{cases} \tag{2.37}$$
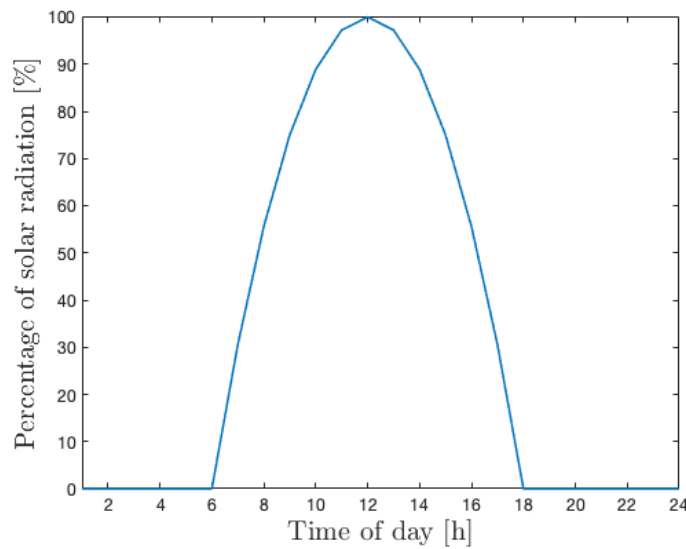
Figure 2.11: Hourly solar radiation in percentage of total daily radiation.

Additionally, solar radiation can be modelled with a random variable to account for the influence of clouds, temperature and other meteorological factors. By implementing a prediction tool to account for these factors, the PV model may become more realistic. According to [49], studies have proven that the variation of the solar radiation reaching the PV module (ΔG) follows a normal distribution. This gives the expression seen in Equation 2.38, where σ_G is the standard deviation and solar radiation is noted as G.

$$f(\Delta G) = \frac{1}{\sqrt{2\pi}} \cdot exp\left(-\frac{\Delta G^2}{2\sigma_G^2}\right) \tag{2.38}$$

By considering this prediction factor, the correlated solar radiation G reaching the PV module at time t can be expressed as given in Equation 2.39, where G_d is the predicted solar radiation.

$$G(t) = G_d(t) + \Delta G(t) \tag{2.39}$$

2.7.2.2 Modelling of PV Generation

The power output of the PV modules is considered solely dependent on the variable G. This can be shown in the calculation of instantaneous power P_{PV} given by Equation 2.40 [36].

$$P_{PV}(G(t)) = \begin{cases} P_r \cdot \frac{G(t)^2}{(G_{std} \cdot R_c)}, & \text{for } 0 \le G(t) < R_c \\ P_r \cdot \frac{G(t)}{G_{std}}, & \text{for } R_c \le G(t) \le G_{std} \\ P_r, & \text{for } G(t) > G_{std} \end{cases} \tag{2.40}$$

In the above expression, P_r is the equivalent rated capacity of the PV system in W, R_c a certain radiation point usually set as 150 W/m^2 and G_{std} the solar radiation in the standard environment set usually as 1,000 W/m^2 [36]. The relation between the output power of the PV and solar radiation can be illustrated by a generalised power curve as such in Figure 2.12.
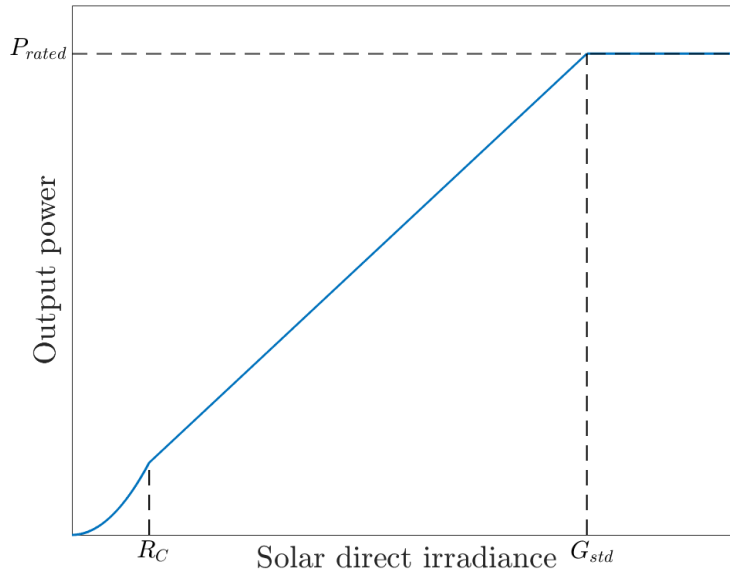
Figure 2.12: A generalised power curve of a PV module.

2.8 Energy Storage Systems

In microgrids, ESS can cope with the intermittent nature of RES. An ESS contributes to ensuring seamless transfers between grid and island connected mode, as well as enhancing the flexibility in power generation, delivery and consumption [5]. Saving electrical energy as chemical energy in batteries is the most common use of ESS. In this thesis work, Battery Energy Storage System (BESS) is further concentrated on the purpose of serving as an uninterrupted power supply system in microgrids operating in parallel with the DG units. It should be noted that, when referring to BESS, this thesis considers the system consisting of a battery, a controller and an inverter.

2.8.1 Modelling of Battery Energy Storage Systems

In reliability studies, BESS representation requires a particular model due to its operational characteristic; its State of Charge (SoC) depends on the system operation [50]. However, it is challenging and complex to include an accurate model for its use in stochastic simulation, as its performance is assumed to be highly dependent on charge/discharge cycles and due to battery degradation. This thesis considers the energy storage balance model and operation strategy as the two main elements in the modelling of BESS, inspired by the work conducted in [51].

The energy storage balance presents the amount of stored energy in the BESS at all times. Moreover, it states the available power to be charged/discharged. In [52], the storage model used is a linear storage model including charge, discharge and SoC variables, whereas self-discharge and battery degradation are neglected. These assumptions are adopted in this work. The storage constraints for the charge/discharge model presented in [52] is shown in Equation 2.41, where P_t^{ch} and P_t^{dch} are the charging and discharging power at time t, respectively, and $P^{ch,max}$ and $P^{dch,max}$ are the rated charging and discharging capacity of the BESS, respectively.

$$0 \le P_t^{ch} \le P^{ch,max}$$
$$0 \le P_t^{dch} \le P^{dch,max}$$

(2.41)

The amount of energy stored in the BESS at time t (E_t^{stored}) can be expressed by the energy storage balance as given in Equation 2.42, where Δt is the time increment, usually 1 hour or 1 minute, and η^{ch} and η^{dch} are the charging and discharging efficiencies [52].

$$E_t^{stored} = E_{t-1}^{stored} + \eta^{ch} \cdot P_t^{ch} \cdot \Delta t - \frac{P_t^{dch}}{\eta^{dch}} \cdot \Delta t \tag{2.42}$$

By assuming ideal charging and discharging efficiencies ($\eta^{ch} = \eta^{dch} = 1$), the energy storage balance can be rewritten as follows in Equation 2.43.

$$E_t^{stored} = E_{t-1}^{stored} + \cdot P_t^{ch} \cdot \Delta t - P_t^{dch} \cdot \Delta t \tag{2.43}$$

Further, the energy storage is also constrained to a limit to avoid full charges and discharges cycles of the battery, as such given in Equation 2.44. Here, E^{reserve} represents the lower limit of the battery to be discharged and E^{max} represents the upper limit of the battery to be charged.

$$E^{reserve} \le E_t^{stored} \le E^{max} \tag{2.44}$$

In this thesis, BESS is used in the cases of power imbalance within the microgrid during island mode with the object of improving the system reliability. Based on this operation strategy, the energy storage balance in Equation 2.43 and the restrictions that are given in Equations 2.41 and 2.44, the available charging and discharging management model of BESS considering MG operation state is built as given in Equations 2.45 and 2.46, respectively.

$$P_t^{ch} = \begin{cases} \frac{E^{max}-E_t^{stored}}{\Delta t} & \text{if } \frac{E^{max}-E_t^{stored}}{\Delta t} < P_t^{sur} < P^{ch,max} \\ P^{sur} & \text{if } P^{ch,max} < P_t^{sur} \le \frac{E^{max}-E_t^{stored}}{\Delta t} \\ \frac{E^{max}-E_t^{stored}}{\Delta t} & \text{if } P^{ch,max} \le P_t^{sur} \text{ and } \frac{E^{max}-E_t^{stored}}{\Delta t} < P^{ch,max} \\ P^{max} & \text{if } P^{ch,max} \le P_t^{sur} \text{ and } P^{ch,max} \le \frac{E^{max}-E_t^{stored}}{\Delta t} \\ 0 & \text{if } P^{sur} \le 0 \text{ or } E^{stored} = E^{max} \end{cases} \tag{2.45}$$

$$P_t^{dch} = \begin{cases} \frac{E_t^{stored} - E^{reserve}}{\Delta t} & \text{if } \frac{E_t^{stored} - E^{reserve}}{\Delta t} < P_t^{sur} < P^{dch,max} \\[2ex] P^{sur} & \text{if } P^{dch,max} < P_t^{sur} \leq \frac{E_t^{stored} - E^{reserve}}{\Delta t} \\[2ex] \frac{E_t^{stored} - E^{reserve}}{\Delta t} & \text{if } P^{dch,max} \leq P_t^{sur} \text{ and } \frac{E_t^{stored} - E^{reserve}}{\Delta t} < P^{dch,max} \\[2ex] P^{max} & \text{if } P^{dch,max} \leq P_t^{sur} \text{ and } P^{dch,max} \leq \frac{E_t^{stored} - E^{reserve}}{\Delta t} \\[2ex] 0 & \text{if } P^{sur} \leq 0 \text{ or } E^{stored} = E^{reserve} \end{cases} \qquad (2.46)$$

In the above equations, P_t^{sur} is the surplus of the microgrid system at time t; for charging operations it presents the difference between the sum of the power generated by the DGs and the sum of the load demand, while for discharging operations it is the difference between the sum of the load demand and the sum of the production of the DGs. This model takes into account the consideration that the battery cannot be simultaneously charged and discharged.

2.9 Literature Review of Reliability Assessment of Future Power Distribution Systems

To address the reliability performance of a distribution system, an appropriate test system with sufficient reliability parameters must be present. Literature provides suitable benchmark test systems for performing reliability analysis of distribution systems; the most commonly used in the research are the Roy Billinton Test System (RBTS) [26, 48, 50, 53, 54, 55, 56, 57, 58, 59] and the different IEEE Reliability Test Systems (IEEE RTS) [41, 44, 60, 61, 62].

In the field of networked microgrids, most researchers have used already defined benchmark systems, by implementing modifications for the construction of networked microgrids [63]. These modifications have mainly been to either implement DERs at different locations and, hence, divide the existing defined distribution system into multiple microgrids, or by adding microgrids to the existing system. However, a newly proposed test system from 2020 [63], argues that these modified systems are not suited to represent real networked microgrid systems. As such, the authors in [63] have presented a system that is designed based on a growing urgent of a suitable benchmark test system and is defined with respect to the requirements stated in the

IEEE Standard 1547-2018 [64]. The system consists of four independent microgrid-structures at which are interconnected to both each other and to the utility grid.

In both distribution and microgrid system reliability analysis, protection devices such as fuses, circuit breakers, sectionaliser, interconnection protection, re-closer and different relays play an important role in the performance. The study in [65] addresses the impact of protection devices on the reliability of a microgrid. In this work, a stochastic model was developed to simulate existing challenges in the current protection scheme during various operating conditions. Furthermore, an evaluation strategy, combined with simulation and load restoration is presented as a solution tool.

Another aspect is the operational strategy. In microgrid systems, the control strategy affects the interruption duration and frequency of the load points and, hence, is directly influencing the system reliability. The study in [53] proposes a method to evaluate the impact of various control strategies in the microgrid on the reliability of the distribution system. The paper addresses comparison of system reliability indices such as SAIFI, SAIDI and EENS for cases with and without island mode, whereas the former case resulted in the best performance.

Distributed generation of both dispatchable and non-dispatchable behaviours are evaluated in several papers. As mentioned before, established test systems are usually modified in a specific way to bring out the features of implementing DG. In order to evaluate the impact in system reliability of including DG in a distribution system, a strategy for the operation of the DG is needed. The research in [66] points out two aspects to include in terms of reliability evaluation and the impact of DG in system operating characteristics: (1) The model of the DG operation and the purpose of its connection; (2) The primary energy source the DG unit is based on.

In [67], the inclusion of DG in the distribution network is considered in two operation modes: dependently and independently of the utility supply. Furthermore, the DG location is considered. The DG is placed at the end of the feeder and, consequently, is studied without considering the alternative back-supply connections to bring out the features of installing DG. The paper also addresses the challenges occurring when DG operating independently of the utility supply, featuring several protections and coordination challenges due to multiple sources and, hence, bi-directional power flow.

In [54], the RBTS is modified to include DGs based on RES to validate the reliability impact. From a reliability perspective, the incorporation of DGs will highly benefit the reliability indices if the downstream network of a failed location would be able to make use of the already available DG unit's restore supply by operating in island mode as a microgrid.

In the distribution reliability evaluation of the presence of DG addressed in [68], it is considered that the DG can supply all or parts of the load in case of main source unavailability and that the occurrence of a failure causes the disconnection of both the main supply and the DG from the system. However, after the isolation of the failure, the DG is re-connected to the system and in this way, may be able to supply load point(s) while the failed component being repaired; as a result, there will be a reduction in the duration-related indices. However, the resulting frequency-related indices are not modified in the presence of DG.

To bring out the features of ESS in the reliability assessment of microgrids, ESS is usually combined with renewable DG to improve the reliability. In [59], a study of the impact of including PV and ESS to a microgrid, where the assessed distribution system is modelled by an analytical approach combined with the Markov method. The findings in this research were that the overall reliability increased. It was experienced that the outage duration decreased; however, the failure frequency increased, due to the implementation of the possibility of a failure of the PV system and ESS.

The most frequently used ESS in microgrids are batteries. However, two-way charging of electric vehicle technology is emerging as a suitable alternative [60]. For example, the study in [61] includes mobile battery energy storage systems to realise islanded operation at which has a positive effect on the reliability.

In the study presented in [56], an evaluation of the reliability of a microgrid containing prioritised loads and distributed RES such as solar and wind is carried out. The presented strategy of the RES is that the combined output of all RES is compared with the load. In this case, where RES cannot supply all of the loads, then the load with the highest priority is supplied first followed by the next load in the priority list and so on. The analysis resulted in a remarkable increase in the reliability of the most sensitive loads in the system.

Power Electronic Systems plays a crucial part in microgrids and subsystems. There are few studies evaluating the impact of power electronic systems on the microgrid's reliability [69, 70, 71]. Renewable-based DGs such as PV and wind are equipped with inverters and step-up transformers with failure rates. The research in [69] states that the inverter is the most critical component of large-scale PV systems; whereas research done in [70] has further located the capacitors to be the most critical elements of the inverters. Findings such as those in [69, 70] underline the importance of including power electronic systems when evaluating the reliability of microgrids. Accordingly, [71] concludes that the reliability of microgrids is greatly affected by the application of large-scale power electronic devices.

In the above-addressed literature, there is no common definition of how to include microgrid operation in the reliability evaluation of distribution systems. Many papers evaluate the impact of including DGs or ESS on distribution system reliability, but few evaluate the implementation of microgrids. As the overall objective of this thesis is to investigate the impact of microgrids on the distribution systems from a reliability perspective and since there is no common definition for doing so, several proposed techniques are applied to the comprehensive assessment. In this way, the identified research gaps provide motivation for the creation of synthesised algorithmic approaches in this thesis for quantifying the impact of microgrids on the reliability of power systems, based on the diverse features of select-few methods proposed in the literature.

Chapter 3

Methodological Approach

As stated in the introduction, this thesis aims to improve the pedagogical dissemination for the evaluation of (i) distribution system without DERs (i.e., passive distribution system), and (ii) distribution system with DERs in the form of a microgrid (i.e., active distribution system). Accordingly, first, a hybrid methodology based on a combination of simulation and analytical approaches is proposed for the reliability analysis of passive distribution systems, motivated by the methods described in [31, 35]. The determination of load point failures used in the simulation algorithm is inspired by the analytical RELRAD approach described in [72].

Additionally, variable load with an hourly resolution is considered in the analysis with the aim of studying a more realistic system, which is more appropriate when considering the integration of RES.

An extension of the developed hybrid methodology is then performed by adding DERs to form a microgrid for assessing the reliability of the active distribution system. As such, suitable integration of wind, solar and battery systems are assessed, inspired by the work presented in [43, 48, 51], respectively. The synthesised method is described in this chapter, where the algorithm is inspired by the published research in [48, 57].

Based on the research presented in [50, 73], an operation strategy for the uniquely designed microgrid for the purpose of reliability assessment, is presented in this chapter.

3.1 Proposed Simulation Algorithm

Time sequential MCS is chosen as the simulation method to obtain the history of all components in the system, and subsequently, obtain load point- and system reliability indices (expected values and probability distributions). As mentioned, the methodology utilised for performing the MCS is based on [31, 35] as well as on the theory presented in Section 2.6.

The proposed procedure for the sequential MCS of passive distribution systems is described by the flow chart in Figure 3.1. At the beginning of each simulation, the Time To Failure (TTF) of all components is generated; as such, a defined year is simulated N times. The simplification of simulating a year several times rather than many years in a row is considered as a valid assumption due to the deterministic reliability data parameters. If the simulation was to run over decades, most components would experience a change in reliability parameters such as failure rate, due to degradation and so on.

In the proposed procedure, first, TTF for each component is determined based on a random number and the respective failure distribution of each component (Equation 2.18). The component with minimum TTF (Equation 2.19) is used to represent the transition time of the system. Then, the location of the corresponding component is found and analysed with respect to the affected load point(s). To account for the restoration duration, a Time To Repair (TTR) is generated for the component according to its repair distribution and additionally, a Time To Switch (TTS) is generated if the component is designed with such equipment. In this way, the entire interruption duration of the respective load point(s) is considered. To account for the possibility that the component may experience more than one failure during the simulated year, a new TTF is generated and added to the transition time of the failed component.

For as long as the minimum TTF is less than one year, the analysis of the next failure event continues. If the transition time of the system is greater than one year, the number and duration of failures for each load point for the respective year are calculated. At the end of the simulation, i.e., when the simulation exceeds the specified number of simulations N, the average value of failure rates and outage duration is calculated as well as the system reliability indices such as SAIFI, SAIDI, CAIDI and EENS.
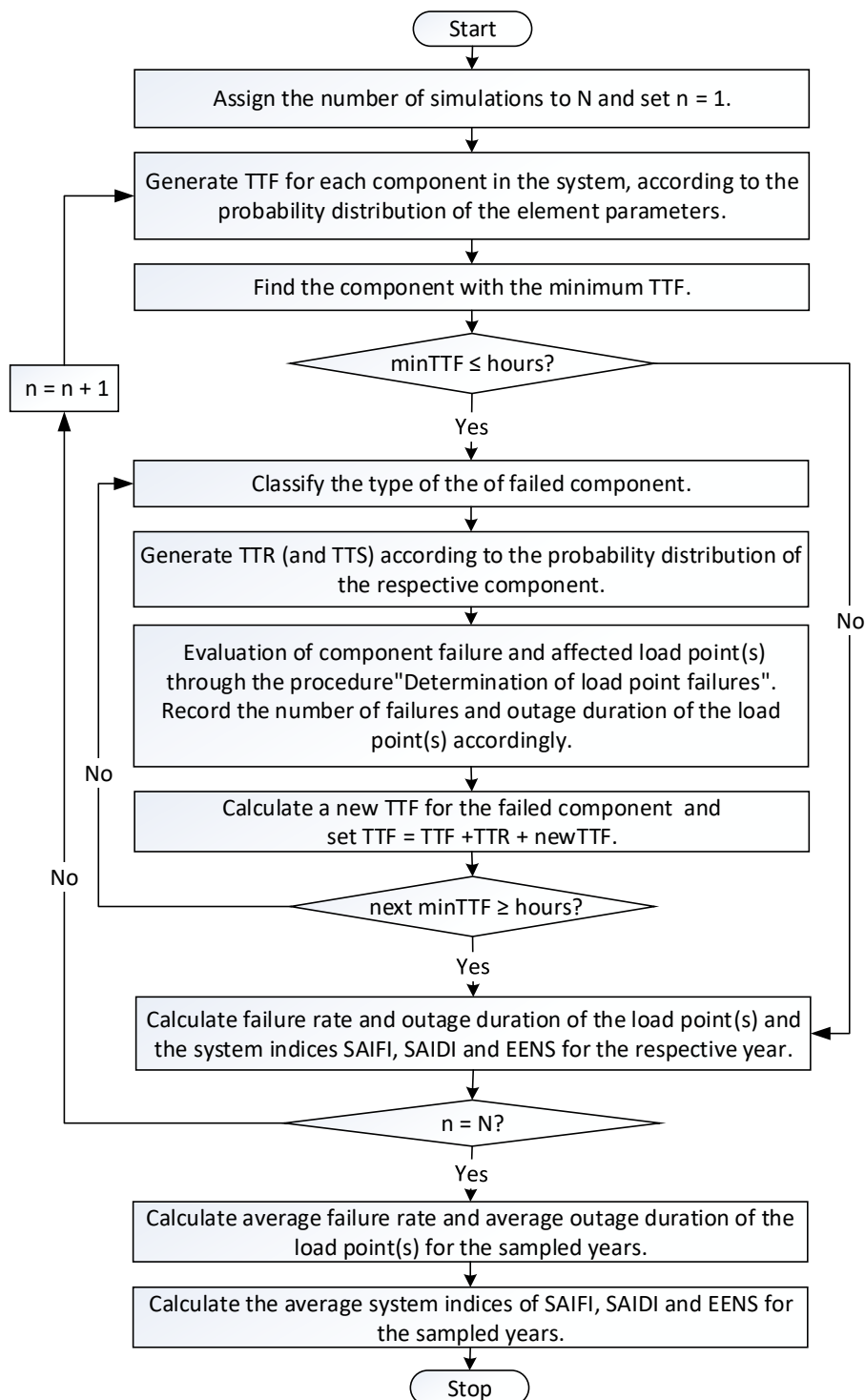
Figure 3.1: Algorithm used to evaluate Passive Distribution networks.

In the conducted analysis, only permanent failures are considered. The analysis is simplified by the assumption that any failure, single-phase or otherwise, will trip all three phases. Further, all failures are assumed independent of each other, and it is assumed that each failure is repaired before the next failure occurs based on [20].

Additionally, the protection equipment such as circuit breakers, disconnectors and fuses are assumed fully reliable and to perfectly isolate all failures. Similar, the upstream network is assumed fully reliable.

3.1.1 Determination of Load Point Failures

To determine the affected load point(s) due to a component's failure, the analytical approach RELRAD [72] and the procedure described in [31] are utilised to algorithmically determine how a component failure affects the system load points. The choice of applying the RELRAD technique is based on the decision of solely assessing radial distribution systems and the desire for low computations.

For the process of locating the load points and identifying their outage duration, upon the occurrence of failure of a component, knowledge of the following are crucial: network configuration, system protection and maintenance philosophy. Based on the supposition that this knowledge is in place, a procedure is developed by dividing the load points affected by the failed feeder in two lists: 1) "failed load points" and 2) "restored load points".

Under the assumption that the system can be divided into the combination of the main feeder and sub-feeders, the direct search procedure for determining the failed load points and their operation-restoration duration, based on the pre-defined input parameters, is described by the illustration in Figure 3.2. It should be noted that the protection devices (if any) are located and operated as described in Section 2.3.2 by Figure 2.4.
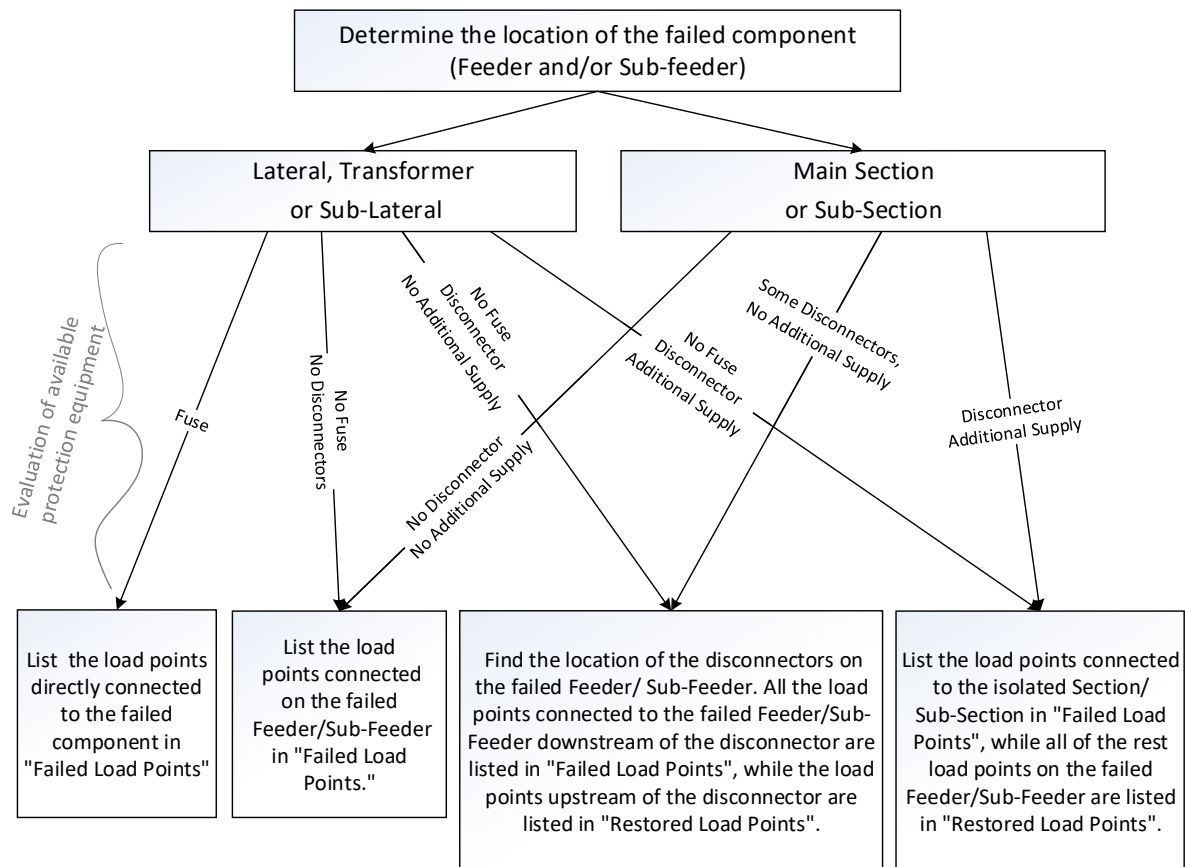
Figure 3.2: Evaluation of component failure and affected load points based on available protection equipment.

3.2 Variable Load Model

The load profile during a year varies with the seasons, the weather conditions and the type of day, e.g., whether it is a weekday or weekend. To account for this behaviour, a generalised hourly time-varying load model (i.e., hourly peak loads) representing the pattern during normal conditions is applied from [74] and illustrated in Figure 3.3.

In detail, the load profiles are constructed of three weighted factors: weekly variations (52 weeks during one year), daily variations (7 days during one week) and hourly variations (24 hours during one day). It should be noted that, in total, this contributes to 8736 load values per year (52 weeks/year × 7 days/week × 24 hours/day). The predicted load P_L for load point i at time t is calculated as shown in Equation 3.1.

$$P_{Li}(t) = W_w(w) \cdot W_d(d) \cdot W_h(h) \cdot P_{Li,peak} \tag{3.1}$$

Here, $W_w(w)$ is the weekly weight factor at week w, $W_d(d)$ is the daily weight factor at day d and $W_h(h)$ is the hourly weight factor at hour h.
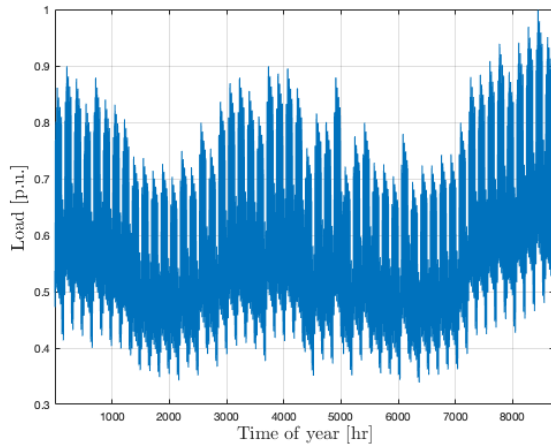
(a) Yearly load profile
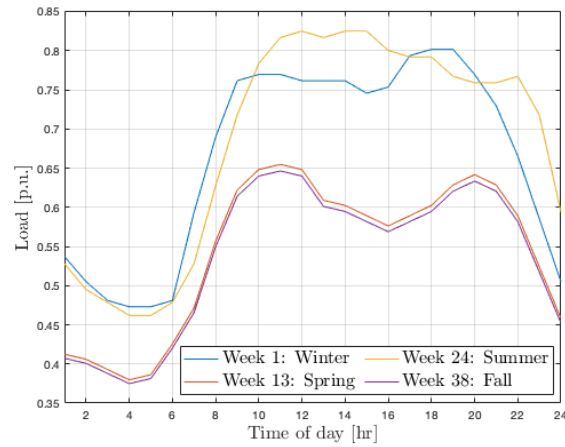
(b) Daily load profile for each season.

Figure 3.3: The generalised time varying load profile for a year.

3.3   Prioritised Loads Strategy

In this thesis, the procedure of load prioritisation is inspired by [73] to determine which load point is of higher and lower priority and, thus, supply accordingly. This is treated in the event that the microgrid is in island mode due to insufficient generation. The loads are prioritised to avoid that the entire microgrid is experiencing an outage. By including load prioritising, sensitive loads may remain connected and supplied while less sensitive loads can be subjected to curtailment.

To implement a reasonable strategy in the reliability judgement, a prioritisation matrix P is defined for the load points within the microgrid (in the range of [0,1]), indicating its priority as follows:

$$P = [LP_1, ..., LP_n] \cdot \begin{bmatrix} 1.0 \\ : \\ 1/n \end{bmatrix} \tag{3.2}$$

In the above matrix, 1 implies the highest priority and accordingly $1/n$ implies the lowest priority (0 signifies no priority at all). In the algorithm, a for-loop is constructed to go through all the load points within the microgrid in the case of island mode. By starting with the load point with the highest priority, its hourly load value is compared with the production at that specific time slot. If the production is higher or equal, the load point is supplied and the remaining production (remaining production = production - load of highest priority) is then compared with the next load point according to its priority order. This is performed for all the load points within the microgrid. If the production is less than the load, the respective load point and the remaining load points of lower priority remain unsupplied.

3.4 Incorporation of Distributed Generation

In this thesis, the complexity due to the effects of the random variables inherent in RES and their interaction has been resolved by simulating the atmospheric conditions and the corresponding system operations. As WT and PV systems are energy limited, intermittent and sporadic in nature, MCS is utilised to account for their stochastic characteristics.

To incorporate the possibility of failures of the considered DGs, reliability parameters of the DGs are treated the same as for the other component data of the distribution system. Additionally, the available outputs of the DGs are estimated and measured against the corresponding load to evaluate the possibility of restoring load points during an outage of the main supply. The proposed procedure of implementing DGs of intermittent behaviour is illustrated in Figure 3.4.

3.4.1 Wind System Model

To account for the intermittent behaviour of wind energy, a stochastic wind speed model is utilised to simulate the outputs of the WT system. This stochastic model is based on a simulation technique to describe the non-deterministic behaviour and the randomness of the wind speed, as presented in Section 2.7.1.1. The probability of occurrence of a particular wind speed is assumed as described by the two-parameter Weibull distribution. Further, a non-sequential MCS technique is utilised to generate random numbers which are converted to wind speed values which are then converted to output power, as described in Section 2.7.1.2.

Step by Step Approach to model WT Generation:

Step 1: Classify the Weibull parameters c and k, based on the average and standard deviation of wind speed.

Step 2: Generate a random number U following uniform distribution in the range [0, 1].

Step 3: Calculate the wind speed V_i by the use of Equation 2.32.

Step 4: Calculate the output power of the system by the use of the power characteristics of the WT given in Equation 2.33.
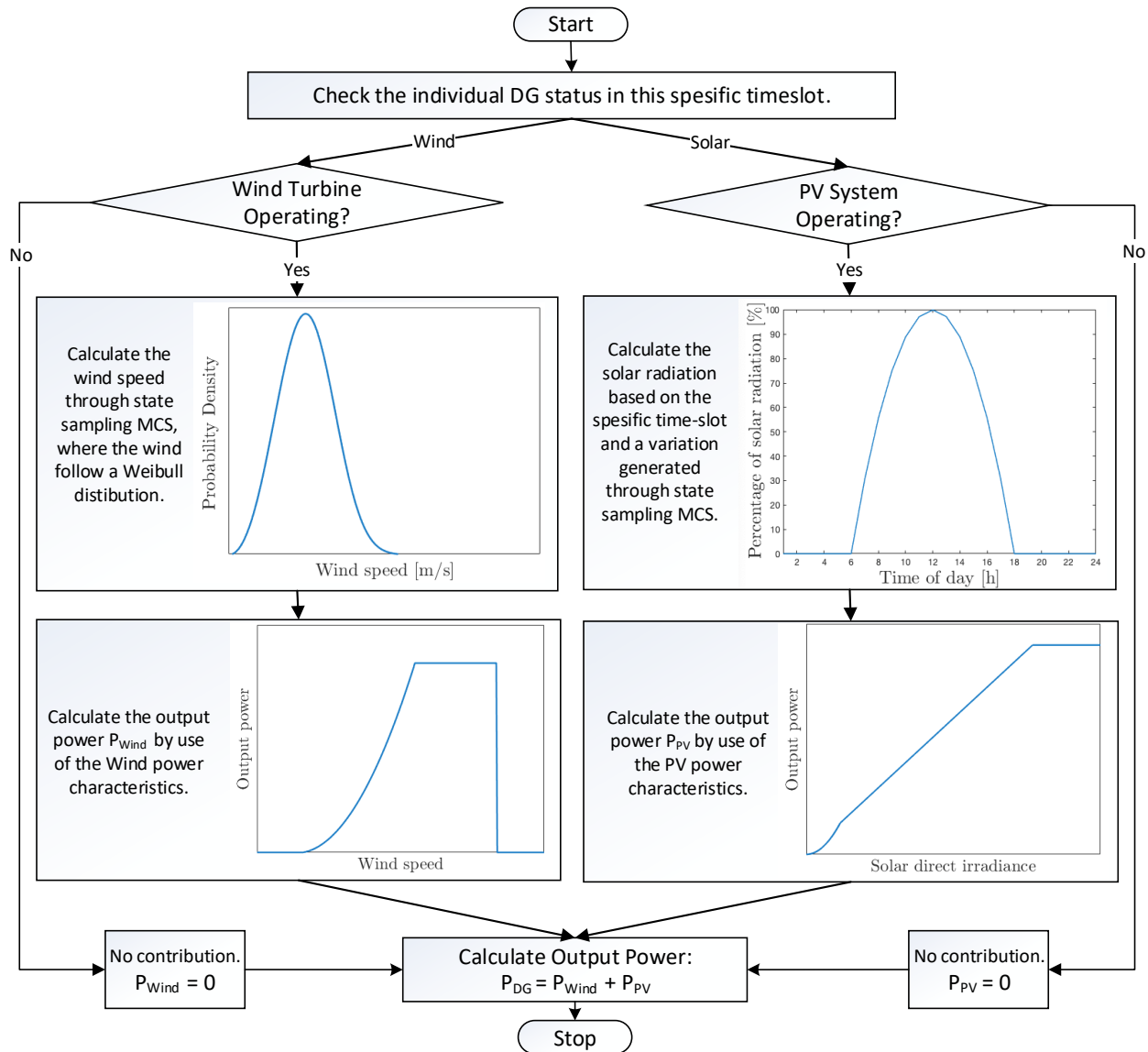
Figure 3.4: Procedure for evaluating the available output power of the considered DGs.

3.4.2 PV System Model

To model the production of the PV system, the hourly variation of solar radiation is simulated, based on the literature [36, 48, 49]. To account for the influence of cloud, temperature and other meteorological factors, which affect the amount of solar radiation accessed by the modules, a prediction error of the solar radiation is simulated following a normal distribution with zero expectation and constant variance, as described in Section 2.7.2.2.

Step by Step Approach to model PV Generation:

Step 1: Classify the month (1-12) and hour of day (1-24) for time t [1, 8736].

Step 2: Based on the month and hour of day, calculate the estimated solar radiation G_d by the use of Equation 2.37.

Step 3: Generate a random number representing attenuation ΔG following normal distribution.

Step 4: Calculate the total solar radiation G as the sum of G_d and ΔG, as in Equation 2.39

Step 5: Calculate the output power of the system by the use of the power characteristics of the PV module given in Equation 2.40.

3.5 Battery Energy Storage System Model

To smoothen the fluctuation of the output of the WT and PV systems, a BESS is implemented within the microgrid to improve the power quality and supply reliability, motivated by [51, 52]. By assuming a rather simple strategy, as presented in Equations 2.45 and 2.46, a battery is included to either release or restore the excessive energy when the microgrid is operating in island mode. Thus, when DGs' output is greater than the local load, residual power is stored in the battery; when DGs' output is less than load, the stored energy is released to supply the remaining load.

In this thesis, a generic battery storage system is developed, which serves the main purpose of this study. The system is considered charged by the main grid during interconnected mode and, thus, assumed to be fully charged when the microgrid goes into island mode.

Furthermore, in this thesis, it is assumed that if the production of the DGs plus the BESS discharging capacity is not sufficient to cover all the loads within the microgrid, then all the load points within the microgrid are considered unsupplied and the BESS is not discharged. This assumption differs from the operation shown in Equation 2.46. Hence, Equation 3.3 is presented

for the applied strategy of discharging the BESS in the microgrid.

$$P_t^{dch} = \begin{cases} P^{sur} & \text{if } P^{dch,max} < P_t^{sur} \leq \frac{E_t^{stored} - E^{reserve}}{\Delta t} \\ 0 & \text{else} \end{cases} \tag{3.3}$$

To account for the unavailability of the BESS in the simulations of the system, similar to the DG units, a failure rate and a repair time are modelled for the BESS.

3.6 Proposed Operating Strategy for Microgrids

A realistic, yet simple strategy for the operation of the microgrid is suggested and employed in this thesis. The managing strategy is tailored to fit distribution systems of radial structure, where the DERs are located in a sub-feeder. Therefore, the microgrid is modelled as a sub-feeder that can be isolated from the upstream network and operated in island mode independently during an emergency to supply its local load points.

For evaluating the reliability impact of adding a microgrid to the distribution system, operation-related questions need to be acknowledged. As there does not exist a defined strategy in the literature, this thesis suggests answers based on well-established assumptions and inspirations from [26, 57]. The strategy is essential for the thesis as it lays the foundation for the reliability evaluation of a distribution system with a microgrid.

The operation strategy is explained by Table 3.1 and Table 3.2, where the microgrid is isolated because of a failure on either a section on the main feeder or the sub-feeder. The operation of the DERs will only influence the load points within the microgrid during island mode operation, based on the assumption that the main supply is 100% reliable. Further, the constraints of the line capacities are neglected by the assumption of sufficient capacity for all scenarios. The DER units are assumed connected in series with fuses, which will immediately trip in the event of a failure of a DER unit. Accordingly, the failure of a DER unit will only impact the system if the failure occurs during island operation. The isolation process of the microgrid is assumed 100% reliable.

The entire distribution system including the microgrid is assumed equipped with disconnectors and fuses located in the sections and laterals, respectively. The disconnectors are set to operate with a switching time, while the fuses trip immediately in case of a failure of the respective component. Both the main feeders and sub feeders are equipped with a circuit breaker between themselves and the upstream network. The circuit breaker reacts instantly in case of a failure on the respective feeder. All the protection equipment is assumed 100% reliable.

Additional supply is assumed unavailable as it is common to model DER in a similar way as back-feed and, hence, it would overlook the impact of the DER. Based on these circumstances, the option for additional supply is not considered in this thesis. This may be recognised as a reasonable assumption, as microgrids are often suggested to be implemented in rural areas where the grid is weak.

Table 3.1: System components with time sequential simulated operation histories.

Location of failure	Failure of system component	Protection device operation	Microgrid operation
Main feeder	Section	Disconnects	Island mode
	Lateral	Fuse trips	Interconnected mode
	Transformer	Fuse trips	Interconnected mode
Microgrid Sub-feeder	Sub-section	Disconnects	Island mode
	Sub-lateral	Fuse trips	Interconnected mode
	Transformer	Fuse trips	Interconnected mode
	DER	Fuse trips	Only evaluated in island mode

Table 3.2: Strategy of microgrid operating in island mode.

Operation of the DER	Failure of a Section	Failure of a Sub-section
Up	The load points within the microgrid are served if production ≥ load.	After the failed part of the system is isolated, load points located upstream of the failure are reconnected with the main feeder while load points located downstream of the failure are supplied by the DERs if production ≥ load. The DERs are operated as additional supply.
Down	The load points within the microgrid are experiencing an outage duration equal the remaining operation in island mode.	The part supplied by the DERs are disconnected for the remaining repair time of the failed component.

During operating in island mode, the microgrid follows the strategy as explained in Table 3.2. In this case, the DER units are assumed placed at the end of the sub-feeder. This allows it to be evaluated as an additional supply when the production is sufficient to cover the local load points.

For a failure on the main feeder section, the location of the failure is relevant for the island process of the microgrid. If the failure occurs downstream of the microgrid connection on the main feeder, the microgrid is isolated until the failure is isolated (i.e., the switching time of the disconnector) and then reconnected to the main feeder. However, for a failure located upstream of the microgrid connection, the microgrid is isolated for the entire repair time of the failed section. As such, the microgrid is modelled similarly as a single load point from the perspective of the distribution system.

Further, the microgrid is assumed unable to perform black start. This implies that the DER units themselves are not able to restore the operation of the microgrid after a failure of the DERs without assistance from the utility grid.

The flow chart in Figure 3.5 is presented as a summary of the described operation strategy above in accordance with the procedure of the practised time-sequential MCS for evaluating distribution system reliability with an incorporated microgrid.
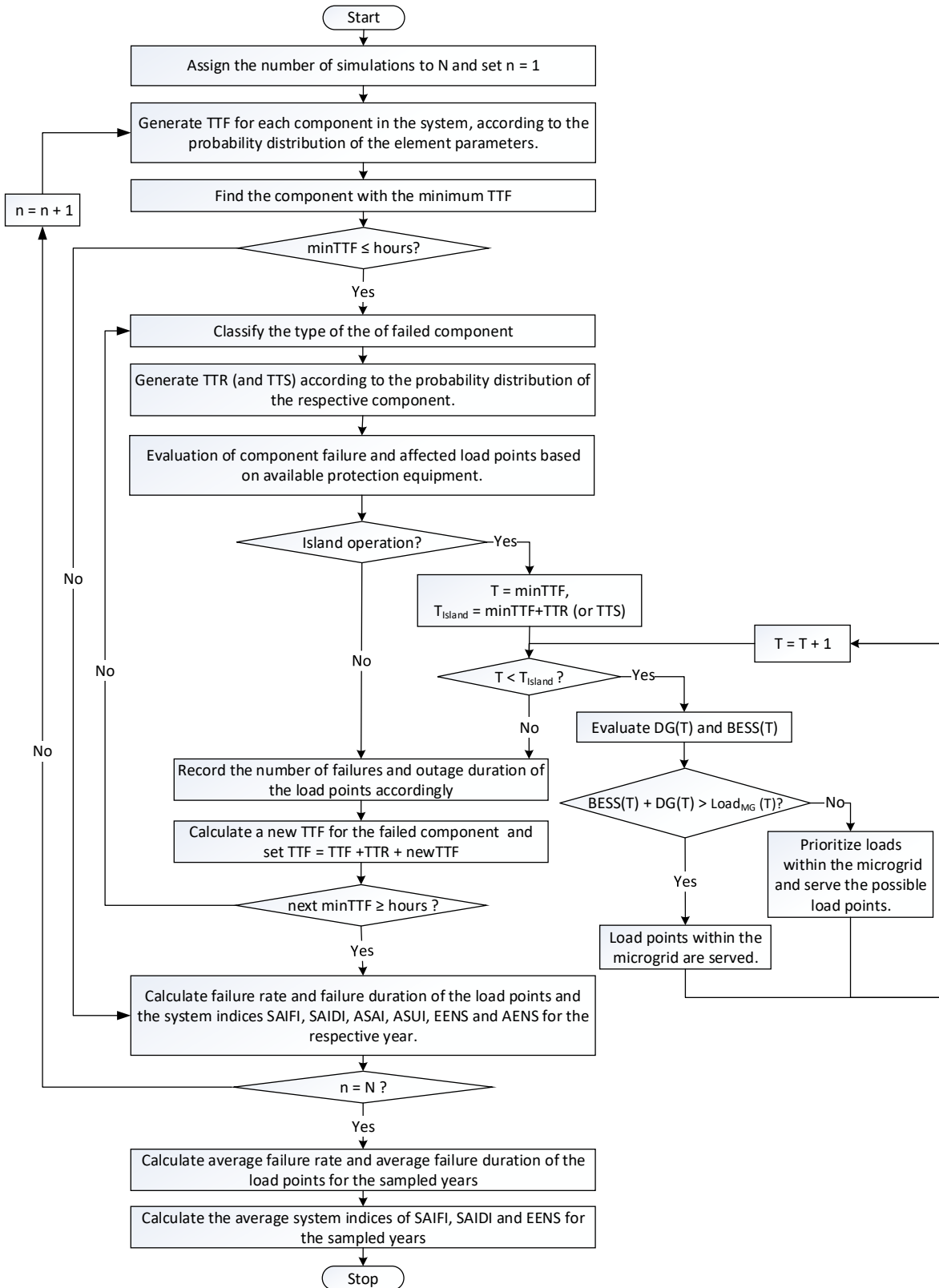
Figure 3.5: Algorithm used to evaluate the reliability of distribution system with microgrid.

Chapter 4

Description of the Simulation Program for Reliability Analysis of Passive Distribution Systems

This chapter contains a detailed description of the validation process conducted for passive distribution system reliability evaluation with the methodology as described in Section 3.1. The validation aspect is presented only for passive distribution systems as there are limited parameters given in the literature making it difficult to validate the work on systems with DERs.

Additionally, a description of how the input parameters are arranged in the developed MATLAB scripts are presented; this is applicable for the evaluation of both passive and active distribution system reliability. Finally, the effect of variable load consideration is represented through an illustrative example.

In the process of developing a suitable program, the focus was first on constructing a program suited for systems of simple structures and then on adding complexities. The program is developed to deal with reliability analysis of distribution systems with the structure of multiple single radial feeders. Subsequently, distribution systems of composite structure (such as the ones including sub-feeders) were studied. Thus, the developed program was modified to include sub-feeders and distinguish protection equipment. Suitable extensions have been made for studying the subsequent effect of adding a microgrid to the distribution system and detailed case studies conducted; these case studies are presented in the next chapter.

4.1   Classification of Input Variables

The MATLAB scripts are created with the objective of reading the required input parameters from an Excel sheet. Accordingly, the inputs are arranged in a simple structure in Microsoft Office Excel to include the parameters of the components as well as the system configuration. The system configuration is assumed pre-defined in the input data, as presented in Tables 4.1 to 4.6, with an aim to minimise the computation time. Depending on the structure of the system and the included gear (i.e., protection devices) in the analysis, the input parameters need to be modified. The reading to/from an Excel file minimises the work of changing the systems of interest due to the generalised code structure. Additionally, the procedure and results of the analytical analysis for each system are organised in the same Excel sheet thoroughly to establish a basis for comparison.

As mentioned before, the scripts are primarily developed to consider reliability analysis of distribution systems of multiple single radial feeders, such as Bus 2 (illustrated in Figure 4.2) and Bus 5 of RBTS. However, for studying the subsequent effect of adding a microgrid to the distribution system, Bus 6 of RBTS has been found to be more appropriate, as it includes several sub-feeders, which are suited for more complex analysis. As such, the Scripts are modified to include sub-feeders. Consequently, for distribution networks with defined sub-feeders (e.g., Bus 6), additional input variables needed to be defined as shown in Tables 4.3 and 4.5.

Table 4.1: Input data of the transformers.

Transformer number	Load point number
T1	LP_{T1}
T2	LP_{T2}
:	:
Tn	LP_{Tn}

Furthermore, parameters such as failure rates, repair times, switching time and the number of simulations need to be defined. In MCS, it is important to define a stopping criterion. In this work, the number of simulations has been carefully chosen such that the convergence is achieved and yields the desired level of accuracy [7, 31, 35].

Table 4.2: Input data of the laterals.

Lateral number	Length of lateral line [km]	Load point number
L1	l_{L1}	LP_{L1}
L2	l_{L2}	LP_{L2}
:	:	:
Ln	l_{Ln}	LP_{Ln}

Table 4.3: Input data of the sub-laterals.

Sub-lateral number	Length of sub-lateral line [km]	Sub-feeder number	Load point number
SL1	l_{SL1}	SF_{SS1}	LP_{SL1}
SL2	l_{SL2}	SF_{SS2}	LP_{SL2}
:	:	:	:
SLn	l_{SLn}	SF_{SSn}	LP_{SLn}

Table 4.4: Input data of the sections.

Section number	Length of section line [km]	Feeder number
S1	l_{S1}	F_{S1}
S2	l_{S2}	F_{S2}
:	:	:
Sn	l_{Sn}	F_{Sn}

Table 4.5: Input data of the sub-sections.

Sub-section number	Length of Sub-section line [km]	Feeder number	Sub-feeder number
SS1	l_{SS1}	F_{SS1}	SF_{SS1}
SS2	l_{SS2}	F_{SS2}	SF_{SS2}
:	:	:	:
SSn	l_{SSn}	F_{SSn}	SF_{SSn}

Table 4.6: Input data of the load points.

Load point number	From Section	To Section	Feeder number	Sub-feeder number	From Sub-section	To Sub-section	Average load [MW]	Peak load [MW]	Number of customers
LP1	S_{FLP1}	S_{TLP1}	F_{LP1}	SF_{LP1}	SS_{FLP1}	SS_{TLP1}	$P_{LP1,avg}$	$P_{LP1,peak}$	C_{LP1}
LP2	S_{FLP2}	S_{TLP2}	F_{LP2}	SF_{LP2}	SS_{FLP2}	SS_{TLP2}	$P_{LP2,avg}$	$P_{LP2,peak}$	C_{LP2}
:	:	:	:	:	:	:	:	:	:
LPn	S_{FLPn}	S_{TLPn}	F_{LPn}	SF_{LPn}	SS_{FLPn}	SS_{TLPn}	$P_{LPn,avg}$	$P_{LPn,peak}$	C_{LPn}

4.2 Validation with Benchmark Test Systems

To verify and validate the methods applied in this thesis work, both the analytical method and the time-sequential Monte Carlo method are utilised for the reliability evaluation of benchmark passive distribution systems. The analytical method was comprehensively studied in the specialisation project [8], which is applied in this thesis by replicating the results presented in [34] for Bus 2, in [33] for Bus 5 and in [31] for Bus 6 of the RBTS, for the respective system configurations.

The time-sequential MCS algorithm as described by the flow chart in Figure 3.1 constructs a fictive history of all the sections, laterals and transformers based on defined reliability data for the respective components and according to the probability distribution of the component parameters. These simulated histories are used to evaluate the number and duration of failures used to assess load point and system reliability indices.
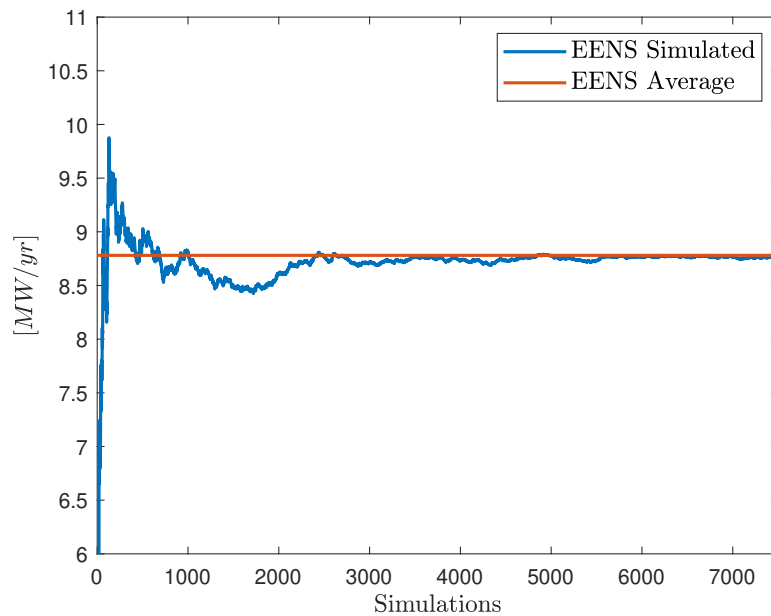

Figure 4.1: The converge process of the EENS index plotted together with the average value.

The convergence process of the indices is illustrated by visualising the index EENS throughout the simulations of the RBTS Bus 2, as illustrated in Figure 4.1. This figure presents the convergence process of the EENS for a simulation of 7,500 runs, where the index is converging after

approx. 6,000 simulation runs. Since some of the indices require a higher number of simulations to converge and the developed simulation program is not directly restricted by simulation time which is relatively low (< 10sec), a simulation run of 15,000 is further selected in this thesis work. This is also in agreement with a similar example presented in [31].

To optimise the algorithm, the line numbering of the original benchmark test systems were changed as illustrated in Figure 4.2 for Bus 2. The motivation was to construct appropriate input parameters to easily understand the system configurations, where all sections were numbered first, followed by the laterals. A similar rearrangement of the numbering is performed on the Bus 5 and Bus 6 systems.
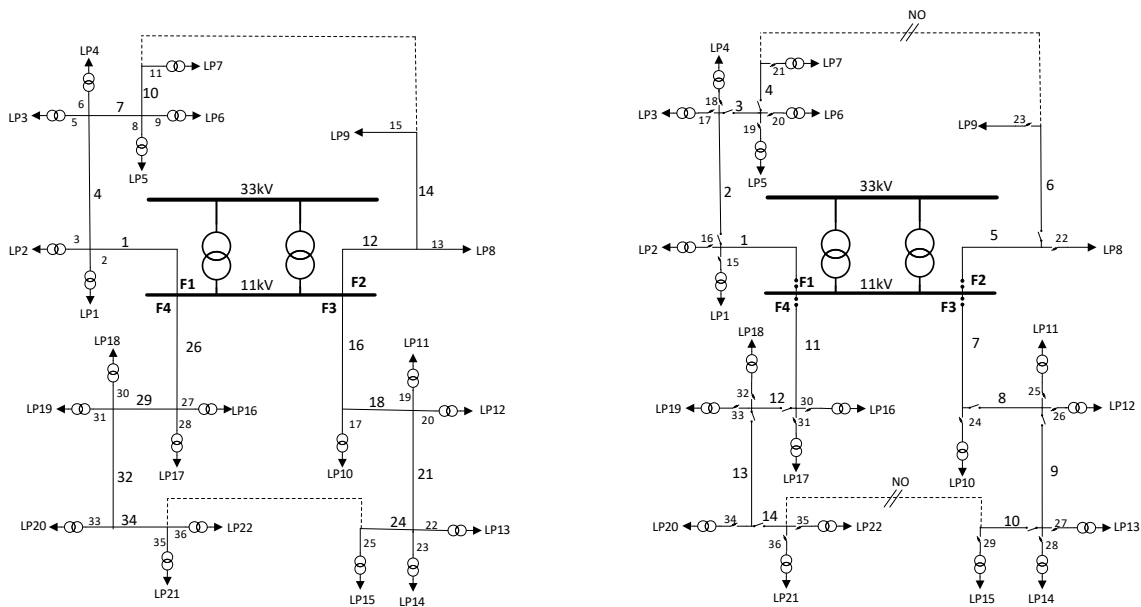
(a) Replicate of RBTS Bus 2 as in [34].   (b) RBTS Bus 2 with updated notation.

Figure 4.2: System configuration of Bus 2 of the RBTS.

The developed program is verified by comparing the average values of the load point and system reliability indices estimated by simulation with those obtained by utilising the analytical approach. As Bus 2 and Bus 5 are of similar structure (multiple single radial feeders), only the result of Bus 2 and 6 are presented in this section, whereas the result of Bus 5 is listed in Appendix C.2.

A selection of the results is presented in the following sections, whereas the entire analysis is given in Appendix. The load point indices presented in the following sections align with those of what is given in [34] and [31] for Buses 2 and 6, accordingly.

4.2.1 RBTS Bus 2

The distribution system for Bus 2 of RBTS is of radial structure and is supplied by two 33/11 kV transformers. The system includes 4 feeders, 14 sections, 22 laterals, 20 transformers and 22 load points supplying various kinds of customers. In this analysis, the system is configured to include circuit breakers in each feeder, a disconnector in each section, a fuse in each lateral and additional supply through back feeders as illustrated in the single line diagram in Figure 4.2b, which aligns the configuration in one of the cases (respectively Case E) presented in [34].

Representative average load point and system reliability indices are presented in Table 4.7 and Table 4.8 respectively, as a result of using both the analytical approach and the developed simulation program. The complete result of the load point indices for Bus 2 is presented in Appendix B.2. From this it can be observed that the results of the analytical and simulation techniques are quite close; the highest difference between the load point indices is 3.2712% for Load Point 18, and as regards the system reliability indices the maximum difference is 1.8877 % for SAIFI. Both errors are within an acceptable range, by comparing and validating with the simulation errors presented in [31] and [75].

Table 4.7: Comparison of selected load point indices for Bus 2.

Load Point	Average failure rate [f/yr]			Average outage duration [h/yr]		
no.	Analytical	Simulated	Difference [%]	Analytical	Simulated	Difference [%]
1	0.2393	0.2378	0.6061	0.7253	0.7371	-1.6285
4	0.2393	0.2369	0.9962	0.7253	0.7209	0.6072
8	0.1398	0.1424	-1.8962	0.5428	0.5493	-1.2134
12	0.2555	0.2511	1.7352	0.8065	0.8072	-0.0805
16	0.2523	0.2497	1.0241	0.7903	0.8102	-2.5263
18	0.2425	0.2371	2.2405	0.7285	0.7047	3.2712
20	0.2555	0.2481	2.8832	0.7935	0.7838	1.2293

Table 4.8: Comparison of the system reliability indices for Bus 2.

Indices	Analytical	Simulated	Difference [%]
SAIFI [int/yr· customer]	0.2482	0.2435	1.8877
SAIDI [h/yr· customer]	0.7656	0.7602	0.7033
CAIDI [h/int· yr]	3.0843	3.0557	0.9273
EENS [MWh/yr]	8.8438	8.8172	0.3013

4.2.2 RBTS Bus 6

Bus 6 of RBTS is a radial distribution system with four feeders, three sub-feeders, 29 sections, 13 sub-sections, 20 laterals, two sub-laterals, 36 transformers and 40 load points; resulting in 100 components that can theoretically fail during operation. This system, analysed in both [31] and [75], contains very specified configurations as illustrated in Figure 4.3. Whereas not all load points are connected through laterals, the location of disconnectors vary in the different feeders; only two feeders have additional supply and the analysis of Feeder 4 uses reliability data for the wrong voltage level when referring to the parameters listed in [34]. All these specialities, which are not clearly stated in the original analysis presented in [31], made the reproduction of the results utilising the analytical approach demanding. Hence, the simulation program utilised for these configurations became less general than the program obtained for RBTS Bus 2. Figure 4.3 matches the analysis of the configurations performed in [31].

Representative average load point and system reliability indices are represented in Table 4.9 and Table 4.10 respectively. The complete result of the load point indices for Bus 6 is presented in Appendix D.2. The maximum difference between reliability indices calculated based on the analytical approach and simulation approach is observed in the outage duration of Load Point 13 with a difference of 4.1354%. In terms of the system reliability indices, SAIFI is observed with the highest difference of 0.2394%. As with the evaluation of Bus 2 and Bus 5, these differences are within an acceptable range, which is deemed as a validation of the created MATLAB scripts.
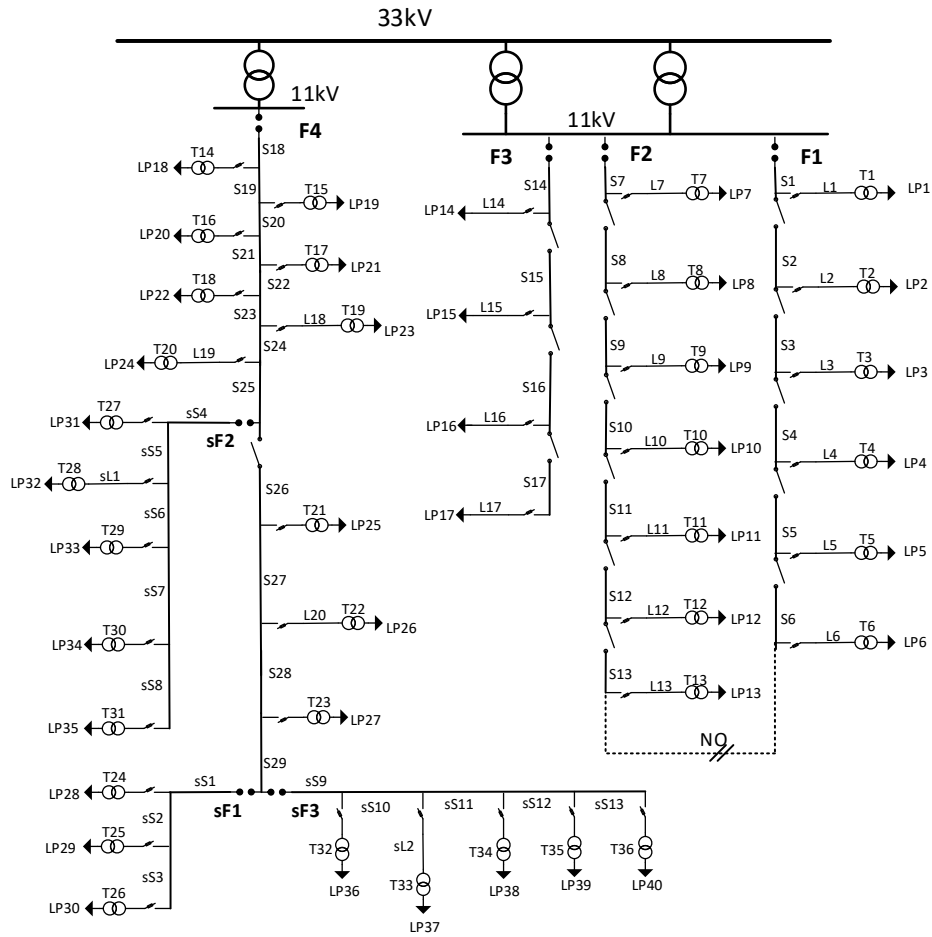
Figure 4.3: System configuration of RBTS Bus 6, as analysed in [31].

Table 4.9: Comparison of selected load point reliability indices for Bus 6.

Load Point	Average failure rate [f/yr]			Average outage duration [h/yr]		
no.	Analytical	Simulated	Difference [%]	Analytical	Simulated	Difference [%]
1	0.3303	0.3365	-1.9026	0.8163	0.8347	-2.2590
5	0.3400	0.3429	-0.8628	0.8260	0.8388	-1.5431
10	0.3595	0.3618	-0.6398	0.8065	0.8160	-1.1782
15	0.2373	0.2314	2.4658	0.8353	0.8189	1.9608
20	1.6725	1.6743	-0.1056	5.5515	5.5741	-0.4064
25	1.6725	1.6726	-0.0060	8.4375	8.4384	-0.0106
30	2.2250	2.2220	0.1348	11.200	11.2170	-0.1521
35	2.5370	2.5502	-0.5203	9.8740	9.9894	-1.1683
40	2.5110	2.5094	0.0637	12.6300	12.6450	-0.1172

Table 4.10: Comparison of the system reliability indices for Bus 6.

Indices	Analytical	Simulated	Difference [%]
SAIFI [int/yr· customer]	1.0065	1.0090	-0.2394
SAIDI [h/yr· customer]	3.8197	3.8280	-0.2167
CAIDI [h/int· yr]	3.7950	3.7939	0.0290
EENS [MWh/yr]	49.2040	49.3060	-0.2071

The main motivation of analysing Bus 6 is to construct a simulation program that includes sub-feeders. As the special configurations of RBTS Bus 6 used in [31] are of little importance when studying the problem statement of this thesis, the system is modified by aligning the configurations to generalise the code after validating the simulation for the respective configurations. A detailed description of the modification conducted is presented in Appendix D.3.

4.2.3   Illustrative Example of Variable Load Model

To present the impact of including variable load on the reliability indices, a comparative study on the modified Bus 6 system is carried out using the simulation approach. For this, the load values in [31] used for the verification are replaced with the load variables from [74], which accommodate both average, peak and variable load values. Note that the average load values in [74] differ from the presented values in [31]. A complete description of the modifications conducted and the system can be found in Appendix D.3.

The difference between the studies with constant and variable load is reflected in the system index EENS. Equation 4.1 shows the calculation of EENS where fixed average load values are used, while Equation 4.2 shows the calculation of EENS with variable load values based on Equation 3.1 where T_O indicates the outage time of load point i.

$$\text{EENS} = \sum_i P_{Li,avg} \cdot U_i \tag{4.1}$$

$$\text{EENS} = \sum_i \sum_{T_o} W_w(w) \cdot W_d(d) \cdot W_h(h) \cdot P_{Li,peak} = \sum_i \sum_{T_o} P_{Li}(T_o) \tag{4.2}$$

It is important to note that there are different ways to calculate EENS using average peak loads in the simulation approach. One way is to use the analytical technique and calculate EENS by using the simulated average unavailability as shown in Equation 4.1. In fact, this is quite adequate if only the average values of the system indices are required. On the other hand, when dealing with variable loads, the respective time t (see Equation 3.1) has to be considered. This is accounted for in the approach summarising the load at time t over the whole outage duration as shown in Equation 4.2, for variable load values. Because of the need to round the simulated time t to whole hours, some errors will arise for the latter technique. Therefore, there will always be a difference when comparing the calculated EENS of the two approaches.

To illustrate this and the impact of including variable load in the reliability analysis, Table 4.11 shows the results for EENS with average loads using the two techniques and the result for EENS with variable loads for Bus 6 with load data as presented in Appendix E. In this table, (T1) represents the first technique that uses the analytical method with average values to calculate EENS and (T2) represents the latter technique that summarises the load during the outage duration of the load points. Consequently, the reliability characteristics of a system may change throughout the days of the year.

Table 4.11: Comparison of system index EENS of Bus 6.

	Average peak load (T1)	Average peak load (T2)	Difference [%]	Variable peak load (T2)
EENS [MWh/yr]	76.3490	78.9677	-3.4299	67.8878

Chapter 5

Case Studies

Suitable extensions have been made to the programs described in Chapter 4 for studying the subsequent effect of adding a microgrid to the distribution system. Detailed case studies have been conducted and presented in this chapter. The following four cases are studied:

Case 1: Passive distribution system (referred to as "Base case").

Case 2: Active distribution system including a microgrid with DG (PV and WTG).

Case 3: Active distribution system including a microgrid with DG (PV and WTG) and prioritised loads.

Case 4: Active distribution system including a microgrid with DG (PV and WTG) and ESS (battery).

All four case studies are performed on the same test system: a modified Bus 6 system of the RBTS, where DERs are added into the existing system to create a defined microgrid configuration. To identify the characteristics of the different cases, load point-, distribution system- and microgrid system reliability indices are assessed and analysed. In addition, a sensitivity analysis of Case 4 is performed to observe the effect of DER (DG + BESS) placement and BESS sizing in the defined microgrid.

The estimates of the reliability indices are obtained by calculating the average values through 15,000 simulation runs. The specifications and observations of the study are stated below.

5.1 Description of Test System

The study is performed on the RBTS Bus 6 [33]. Since the radial main feeders in a distribution system are analysed individually (due to the installed circuit breakers), the impact of adding a microgrid in one radial feeder would not affect the neighbour feeders when the possibility of re-configuration is neglected. Hence, to concentrate the study, evaluation of only Feeder 4 of the Bus 6 system is highlighted. Additionally, the test system is modified from its original configurations, illustrated in Figure 4.3, to a more generalised configuration by adding sufficient protection devices as described in Section 2.3.2. Accordingly, the analysed system consists of one main feeder, 12 main sections, 10 laterals, three sub-feeders, 13 sub-sections, 13 sub-laterals and 23 low voltage transformers connected to 23 load points as illustrated in Figure 5.1. The system consists of a total of 1183 customers sharing a peak load of 10.9284 MW. A complete description of the modifications conducted and the system can be found in Appendix D.3.
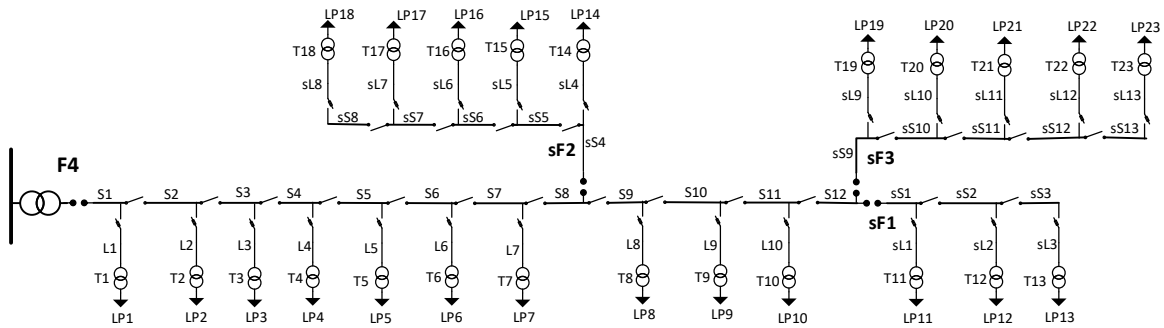

Figure 5.1: System configuration of modified Feeder 4, Bus 6 of the RBTS.

5.1.1 Load data

The required load data used in this case study is presented in Appendix E. Here, average load values and peak load values are listed; where the latter is used in the variable load model as presented in Section 3.2. The applied load parameters for creating a variable load model are sourced from [74], as [33] does not provide a variable load model.

Thus, in this thesis, it is assumed a deterministic behaviour of the varying load during the year following a chronological load model. Moreover, it is assumed that all load points of the distribution network follow the same profile, with different defined annual peak loads collected from [33].

5.1.2 Distributed Energy Resources

In order to evaluate the reliability impact of including DERs in the distribution system, the proposed strategy of the operation of the DERs given in Section 3.4 is used. In this thesis work, the DER units are modelled similar to a back-feed with transfer restriction equal to the DER unit capacity and located at the end of the feeder. The DER units are integrated through a fuse as illustrated in Figure 2.1.

As there are no definite parameters for failure rates and repair times of DG based on RES and BESS presented in the literature, a proposal of somewhat realistic values are presented in this thesis, based on mainly values presented in [54] with support from [48, 57, 58]. The applied reliability indices of the studied DER systems are given in Table 5.1, where the PV system is assumed consisting of PV, converter and inverter; WT system is assumed consisting of WT, boost converter and inverter; BESS is assumed consisting of a battery, battery controller/charger and inverter.

Table 5.1: Reliability indices of components of the DER systems [54].

Description	Failure rate [f/yr]	Repair time [h/f]
WT	0.0500	20.00
PV	0.0200	18.25
Battery	0.0312	51.96
Battery controller/charger	0.1250	45.21
Inverter	0.1430	52.14
Boost converter	0.0657	62.50
Converter AC/DC	0.1520	55.23
PV System (PV + converter + inverter)	**≈ 0.25**	**≈ 41**
WT System (WT + boost converter + inverter)	**≈ 0.35**	**≈ 43**
BESS (Battery + controller + inverter)	**≈ 0.30**	**≈ 49**

The maximum output power of the WT and PV systems are 3 MW and 2 MW, respectively. These ratings are selected considering that the capacity factors of DGs based on RES are quite low. Hence, the combined rated power of all DGs is higher than the total peak load in the micro-grid (i.e., "sF2"), which is approximately 2.4 MW at its highest. The BESS is considered with an installed capacity of 1 MW, a storage volume of 5 MWh and a minimum reserve of 20% of the storage volume (i.e., 1 MWh), based on the work conducted in [51].

Wind Turbine Generation Specifications

In general, wind generation unit modelling depends on the available historical data for a specified site. However, the objective of this project is not to evaluate the on-site reliability but to consider the algorithm used to model the reliability contribution of the intermittent DGs. Hence, somewhat generalised wind parameters are applied in this thesis, extracted from [56, 76]. These are presented in Table 5.2. The output generation of the wind system is modelled as presented in Section 2.7.1 under the assumption that the wind speed obeys a Weibull distribution and that the wind system is simulated as a single wind power unit with an installed capacity equal to the total wind farm capacity.

Table 5.2: Wind speed and wind turbine parameters; extracted from [56, 76].

Average wind speed (v_{avg}) [m/s]	Standard deviation of wind speed (σ) [m/s]	Cut-in speed (v_{ci}) [m/s]	Rated speed (v_r) [m/s]	Cut-out speed (v_{co}) [m/s]
7.5	2.6	3	12	25

PV Generation Specifications

Similar to wind generation, the generation of PV modules depends on location. Distribution of average largest received solar radiation data for each month based on [48] is applied in this work as given in Table 5.3.

Table 5.3: Percentage of solar radiation distribution in every month.

Jan [%]	Feb [%]	Mar [%]	Apr [%]	May [%]	Jun [%]	Jul [%]	Aug [%]	Sep [%]	Oct [%]	Nov [%]	Dec [%]
51.8	62.7	76.9	89.6	97.3	100.0	98.3	91.9	80.7	66.5	54.0	48.3

By utilising these solar radiation parameters and Equation 2.37, an estimate of the hourly solar radiation received by the PV modules for the different months are illustrated in Figure 5.2. The output generation of the PV system is modelled as presented in Section 2.7.2 under the assumption that the solar farm is simulated as a single PV unit with an installed capacity equal to the total solar farm capacity.
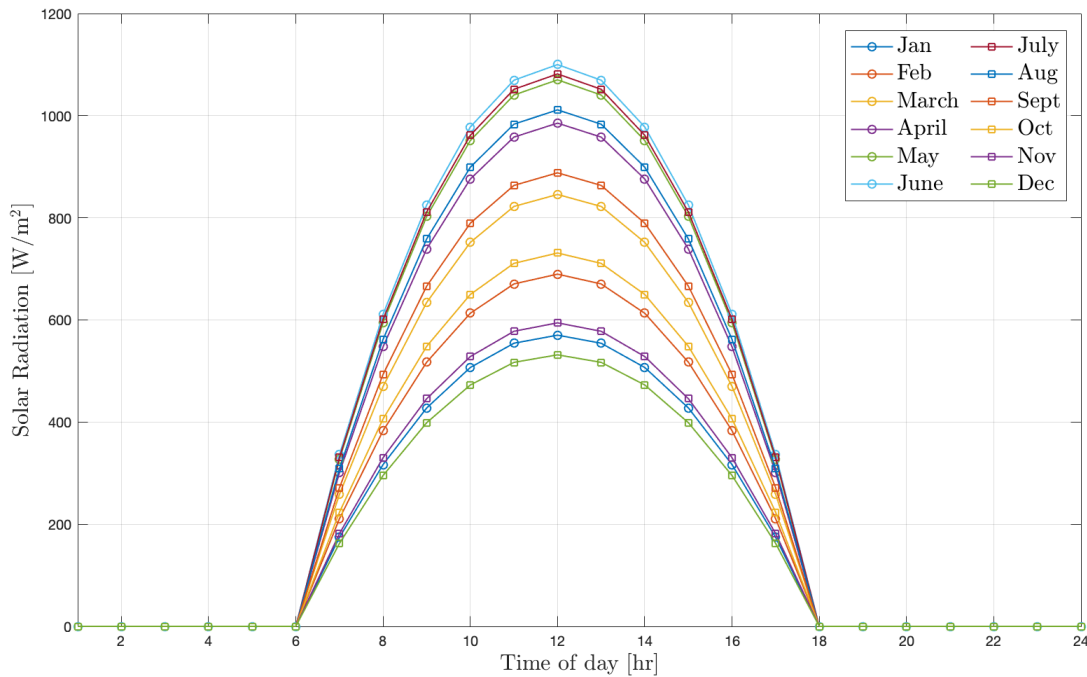

Figure 5.2: Hourly estimate of solar radiation of each month.

BESS Specifications

To reduce the power outage time and increase the efficiency of the microgrid system, an ESS can be implemented. In Case 4, a generic BESS is implemented for the RES to act more flexible, based on the strategy described in Section 3.5. In this thesis, the charge and discharge capacities are assumed equal to the installed capacity, and it is assumed that the BESS is completely charged at the start of each island mode operation.

5.1.3 Prioritised Loads

Load prioritisation is considered for the load points within the defined microgrid when operating in island mode. The procedure of prioritising loads is described in Section 3.3.

To implement a reasonable strategy for this in the reliability judgement, a prioritisation matrix P is defined for the load points within the microgrid (i.e., load points 14-18), each with a weighted factor in the range of [0,1] indicating its priority, 1 being the highest priority:

$$P = \begin{bmatrix} 14 & 1.0 \\ 15 & 0.8 \\ 16 & 0.6 \\ 17 & 0.4 \\ 18 & 0.2 \end{bmatrix} \tag{5.1}$$

5.2 Case 1: Passive Distribution System

This section presents the conducted reliability assessment for the modified Feeder 4 when operating as a passive distribution system, as shown in Figure 5.1. For this case study, the results obtained with the analytical method and with MCS are presented. As the main objective of this case is to establish a base case for further comparison with the other cases, the results of the MCS are compared with the results of the analytical method for validation. Note that the results of this analysis differ from the results obtained in Chapter 4 due to the modified configurations described in Section 5.1. Additionally, probability distributions of the reliability indices are presented in Appendix F.

The estimates of the load point reliability indices such as average failure rate and outage duration for both methods are listed in Table 5.4. Additionally, the difference between the analytical and the simulation estimates are given; the maximum difference in the indices is 1.0892% for Load Point 12. The errors between the methods are within an acceptable range and, therefore, negligible as discussed in Chapter 4. Based on this, the simulated model of the system is confirmed to be correctly implemented with respect to the conceptual model.

The resulting distribution system reliability indices SAIFI, SAIDI, CAIDI and EENS are shown in Table 5.5 from the analytical method and MCS, along with the percentage difference. Similar to load point indices, the difference in the system indices is considered negligible. The EENS-index is calculated for both methods with average load and with variable load, as explained in Section 4.2.3. Whereas the average load is used for comparing the MCS with the analytical method, the variable load is used in MCS for comparison in the following cases.

As the Sub-feeder 2, noted "sF2" in Figure 5.1, is referred to as a microgrid in the further case studies, the system reliability indices of Sub-feeder 2, MAIFI, MAIDI, MCAIDI and EENS are presented in Table 5.6; performed to present a baseline used to explore the effect of defining this part as a microgrid in the following cases.

Table 5.4: Load point reliability indices of Base Case.

Load point no.	Average failure rate [f/yr]			Average outage duration [h/yr]		
	Simulation	Analytical	Difference [%]	Simulation	Analytical	Difference [%]
1	1.6999	1.7115	0.6797	2.7357	2.7305	-0.1918
2	1.7125	1.7213	0.5103	3.4427	3.4293	-0.3909
3	1.7024	1.7115	0.5317	3.7914	3.7965	0.1352
4	1.7036	1.7115	0.4616	4.0520	4.0305	-0.5344
5	1.7033	1.7115	0.4772	4.4587	4.4465	-0.2744
6	1.7016	1.7115	0.5784	5.1048	5.0965	-0.1637
7	1.7018	1.7115	0.5668	5.4917	5.5125	0.3782
8	1.7009	1.7115	0.6174	6.5123	6.5785	1.0065
9	1.7021	1.7115	0.5512	7.2784	7.3065	0.3841
10	1.7031	1.7115	0.4927	8.1775	8.2165	0.4752
11	2.2533	2.2770	1.0423	9.8778	9.9780	1.0045
12	2.2522	2.2770	1.0892	10.6992	10.8100	1.0251
13	2.2577	2.2770	0.8491	11.3515	11.3950	0.3818
14	2.5891	2.5890	-0.0051	7.5579	7.5080	-0.6647
15	2.5865	2.5890	0.0953	7.9483	7.9240	-0.3072
16	2.5845	2.5890	0.1725	8.6588	8.6520	-0.0788
17	2.5886	2.5890	0.0154	9.3243	9.3020	-0.2393
18	2.5859	2.5890	0.1184	10.1457	10.1340	-0.1155
19	2.5483	2.5630	0.5722	10.1986	10.2640	0.6373
20	2.5449	2.5598	0.5788	10.8629	10.8978	0.3201
21	2.5501	2.5630	0.5046	11.3015	11.3300	0.2512
22	2.5535	2.5630	0.3694	12.1267	12.1620	0.2906
23	2.5490	2.5630	0.5462	12.8344	12.8900	0.4316

Table 5.5: Distribution system indices of Base Case.

System Index	Simulation	Analytical	Difference [%]
SAIFI [int/yr·customer]	2.0071	2.0180	0.5402
SAIDI [h/yr·customer]	6.7466	6.7658	0.2845
CAIDI [h/int]	3.3613	3.3527	-0.2571
EENS (Average load) [MWh/yr]	66.4914	63.7982	-4.2215
EENS (Variable load) [MWh/yr]	57.2687	-	-

Table 5.6: System reliability indices of Sub-feeder 2 (denoted as future microgrid) of Base Case.

MAIFI [int/yr·customer]	MAIDI [h/yr·customer]	MCAIDI [int/yr]	EENS [MWh/yr]
2.5869	8.1175	3.1379	13.9830

5.3 Case 2: Active Distribution System with Microgrid Including DGs

As it is of interest to study the impact a microgrid has on the distribution system reliability, a further study is carried out on the modified Feeder 4, where Sub-feeder 2 is modelled as a microgrid with local DGs based on WT and PV. The new system configuration is illustrated in Figure 5.3. The operation strategy of the defined microgrid follows the description in Section 3.6.
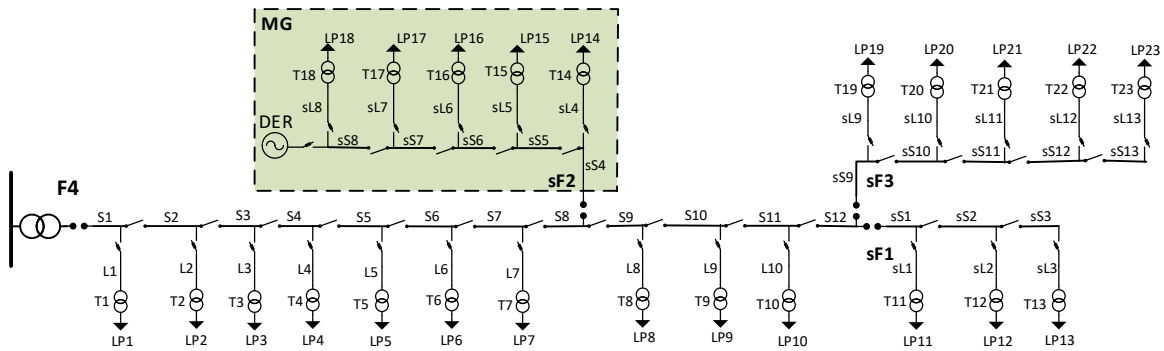

Figure 5.3: System configuration of modified Feeder 4, Bus 6 of the RBTS, where Sub-feeder 2 is defined as a microgrid.

The load point reliability indices for Case 2 are listed in Table 5.7. The estimates of the distribution system reliability indices are presented in Table 5.8 and the microgrid system reliability indices are given in Table 5.9. Similar to Case 1, the indices MAIFI, MAIDI, MCAIDI and EENS are evaluated. In addition, island mode-oriented indices such as IOSR, ILOLP and MIOP are included. Additionally, probability distributions of the reliability indices are presented in Appendix G.

The impact of implementing a microgrid in the distribution system is discussed in Section 5.6.2, by comparing Case 2 and Case 1.

Table 5.7: Load point reliability indices of Case 2.

Load point no.	Average failure rate [f/yr]	Average outage duration [h/yr]
1	1.7202	2.7273
2	1.7265	3.4281
3	1.7216	3.8621
4	1.7187	4.0756
5	1.7183	4.4948
6	1.7181	5.1898
7	1.7190	5.5603
8	1.7197	6.6440
9	1.7152	7.4006
10	1.7208	8.3075
11	2.2858	10.1783
12	2.2819	10.9620
13	2.2850	11.5844
14	2.0703	5.1776
15	2.0652	5.0959
16	2.0666	5.5818
17	2.0682	5.7668
18	2.0689	6.1060
19	2.5697	10.5353
20	2.5728	11.1998
21	2.5723	11.5990
22	2.5729	12.3511
23	2.5738	13.0524

Table 5.8: Distribution system reliability indices of Case 2.

SAIFI [int/yr·customer]	SAIDI [h/yr·customer]	CAIDI [int/yr]	EENS [MWh/yr]
1.9549	6.4852	3.3174	52.7269

Table 5.9: Microgrid system reliability indices of Case 2.

MAIFI [int/yr·customer]	MAIDI [h/yr·customer]	MCAIDI [int/yr]	EENS [MWh/yr]	IOSR [%]	ILOLP [%]	MIOP [%]
2.0684	5.3811	2.6015	8.9574	56.35	43.65	0.10

5.4   Case 3: Active Distribution System with Microgrid and Prioritised Loads

The modelled local generations are highly unreliable and cannot supply all of the load points inside the microgrid continuously when requested. To account for this, an extension of Case 2 is assessed by including the ability to prioritise load points inside the microgrid during island mode operation. The strategy implemented is as described in Sections 3.3, where the local DGs are modelled to supply the load with the highest priority first followed by the next load in the priority list and so on. Table 5.10 presents the load points reliability indices for the case with included prioritising of load points. Additionally, probability distributions of the reliability indices are presented in Appendix H.

As a consequence of the implemented strategy where the load points closest to the circuit breaker are defined with higher priority, the main effect is also reflected in these load points (14-15). Thus, when moving downstream on the feeder, the reliability performance decreases as the DGs are not able to supply all load points inside the microgrid. By reviewing the microgrid load points 14-18, one may notice a distinct difference in the indices, especially in the outage duration. Load Point 14 experiences a relatively lower outage duration of 2.7051 h/yr compared to Load Point 18 with an outage duration of 6.0095 h/yr, which is a direct consequence of defining load point 14 with the highest priority and load point 18 with the lowest. There is also a recognisable difference in the failure rates; whereas load point 14 has a failure rate of 1.3469 failures/yr, load point 18 has a failure rate of 2.0525 failures/yr.

The distribution- and microgrid system reliability indices for Case 3 are presented in Table 5.11 and Table 5.12, respectively. The impact of prioritising loads within the microgrid is discussed in Section 5.6.3, by comparing Case 3 and Case 2.

Table 5.10: Load point reliability indices of Case 3.

Load point no.	Average failure rate [f/yr]	Average outage duration [h/yr]
1	1.7009	2.7399
2	1.7131	3.4032
3	1.7039	3.8007
4	1.7042	3.9608
5	1.7065	4.4201
6	1.7029	5.0740
7	1.7036	5.5224
8	1.7016	6.5526
9	1.7015	7.2983
10	1.7037	8.1890
11	2.2674	10.0705
12	2.2689	10.8470
13	2.2636	11.4140
14	1.3469	2.7051
15	1.5755	3.0396
16	1.6731	3.7451
17	1.8772	4.7593
18	2.0525	6.0095
19	2.5611	10.4684
20	2.5572	11.0628
21	2.5644	11.5352
22	2.5594	12.2477
23	2.5609	12.9878

Table 5.11: Distribution system reliability indices of Case 3.

SAIFI [int/yr·customer]	SAIDI [h/yr·customer]	CAIDI [int/yr]	EENS [MWh/yr]
1.8678	6.1356	3.2849	50.4531

Table 5.12: Microgrid system reliability indices of Case 3.

MAIFI [int/yr·customer]	MAIDI [h/yr·customer]	MCAIDI [int/yr]	EENS [MWh/yr]	IOSR [%]	ILOLP [%]	MIOP [%]
1.5131	3.2414	2.1422	7.0504	56.55	43.45	0.10

5.5 Case 4: Active Distribution System with Microgrid Including DGs and ESS

Storage systems are usually configured with intermittent generation such as WT and PV to smooth the fluctuations of these DERs' output. Thus, a hybrid system consisting of WT, PV and ESS systems is proposed to enhance the power supply reliability in microgrid and, hence, in the distribution system. In other words, an extension of Case 2 is conducted by including a BESS in the same sub-section as the DGs within the microgrid, based on the strategy described in Section 3.5. The load point reliability indices conducted through Case 4, are listed in Table 5.13. Additionally, probability distributions of the reliability indices are presented in Appendix I.

Table 5.13: Load point reliability indices for Case 4.

Load point no.	Average failure rate [f/yr]	Average outage duration [h/yr]
1	1.7095	2.7442
2	1.7184	3.4119
3	1.7052	3.8112
4	1.7067	4.0421
5	1.7043	4.4419
6	1.7097	5.1258
7	1.7091	5.4907
8	1.7041	6.5559
9	1.7111	7.2674
10	1.7081	8.2272
11	2.2662	10.1062
12	2.2701	10.9073
13	2.2663	11.5004
14	1.5404	3.3445
15	1.5403	3.0445
16	1.5400	3.3369
17	1.5443	3.2868
18	1.5373	3.4321
19	2.5585	10.4786
20	2.5520	11.0648
21	2.5561	11.4656
22	2.5599	12.2255
23	2.5588	12.8774

The distribution- and microgrid system reliability indices for Case 4 are presented in Table 5.14 and Table 5.15, respectively. The impact of supporting the RES with BESS is discussed in Section 5.6.4, by comparing Case 4 and Case 2.

Table 5.14: Distribution system reliability indices of Case 4.

SAIFI	SAIDI	CAIDI	EENS
[int/yr·customer]	[h/yr·customer]	[int/yr]	[MWh/yr]
1.8740	6.1671	3.2910	48.8607

Table 5.15: Microgrid system reliability indices of Case 4.

MAIFI	MAIDI	MCAIDI	EENS	IOSR	ILOLP	MIOP
[int/yr·customer]	[h/yr·customer]	[int/yr]	[MWh/yr]	[%]	[%]	[%] [p.u.]
1.5402	3.3391	2.1680	5.5212	84.47	15.53	0.10

5.6 Comparison and Discussion

This section presents a comparison of the different cases, followed by a discussion of the performed research. Load point-, microgrid- and distribution system reliability indices are presented to achieve a sufficient analysis of the performed case studies.

Consistently, failure frequency and outage duration probability distribution of Load Point 14 is highlighted throughout this section to explore the different considerations.

The trends in the load point reliability indices are discussed based on the defined system configuration. The impact of implementing microgrid to the distribution system is discussed by comparing Case 1 and Case 2. The effect of prioritising loads is addressed by comparing Case 2 and Case 3, while the effect of facilitating the RES with a BESS is discussed by comparing Case 2 and Case 4.

Load Point Reliability Indices

The most significant effect is experienced by comparing the load point reliability indices of the four cases as illustrated by Figure 5.4, including the failure rate (Figure 5.4a), outage duration (Figure 5.4b) and EENS (Figure 5.4c) for every load point in the system.
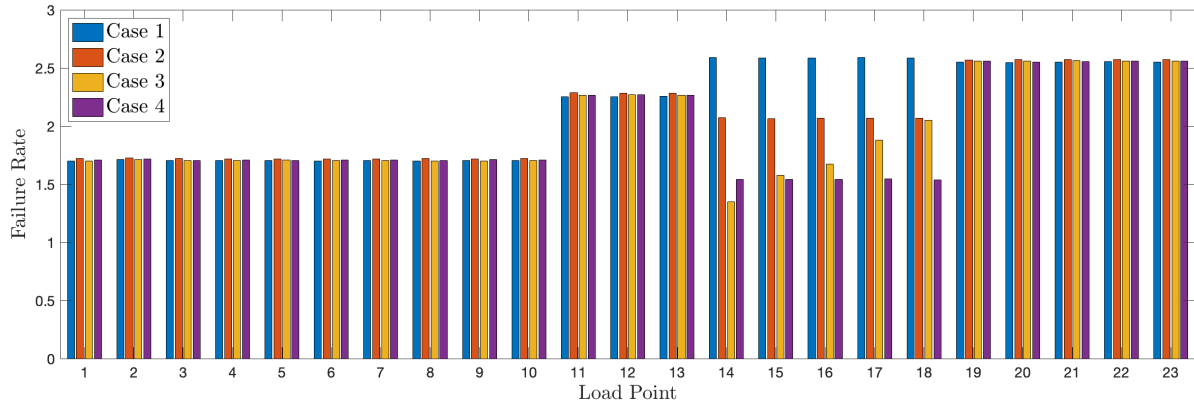
(a) Failure rate for load points.
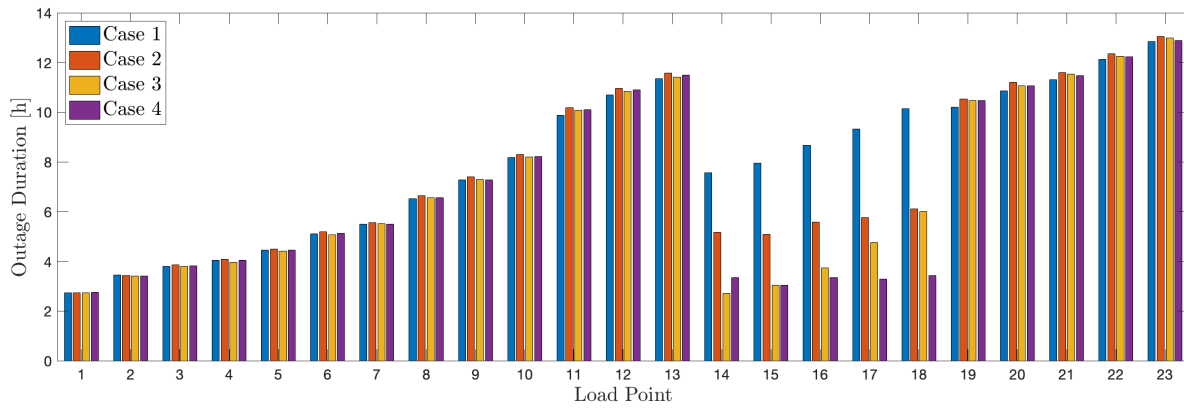
(b) Outage duration for load points.
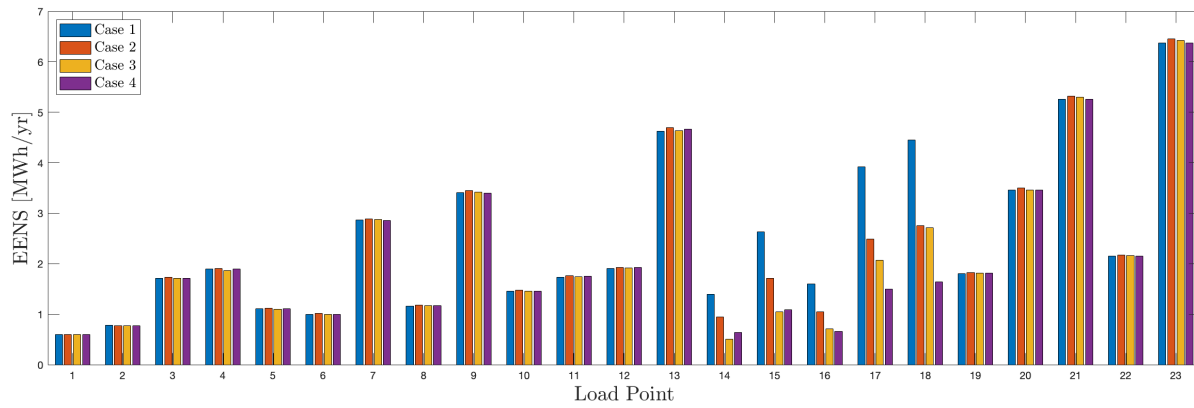
(c) EENS for load points.

Figure 5.4: Comparison of load points reliability indices.

Microgrid Reliability Indices

The microgrid reliability indices MAIFI, MAIDI, MCAIDI and EENS, for the four cases are compared in Figure 5.5. These indices pertain to Sub-Feeder 2 which is where the cases are distinct. Hence, the local system indices show variation with a clear pattern between the cases.

(a) MAIFI

(b) MAIDI

(c) MCAIDI
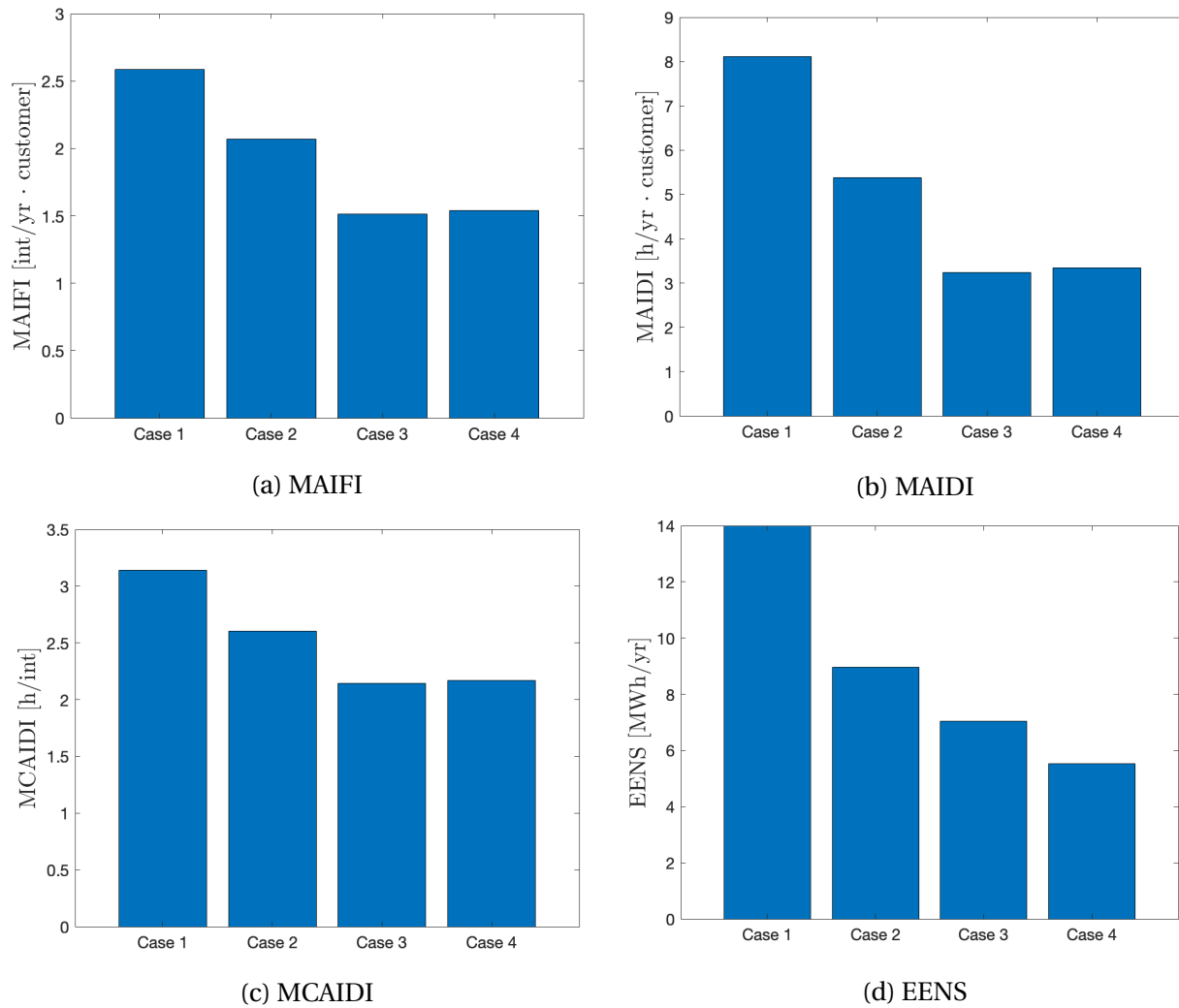
(d) EENS

Figure 5.5: Comparison of microgrid system reliability indices.

System Reliability Indices

An overall comparison of the four cases is presented by comparing the four system reliability indices; SAIFI, SAIDI, CAIDI and EENS for the distribution system in Figure 5.6. As the microgrid only serves 13.27% of the total customers, an improvement in the reliability of these customers has a negligible effect on the overall system reliability. A zoom function is used when displaying the customer-oriented indices in Figures 5.6a, 5.6b and 5.6c to illustrate the differences among the cases.

(a) SAIFI

(b) SAIDI

(c) CAIDI
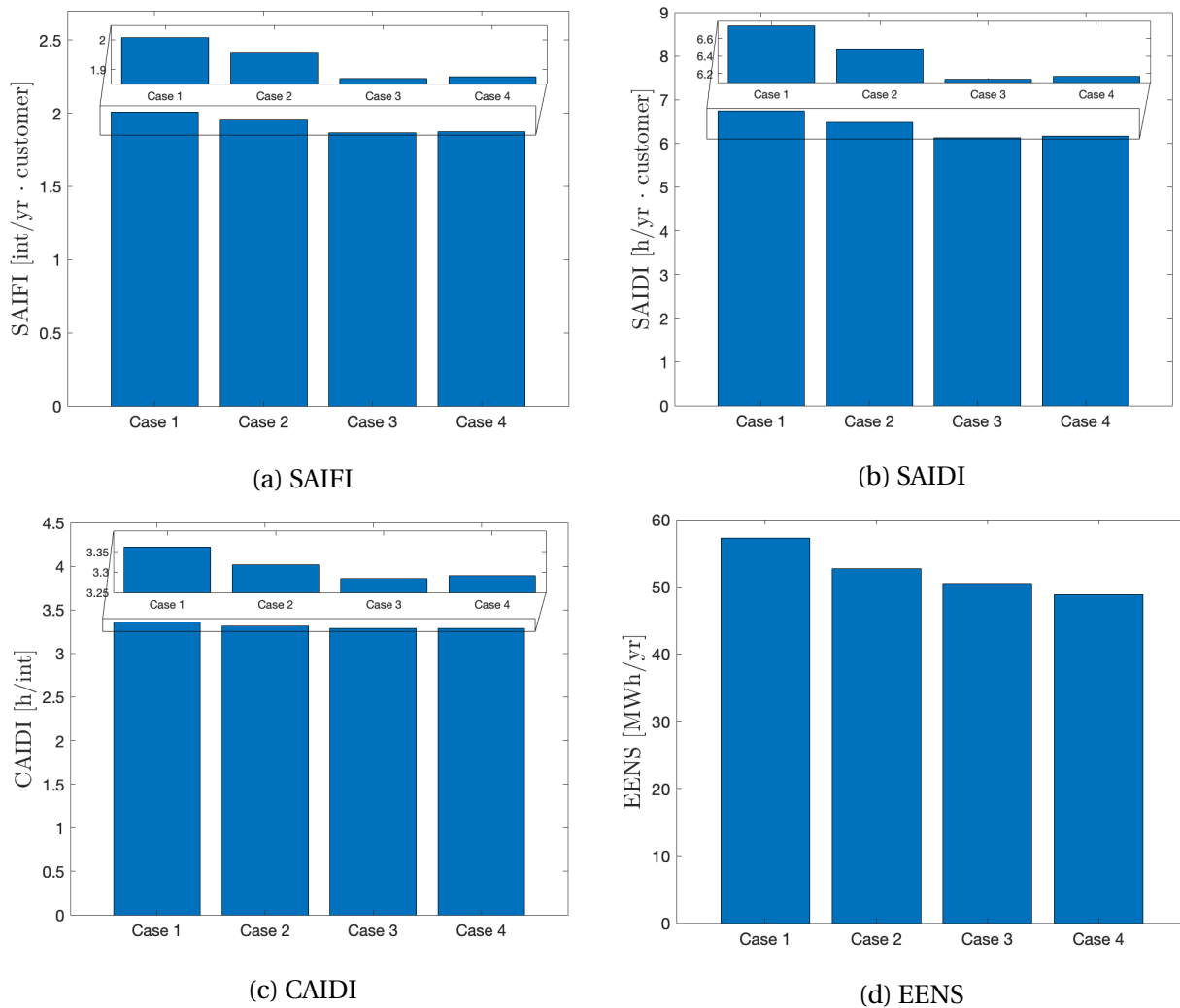
(d) EENS

Figure 5.6: Comparison of distribution system reliability indices.

5.6.1   Simulation Response Due to the System Configuration

The expected trends are shown by studying the variation in failure rates, outage duration and EENS for the different load points for Case 1 (configuration in Figure 5.1) illustrated in 5.4 are discussed in this section.

By analysing the variations of failure rates for the different load points illustrated by Figure 5.4a, it is clear that all load points on the same feeder (or sub-feeder) experience equal failure rate. The load points 1-10 on Feeder "F4" are dependent on an equal amount of components (with equal failure rates) to operate successfully, while the load points 11-14 are dependent on additionally three sub-sections on Sub-feeder "sF1" which is why their failure rate is higher. The load points 14-18 in Sub-feeder "sF2" are dependent on five sub-sections in addition to "F4", which further increases the failure rate. As the number of sub-sections on "sF3" align with those of sub-sections on "sF2" (i.e., failure rate and length), the failure rates of the load points 19-23 align with those of the load points 14-18.

The variation in outage duration among the load points illustrated by Figure 5.4b occur as expected when analysing the system configuration. The outage duration experienced by the load points when studying Case 1, increases along the feeder due to the effect of disconnectors and their location along the feeder. As the sub-feeders are equipped with individual circuit breakers, a failure on a sub-section will not impact the main feeder. Hence, there is an approximately linear increase in outage duration for load points 1-13, load points 1-7 $\rightarrow$ 14-18 and load points 1-10 $\rightarrow$ 19-23.

The EENS index for the individual load points illustrated in Figure 5.4c shows a larger variation. The EENS depends directly on the outage duration and the power consumption of the individual loads, which vary significantly. The difference in the pattern between the outage duration in Figure 5.4b and EENS in Figure 5.4c is due to the difference in the individual power demand of the load points.

5.6.2 Impact of Implementing Microgrid in the Distribution System

The impact of placing DGs on Sub-feeder 2 and allowing this sub-feeder to operate as a microgrid is noticeable in the reliability performance of the local load points (i.e., load point 14-18), while the load points outside the defined microgrid remain unaffected as a consequence of the applied operation strategy. This is clearly illustrated by comparing the estimated load point reliability indices in Figure 5.4 of Case 2 with those of Case 1. As a consequence of implementing the local generation as a back-feed, the microgrid load points participate in a more even distribution of outage duration, compared to Case 1 as shown in Figure 5.4b.

The reliability improvements are highly reflected through the microgrid reliability indices, by comparing Case 1 and Case 2 in Figure 5.5. For Case 2, MAIFI is improved (i.e., decreased) approximately by 20.0%, MAIDI with 33.7% and EENS with 35.9%. As the impact is experienced for the load points within the microgrid, the overall enhancement experienced by the distribution system is far less as indicated in Figure 5.6. In this respect, SAIFI has improved approximately by 2.6%, SAIDI by 3.9% and EENS by 7.9%.

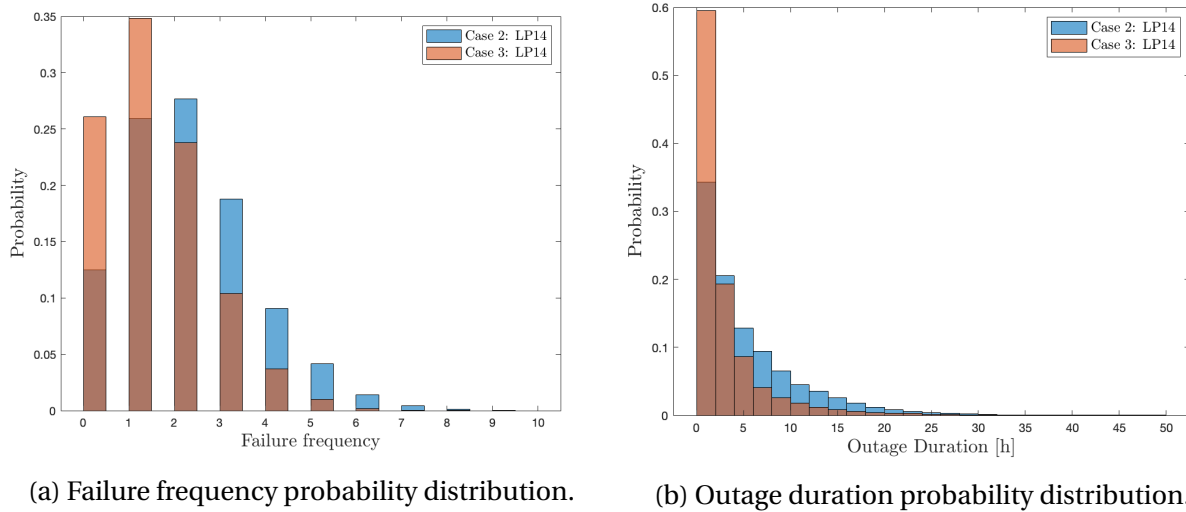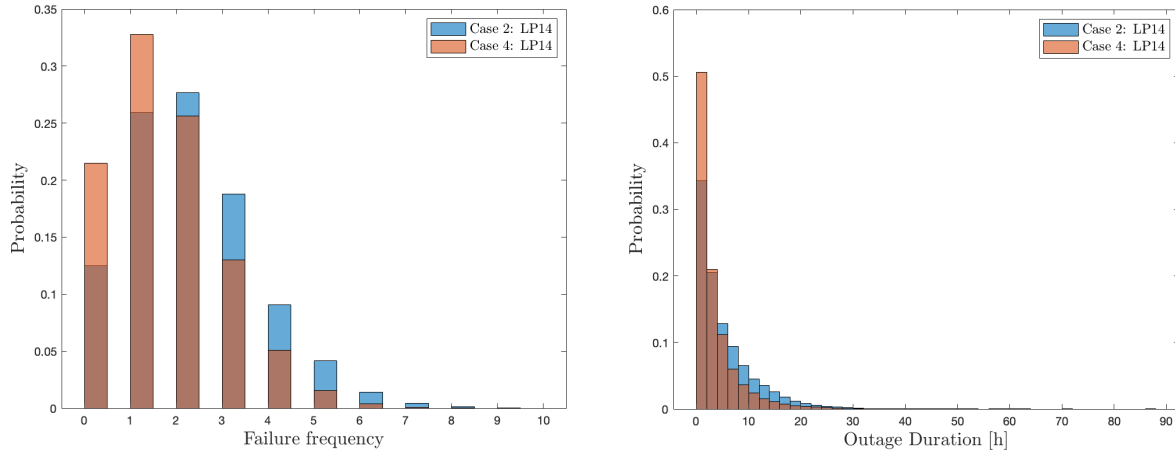(a) Failure frequency probability distribution.

(b) Outage duration probability distribution.
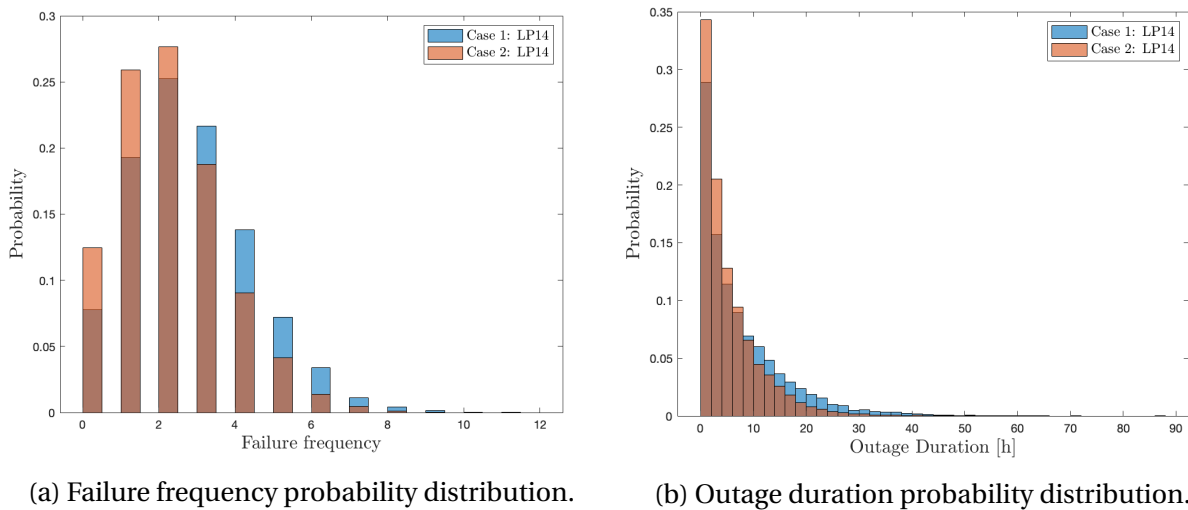
Figure 5.7: Comparison of probability distribution of Case 1 and Case 2 for reliability indices of Load Point 14.

Further, the local improvement of Load Point 14 is clearly seen by studying the probability distribution of failure frequency and outage duration illustrated in Figure 5.7. In both the probability distributions, the same tendency of a little covariate shift is present between the two cases, implying that the number of interruption occurrences and duration of interruptions per year is decreased by implementing a microgrid. Placing the microgrid further away from the utility grid in the main section and allowing the microgrid to supply load points outside the microgrid would increase the reliability of the distribution system.

5.6.3   Impact of Prioritising Loads Within the Microgrid

The impact of introducing the ability to prioritise loads within the microgrid during island operation is evaluated by comparing Case 2 with Case 3. The high priority load points (load points 14-15) experiences a significant reliability improvement as illustrated by Figure 5.4 compared with the regular island operation strategy of Case 2.

In terms of the microgrid reliability indices, the MAIFI experiences an approximate improvement of 26.8%; MAIDI an improvement of 39.8%; EENS an improvement of 21.3%. As the effect is limited to the load points within the microgrid, the overall enhancement experienced by the distribution system is far less as indicated in Figure 5.6. The SAIFI is enhanced with 4.46%, SAIDI with 5.39% and EENS with 4.31%, by implementing prioritising of load points inside the microgrid.

The probability distribution of failure frequency and outage duration for Load Point 14, which is considered as the highest prioritised load, are displayed in Figure 5.8. By comparing Case 3 with Case 2, an improvement is noticeable by the substantial covariate shift indicating that the number of interruption occurrences and duration of interruptions per year is significantly decreased. It is noteworthy that the class interval width (outage duration in hours) in Figure 5.8b is almost reduced by 50% compared to Figure 5.7b of Case 2, which implies that the upper limit of outage duration is decreased for Load Point 14.

(a) Failure frequency probability distribution.

(b) Outage duration probability distribution.

Figure 5.8: Comparison of probability distribution of Case 2 and Case 3 for reliability indices of Load Point 14.

5.6.4 Impact of Supporting the RES with BESS

The intermittent DGs are facilitated by adding a BESS to the microgrid, to be able to restore the load to a greater extent when operating in island mode. The effect of including a BESS is examined through the comparison of Case 2 and Case 4. The extra generation capacity by the DGs and BEES during the restoration period, allows the load point demand to be satisfied without causing disruptions. As a result, the failure rates of the microgrid load points experiencing an improvement of approximately 25%, as illustrated in Figure 5.4a. Additionally, the same trend is reflected in the outage duration and EENS shown in Figures 5.4b and 5.4c.

Consequently, the microgrid reliability indices also experience an improvement, illustrated in Figure 5.5. By introducing the BESS in the microgrid, the indices MAIFI, MAIDI and EENS are improved approximately 25.5%, 38.0% and 38.4%, respectively. Furthermore, the indices IOSR and ILOLP experience a significant enhancement of approximately 50% (increased) and 64.42% (decreased), respectively. As the impact is limited to the load points inside the microgrid, the impact on the distribution system reliability indices are significantly lower. SAIFI is improved with approximately 4.14%, SAIDI with 4.91% and EENS with 7.33%, upon comparing the respective indices for Case 4 and Case 2.

(a) Failure frequency probability distribution.

(b) Outage duration probability distribution.

Figure 5.9: Comparison of probability distribution of Case 2 and Case 4 for reliability indices of Load Point 14.

The local improvement in reliability of Load Point 14 is seen in the probability distribution of failure frequency and outage duration in Figure 5.9. It may be observed that the distributions are more shifted to the left for Case 4 compared to Case 2, implying that the respective load point demands have a higher probability of being met without causing disruptions with the inclusion of the BESS when compared to the scenario without the BESS.

5.7 Sensitivity Analysis of Case 4

The sensitivity associated with optimal placement and operation of DG and ESS with a primary objective of improving the reliability performance of the microgrid is briefly studied in this section. The installation of DGs and ESS within a microgrid imposes additional modelling requirements. Thus, an extended evaluation of the reliability of the microgrid is considered to study the effect of DG+BESS placement and BESS sizing. Firstly, a study of the effect of DER placement in the microgrid is carried by adding the same capacity of DER in different locations. Secondly, a study of the effect of BESS capacity value in the microgrid is performed by changing the capacity of BESS in the same location. Other characteristics such as voltage levels, transmission loss and cost aspects should be included in an optimisation analysis of DER. However, these considerations are outside the scope of this thesis, but existing techniques for including them are available in [62, 77, 78, 79].

5.7.1 Placement of DER

For DG and ESS units to benefit consumers as well as the utilities in the system in an optimal manner, the units should be installed strategically. Consequently, the locations considered are close to the load points within the microgrid. The defined microgrid has several nodes allowing a connection of the DER units. In this thesis, the investigated DER placement is as follows:

Case A: DER located in Sub-section 8

Case B: DER located in Sub-section 7

Case C: DER located in Sub-section 6

Case D: DER located in Sub-section 5

Case E: DER located in Sub-section 4

Load point indices such as failure rate, outage duration and EENS are presented for the microgrid load points in Figures 5.10a, 5.10b and 5.10c, respectively. By comparing the resulting load point indices for the studied cases, it can be observed that only the outage duration and EENS change by moving DER while the failure rate remains unchanged.
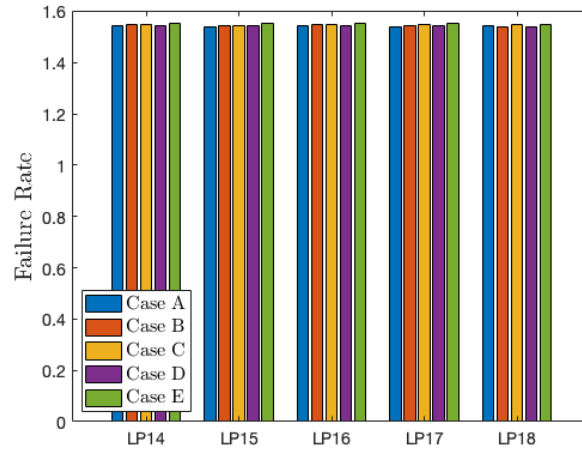
(a) Failure rates for load points within the microgrid.
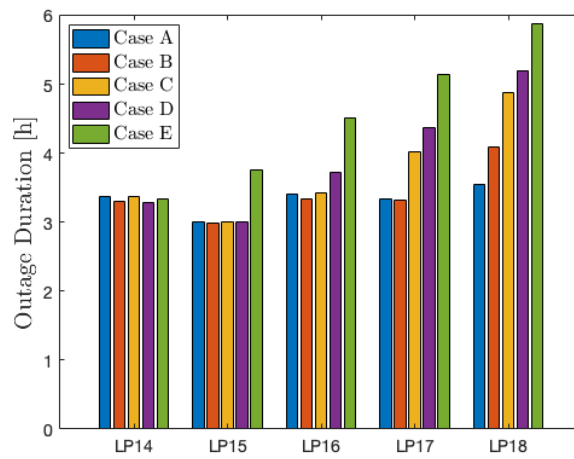
(b) Outage duration for load points within the microgrid.
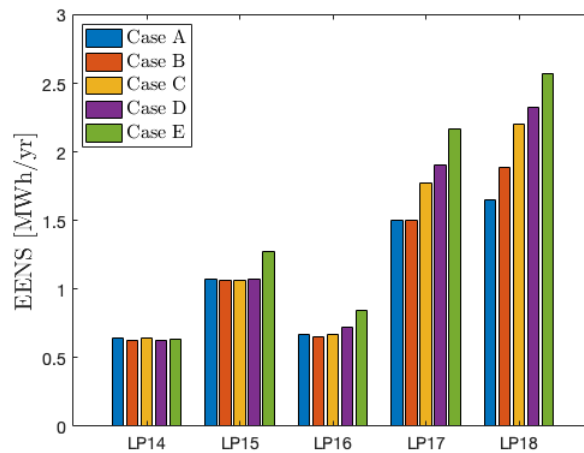
(c) EENS for load points within the microgrid.

Figure 5.10: Comparison of load point indices for the load points within the microgrid.

As expected, the best outcome, in terms of outage duration and EENS for the load points, is obtained for the case where DER is placed at the end of the feeder (Case A) and the worst is obtained when DER is located at the start of the feeder (Case E). These results are in agreement with the findings in [67].

(a) MAIFI

(b) MAIDI

(c) MCAIDI

(d) EENS
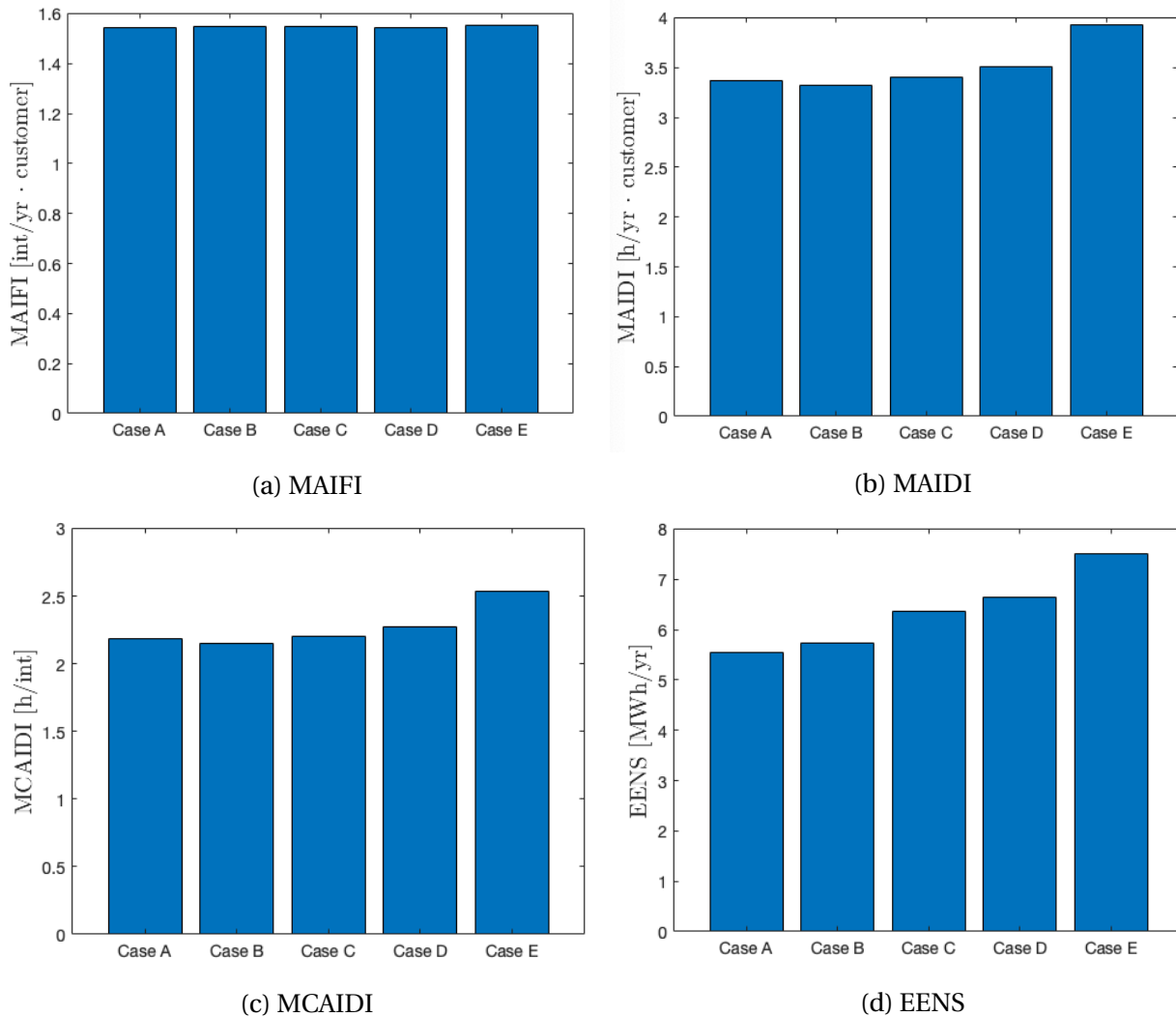
Figure 5.11: Comparison of microgrid system reliability indices.

From Figure 5.11, it is possible to identify the improvement of reliability indices for the studied microgrid. Although the index MAIFI does not change significantly for the cases, there is a noticeable improvement in MAIDI and EENS. The outcomes are as expected according to the load point reliability indices; Case A gives the overall best performance in terms of the duration-related indices. Thus, by comparing the studied cases, locations closer to the end of the feeder

give a better performance in terms of reliability. Thus, to maximise the benefits of installed DER in the microgrid, their location is chosen at the far end of the feeder (i.e., on Sub-section 8) in the studies of Case 2, Case 3 and Case 4.

5.7.2 Sizing of BESS

The effect of changing the installed charge/discharge capacity of BESS in the microgrid is considered while keeping the storage duration fixed at 5 hours and the depth of discharge at 80%. By recognising that the maximum peak load of the microgrid load is 2.4 MW, the capacity value of BESS is varied between 0 and 4 MW. The microgrid system indices EENS and IOSR are used to illustrate the effect of varying the capacity from a reliability perspective, as presented in Figures 5.12 and 5.13, accordingly.
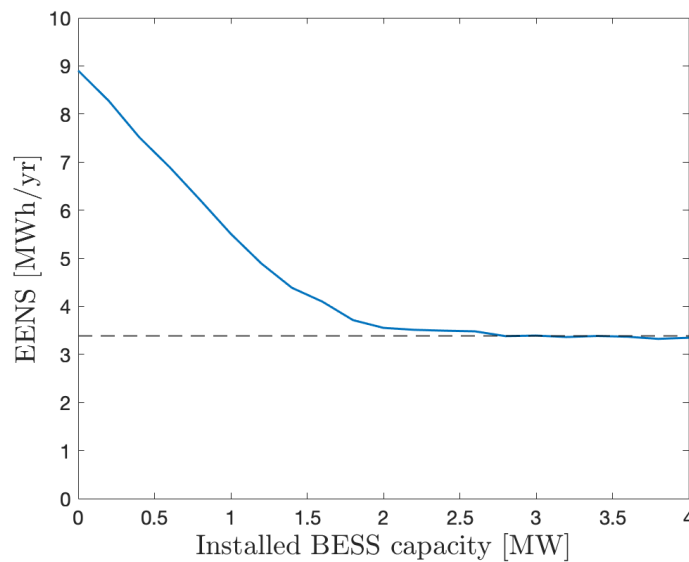
Figure 5.12: The change of EENS with increasingly BESS charge/discharge capacity.

From Figure 5.12, it is possible to observe that EENS converges with the increased capacity of BESS. For low installed charge/discharge capacity (i.e., approx. < 2 MW), the EENS of the microgrid system decreases as the charge/discharge capacity of BESS increases. As the capacity reaches and exceeds the peak load (2.4 MW), EENS stabilises towards a value of approx. 3.4 MWh/yr.
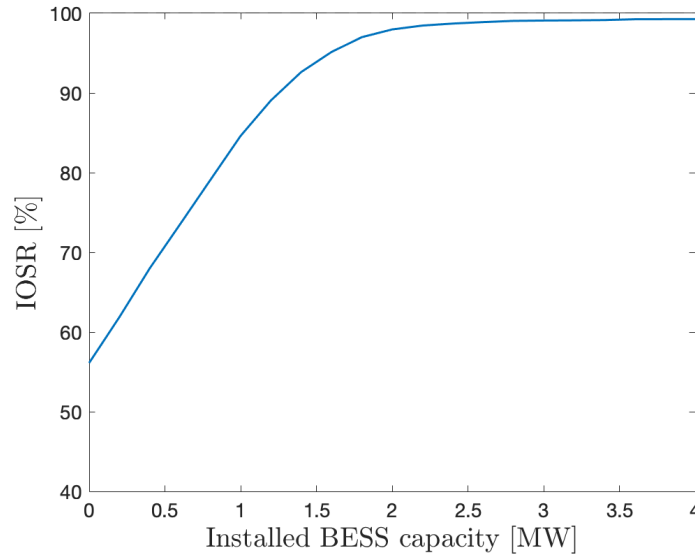
Figure 5.13: The change of IOSR with increasingly BESS charge/discharge capacity.

By considering the success rate of the microgrid operating in island mode, Figure 5.13 demonstrates the effect the capacity value of BESS has on IOSR. Here, the index IOSR converges towards a value close to 100% with the increasing capacity of BESS. However, it is important to note that IOSR will never reach a rate of 100% due to the assumption that the DGs and BESS can fail. By comparing the scenario of 0 MW with that of 2.5 MW, IOSR increases with a rate of over 40%, which is considered a substantial improvement.

Chapter 6

Conclusions and Future Work

6.1 Conclusions

The main objective of this thesis was to evaluate how microgrids can contribute to distribution system reliability. A major part of this thesis work dealt with a pedagogical dissemination of the conducted research on distribution system reliability; this enabled a transparent and easy-to-understand implementation of microgrids in the reliability assessment of distribution systems. As such, analytical and MCS methods have been examined for obtaining distribution system reliability (adequacy) indices, with emphasis placed on failure rate, outage duration, SAIFI, SAIDI, CAIDI and EENS.

As a basis for comparison, MATLAB scripts for time-sequential MCS of passive distribution systems have been developed, verified, validated, and comprehensively described in Chapter 3 and 4. The scripts were tested on three test systems: Bus 2, Bus 5 and Bus 6 of the RBTS. The reliability indices estimated from the simulations were verified with the result from the analytical method. The difference between the two methods was considered to be within an acceptable range, in accordance with other literature [31, 75]. Because of this, the created scripts can serve as a benchmark for further research.

As a consequence of the lack of test systems serving the purpose of addressing the distribution system reliability with the presence of microgrids in the literature, a modification to Feeder 4 of Bus 6 from the RBTS has been defined and applied, as described in Section 5.1. In this thesis, the attention has been on incorporating DGs such as WT and PV systems, BESS and a proposed operation strategy to assess microgrid reliability. As such, appropriate models of DER have been presented and addressed. MATLAB scripts for time-sequential MCS of distribution

system with the presence of microgrid have been created for the purpose of establishing the impact microgrid has on the distribution system. These scripts have been verified with the analytical method by assuming constant generation and load, before DGs of intermittent behaviour and time-varying loads were introduced.

Further, four case studies have been conducted in this work to seek understanding in a transparent manner: two studies to present the impact of implementing microgrid to the reliability assessment, and two incentives to enhance the microgrid operation (i.e., during island mode operation). The studies indicated that the integration of microgrid containing intermittent wind and solar energy sources improves the reliability performance. In particular, the load points within the defined microgrid experienced a significant reliability improvement. However, as the microgrid evaluated in the case studies only serve 13.27% of the customers located in the evaluated distribution system, the impact on the distribution system reliability indices was rather small. Hence, the improvement is expected to be higher for larger systems containing DGs.

Through incorporating a prioritisation strategy of the loads within the microgrid, the high priority loads experienced a significant improvement, which implies that sensitive loads would benefit greatly from this incentive. On the other hand, facilitating the RES with BESS showed to have a positive impact on the entire microgrid, where the battery size had a considerable impact on the result. The placement of the DER has been treated; as a result, the optimal placing of the DER facilities was found to be in the feeder end. Furthermore, the sizing of BESS was established to be somewhat optimal with a charging/discharging capacity equal to the highest load peak of the microgrid load. A combination of the two incentives would highly benefit the microgrid operation.

The overall conclusion of this presented work is that the reliability impact of implementing a microgrid in a distribution system is positive but profoundly depends on the size of the microgrid fraction and the proposed microgrid operation strategy. In addition, optimal placement and sizing of the DERs have demonstrated to impact reliability and should accordingly be taken into consideration.

6.2 Future work

Possible continuation of this thesis work could follow several paths. This section presents some suggestions that can form the basis for future research.

Operation Strategy: As the microgrid operation strategy sets the direction for the reliability evaluation, the outcome would differ considerably by modifying the proposed strategy. A suggestion would be to enable the microgrid to support loads outside the defined microgrid to obtain an increase in reliability.

System Design: An alternative design could be to install disconnectors at the end of each section, allowing the sections to be isolated individually. This is perhaps a more realistic design, but consequently, a more expensive solution as the system would require almost double the amount of equipment. This would lead to minor changes in the developed reliability evaluation program, and thereby, be easy to implement in combination with a cost analysis.

Assessing Real Distribution Systems: If one were to evaluate the reliability impact of implementing a microgrid in a practical distribution system, the input data should match the site of interest. Accordingly, besides the tailored system data, the input data to the respectively DG units of interest needs to be configured. For example, the applied solar radiation should match the radiation of the respective site. The shape of the solar radiation used in this thesis assumes the equal length of day and night throughout the year, which does not fit with the yearly variations in a country like Norway. However, the developed simulation program would be able to simulate the reliability parameters of real distribution systems and contribute to the evaluation of planning integration of a proposed microgrid in the network. Additionally, a more detailed study could be conducted by incorporating realistic load values and types to generate a better prioritising process of load points. The same also applies to including more realistic reliability parameters of the system components.

Power Flow Considerations: Another aspect would be to include consideration of power flow in the evaluation. As such, an analysis stating if the operation is feasible or not concerning stability requirements could be achievable. Power flow analysis of distribution systems was studied in relation to this thesis, but not included due to lack of suitable references to validate poten-

tial work, and time constraints. Including power flow in the reliability analysis would significantly increase the overall complexity of the analysis, but is highly relevant as the DG introduce bi-directional power flow which might increase the difficulties of proper control. The forward-backwards sweep method is considered suitable for the power flow analysis of distribution systems; Professor Olav B. Fosso at the Department of Electric Power Engineering at NTNU has proposed and published a fully available algorithm utilising the method for distribution systems of radial structure in [80], which could be applied. Accordingly, a possible future work could be to incorporate the available power flow algorithm into the reliability simulation program.

Cost Perspective: The cost-benefit aspect is essential for evaluating if microgrid operation is preferred as part of future technological developments. As such, reliability analysis can be conducted to (1) determine the cost of reliability or performance at a given cost or (2) determine the worth of reliability and its impact on cost versus improvements to the system.

If this thesis work were to continue, the most attractive follow up would be to further include power flow and cost-benefit analysis to evaluate the reliability impact of introducing microgrid operation in the distribution systems.

Bibliography

[1] United Nations Development Programme, "Goal 7: Affordable and Clean Energy," *Sustainable Development Goals*, 2016.

[2] P. Cicilio, M. Orosz, A. Mueller, and E. Cotilla-Sanchez, "μGrid: Reliable Minigrid Design and Planning Toolset for Rural Electrification," *IEEE Access*, vol. 7, pp. 163 988–163 999, 2019.

[3] I. E. Agency, "Energy Access Outlook 2017," p. 140, 2017. [Online]. Available: https://www.oecd-ilibrary.org/content/publication/9789264285569-en

[4] IEA, "Digitalisation and Energy," Paris, 2017. [Online]. Available: https://www.iea.org/reports/digitalisation-and-energy

[5] S. Parhizi, H. Lotfi, A. Khodaei, and S. Bahramirad, "State of the Art in Research on Microgrids: A Review," *IEEE Access*, vol. 3, pp. 890–925, 2015.

[6] S. Abu-Sharkh, R. Arnold, J. Kohler, R. Li, T. Markvart, J. Ross, K. Steemers, P. Wilson, and R. Yao, "Can microgrids make a major contribution to UK energy supply?" *Renewable and Sustainable Energy Reviews*, vol. 10, no. 2, pp. 78 – 127, 2006. [Online]. Available: http://www.sciencedirect.com/science/article/pii/S1364032104001194

[7] R. Billinton, "Reliability assessment of electric power systems using monte carlo methods," New York, 1994.

[8] K. B. Johansen and H. Enevoldsen, "Contribution of Microgrid to the Reliability of Distribution Systems," Dec. 2020, TET4520 Specialisation thesis.

[9] H. L. Willis, "Distributed power generation : planning and evaluation," New York, 2000.

[10] *IEEE Standard for the Specification of Microgrid Controllers*, IEEE Std 2030.7-2017 Edition, 2018.

[11] *IEEE Recommended Practice for the Planning and Design of the Microgrid*, IEEE Std 2030.9-2019 Edition, 2019.

[12] T. Funabashi, *Integration of Distributed Energy Resources in Power Systems: Implementation, Operation and Control.* San Diego: Elsevier Science & Technology, 2016.

[13] P. Salmerón Revuelta, S. Pérez Litrán, and J. Prieto Thomas, "Distributed Generation," in *Active Power Line Conditioners.* San Diego: Academic Press, 2016, pp. 285 – 322.

[14] A. Bidram and A. Davoudi, "Hierarchical Structure of Microgrids Control System," *IEEE Transactions on Smart Grid*, vol. 3, no. 4, pp. 1963–1976, 2012.

[15] G. K. A. Dimenas, A. Tisikalakis and G. Korres, "Microgrids control issues," *Microgrids: Architectures and Control*, 2014.

[16] *IEEE Guide for Design, Operation, and Integration of Distributed Resource Island Systems with Electric Power Systems*, IEEE Std 1547.4-2011 Edition, 2011.

[17] American National Standards Institute, "American National Standard for Electric Power Systems and Equipment—Voltage Ratings (60 Hertz)," *ANSI/NEMA C.84.1-2006*, no. 2, 2006.

[18] *IEEE Standard for Interconnecting Distributed Resources with Electric Power Systems*, IEEE Std 1547-2003 Edition, 2003.

[19] R. Billinton and R. N. Allan, "Power system reliability in perspective," *Electronics and Power*, vol. 30, no. 3, pp. 231–236, 1984.

[20] B. Allan, "Reliability Evaluation of Power Systems," New York, NY, 1996.

[21] R. Billinton and P. Wang, "A generalized method for distribution system reliability evaluation," *IEEE WESCANEX 95. Communications, Power, and Computing. Conference Proceedings*, vol. 2, pp. 349–354, 1995.

[22] *IEEE Guide for Electric Power Distribution Reliability Indices*, IEEE Std 1366, 2001 Edition, 2001.

[23] R. Billinton and R. Allan, *Reliability Evaluation of Power Systems*, 2nd ed. New York, NY: Springer US, 1996.

[24] M. Čepin, *Assessment of Power System Reliability: Methods and Applications.* London: Springer London, Limited, 2011.

[25] *IEEE Guide for Electric Power Distribution Reliability Indices*, IEEE Std 1366, 2001 Edition, 2001.

[26] P. M. Costa and M. A. Matos, "Assessing the contribution of microgrids to the reliability of distribution networks," *Electric Power Systems Research*, vol. 79, no. 2, pp. 382 – 389, 2009. [Online]. Available: http://www.sciencedirect.com/science/article/pii/S0378779608002058

[27] S. Wang, Z. Li, L. Wu, M. Shahidehpour, and Z. Li, "New Metrics for Assessing the Reliability and Economics of Microgrids in Distribution System," *IEEE Transactions on Power Systems*, vol. 28, no. 3, pp. 2852–2861, 2013.

[28] S. Kennedy and M. M. Marden, "Reliability of islanded microgrids with stochastic generation and prioritized load," in *2009 IEEE Bucharest PowerTech*, 2009, pp. 1–7.

[29] J. A. P. Lopes, C. L. Moreira, and A. G. Madureira, "Defining control strategies for MicroGrids islanded operation," *IEEE Transactions on Power Systems*, vol. 21, no. 2, pp. 916–924, 2006.

[30] J. A. Momoh, "Electric power distribution, automation, protection, and control," Boca Raton, Fla, 2008.

[31] P. Wang and L. Goel, "Power Distribution System Reliability Evaluation Using Both Analytical Reliability Network Equivalent Technique and Time-sequential Simulation Approach," in *Simulation Methods for Reliability and Availability of Complex Systems*, ser. Springer Series in Reliability Engineering. London: Springer London, 2010, pp. 145–172.

[32] G. Kjolle and K. Sand, "RELRAD-an analytical approach for distribution system reliability assessment," in *Proceedings of the 1991 IEEE Power Engineering Society Transmission and Distribution Conference*, 1991, pp. 729–734.

[33] R. Billinton and S. Jonnavithula, "A test system for teaching overall power system reliability assessment," *IEEE Transactions on Power Systems*, vol. 11, no. 4, pp. 1670–1676, 1996.

[34] R. N. Allan, R. Billinton, I. Sjarief, L. Goel, and K. S. So, "A reliability test system for educa-

tional purposes- basic distribution system data and results," *IEEE Transactions on Power Systems*, vol. 6, no. 2, pp. 813–820, 1991.

[35] R. Billinton and P. Wang, "Teaching distribution system reliability evaluation using Monte Carlo simulation," *IEEE Transactions on Power Systems*, vol. 14, no. 2, pp. 397–403, 1999.

[36] J. Park, W. Liang, J. Choi, A. A. El-Keib, M. Shahidehpour, and R. Billinton, "A probabilistic reliability evaluation of a power system including Solar/Photovoltaic cell generator," in *2009 IEEE Power Energy Society General Meeting*, 2009, pp. 1–6.

[37] J. F. Manwell, "Wind energy explained : theory, design and application," Chichester, U.K., 2009.

[38] S. Deshmukh, "Evaluation of Reliability Indices and Cost Worth Analysis for Generating Power Plants," *InternationalJournal of Engineering Reserarch*, 12 2013.

[39] M. Rausand and A. Høyland, *System Reliability Theory: Models, Statistical Methods, and Applications*, 2nd ed., ser. Wiley series in probability and statistics.   Hoboken, N.J: Wiley-Interscience, 2004.

[40] Y. Sun, M. H. J. Bollen, and G. W. Ault, "Probabilistic Reliability Evaluation for Distribution Systems with DER and Microgrids," in *2006 International Conference on Probabilistic Methods Applied to Power Systems*, 2006, pp. 1–8.

[41] Z. Bie, P. Zhang, G. Li, B. Hua, M. Meehan, and X. Wang, "Reliability Evaluation of Active Distribution Systems Including Microgrids," *IEEE Transactions on Power Systems*, vol. 27, no. 4, pp. 2342–2350, 2012.

[42] C. G. Justus, W. R. Hargraves, A. Mikhail, and D. Graber, "Methods for Estimating Wind Speed Frequency Distributions," *Journal of applied meteorology (1962)*, vol. 17, no. 3, pp. 350–353, 1978.

[43] S. Shi and K. L. Lo, "Reliability assessment of power system considering the impact of wind energy," in *2012 47th International Universities Power Engineering Conference (UPEC)*, 2012, pp. 1–6.

[44] A. A. Chowdhury, "Reliability models for large wind farms in generation system planning," *IEEE Power Engineering Society General Meeting, 2005*, vol. 2, pp. 1926–1933, 2005.

[45] P. Giorsetto and K. F. Utsurogi, "Development of a New Procedure for Reliability Modeling of Wind Turbine Generators," *IEEE Transactions on Power Apparatus and Systems*, vol. PAS-102, no. 1, pp. 134–143, 1983.

[46] Breeze, P., *Solar power generation*, 1st ed.   Academic Press, 2016.

[47] Bjørkedal, Ø., Løvholm, A.L. and Liléo, S., "Resource mapping of solar energy: an overview of available data in Norway," *Kjeller Vindteknikk*, 2013.

[48] H. Liang, J. Su, and S. Liu, "Reliability evaluation of distribution system containing microgrid," in *CICED 2010 Proceedings*, 2010, pp. 1–7.

[49] S. Lin, M. Han, R. Fan, and X. Hu, "Configuration of energy storage system for distribution network with high penetration of PV," in *IET Conference on Renewable Power Generation (RPG 2011)*, 2011, pp. 1–6.

[50] C. L. Borges and E. Cantarino, "Microgrids Reliability Evaluation with Renewable Distributed Generation and Storage Systems," *IFAC Proceedings Volumes*, vol. 44, no. 1, pp. 11 695–11 700, 2011, 18th IFAC World Congress. [Online]. Available: https://www.sciencedirect.com/science/article/pii/S1474667016454947

[51] H. D. Mediaas, "Contribution of Energy Storage to Generation Adequacy," Master's thesis, NTNU, June 2020.

[52] S. Zaferanlouei, M. Korpås, J. Aghaei, H. Farahmand, and N. Hashemipour, "Computational Efficiency Assessment of Multi-Period AC Optimal Power Flow including Energy Storage Systems," in *2018 International Conference on Smart Energy Systems and Technologies (SEST)*, 2018, pp. 1–6.

[53] A. Heidari, V. G. Agelidis, H. Zayandehroodi, J. Pou, and J. Aghaei, "On Exploring Potential Reliability Gains Under Islanding Operation of Distributed Generation," *IEEE Transactions on Smart Grid*, vol. 7, no. 5, pp. 2166–2174, 2016.

[54] T. Adefarati and R. Bansal, "Reliability assessment of distribution system with the integra-

tion of renewable distributed generation," *Applied Energy*, vol. 185, pp. 158–171, 2017. [Online]. Available: https://www.sciencedirect.com/science/article/pii/S0306261916315318

[55] W. S. Andrade, C. L. T. Borges, and D. M. Falcao, "Reliability evaluation of distribution systems with renewable distributed generation and load variation models," in *CIRED 2009 - 20th International Conference and Exhibition on Electricity Distribution - Part 1*, 2009, pp. 1–4.

[56] O. A. Ansari, N. Safari, and C. Y. Chung, "Reliability assessment of microgrid with renewable generation and prioritized loads," in *2016 IEEE Green Energy and Systems Conference (IGSEC)*, 2016, pp. 1–6.

[57] A. Abul'Wafa and A. Taha, "Reliability Evaluation of Distribution Systems under μ Grid-Tied and Islanded μ Grid Modes Using Monte Carlo Simulation," *Smart Grid and Renewable Energy*, no. 5, pp. 52–62, 2014.

[58] A. A. Alkuhayli, S. Raghavan, and B. H. Chowdhury, "Reliability evaluation of distribution systems containing renewable distributed generations," in *2012 North American Power Symposium (NAPS)*, 2012, pp. 1–6.

[59] T. Tuffaha and M. AlMuhaini, "Reliability assessment of a microgrid distribution system with pv and storage," in *2015 International Symposium on Smart Electric Distribution Systems and Technologies (EDST)*, 2015, pp. 195–199.

[60] H. Farzin, M. Fotuhi-Firuzabad, and M. Moeini-Aghtaie, "Reliability Studies of Modern Distribution Systems Integrated With Renewable Generation and Parking Lots," *IEEE Transactions on Sustainable Energy*, vol. 8, no. 1, pp. 431–440, 2017.

[61] Y. Zheng et al, "Optimal integration of mobile battery energy storage in distribution system with renewables," *Journal of Modern Power Systems and Clean Energy*, vol. 3, no. 4, pp. 589–596, 2015.

[62] K. Mahesh, P. A. Nallagownden, and I. A. Elamvazuthi, "Optimal placement and sizing of DG in distribution system using accelerated PSO for power loss minimization," in *2015 IEEE Conference on Energy Conversion (CENCON)*, 2015, pp. 193–198.

[63] M. N. Alam, S. Chakrabarti, and X. Liang, "A Benchmark Test System for Networked Micro-grids," *IEEE Transactions on Industrial Informatics*, vol. 16, no. 10, pp. 6217–6230, 2020.

[64] IEEE, "IEEE Standard for Interconnection and Interoperability of Distributed Energy Resources with Associated Electric Power Systems Interfaces," *IEEE Std 1547-2018 (Revision of IEEE Std 1547-2003)*, pp. 1–138, 2018.

[65] T. T. Pham, T. C. Kuo, and D. M. Bui, "Reliability evaluation of an aggregate battery energy storage system in microgrids under dynamic operation," *International Journal of Electrical Power* & *Energy Systems*, vol. 118, p. 105786, 2020. [Online]. Available: https://www.sciencedirect.com/science/article/pii/S0142061519329989

[66] W. S. Andrade, C. L. T. Borges, and D. M. Falcao, "Modeling reliability aspects of distributed generation connected to distribution systems," in *2006 IEEE Power Engineering Society General Meeting*, 2006, pp. 1–6.

[67] R. Allan and R. Billinton, "Probabilistic assessment of power systems," *Proceedings of the IEEE*, vol. 88, no. 2, pp. 140–162, 2000.

[68] C. L. T. Borges and D. M. Falcao, "Impact of distributed generation allocation and sizing on reliability, losses and voltage profile," in *2003 IEEE Bologna Power Tech Conference Proceedings,*, vol. 2, 2003, pp. 1–5.

[69] A. Ahadi, N. Ghadimi, and D. Mirabbasi, "Reliability assessment for components of large scale photovoltaic systems," *Journal of Power Sources*, vol. 264, pp. 211–219, 2014. [Online]. Available: https://www.sciencedirect.com/science/article/pii/S037877531400531X

[70] P. Zhang, W. Li, S. Li, Y. Wang, and W. Xiao, "Reliability assessment of photovoltaic power systems: Review of current status and future perspectives," *Applied Energy*, vol. 104, pp. 822–833, 2013. [Online]. Available: https://www.sciencedirect.com/science/article/pii/S0306261912008926

[71] W. Zhong, L. Wang, Z. Liu, and S. Hou, "Reliability Evaluation and Improvement of Islanded Microgrid Considering Operation Failures of Power Electronic Equipment," *Journal of Modern Power Systems and Clean Energy*, vol. 8, pp. 111–123, 01 2020.

[72] G. Kjolle and K. Sand, "RELRAD-an analytical approach for distribution system reliability assessment," in *Proceedings of the 1991 IEEE Power Engineering Society Transmission and Distribution Conference*, 1991, pp. 729–734.

[73] O. A. Ansari, N. Safari, and C. Y. Chung, "Reliability assessment of microgrid with renewable generation and prioritized loads," in *2016 IEEE Green Energy and Systems Conference (IGSEC)*, 2016, pp. 1–6.

[74] P. M. Subcommittee, "IEEE Reliability Test System," *IEEE Transactions on Power Apparatus and Systems*, vol. PAS-98, no. 6, pp. 2047–2054, 1979.

[75] R. Billinton and P. Wang, "Teaching distribution system reliability evaluation using Monte Carlo simulation," *IEEE Transactions on Power Systems*, vol. 14, no. 2, pp. 397–403, 1999.

[76] A. Leite, C. Borges, and D. Falcao, "Probabilistic Wind Farms Generation Model for Reliability Studies Applied to Brazilian Sites," *IEEE Transactions on Power Systems*, vol. 21, no. 4, pp. 1493–1501, 2006.

[77] R. S. Al Abri, E. F. El-Saadany, and Y. M. Atwa, "Optimal Placement and Sizing Method to Improve the Voltage Stability Margin in a Distribution System Using Distributed Generation," *IEEE Transactions on Power Systems*, vol. 28, no. 1, pp. 326–334, 2013.

[78] M. Suresh and J. B. Edward, "A hybrid algorithm based optimal placement of DG units for loss reduction in the distribution system," *Applied Soft Computing*, vol. 91, p. 106191, 2020. [Online]. Available: https://www.sciencedirect.com/science/article/pii/S1568494620301319

[79] H. Manafi, N. Ghadimi, M. Ojaroudi, and P. Farhadi, "Optimal Placement of Distributed Generations in Radial Distribution Systems Using Various PSO and DE Algorithms," *Elektronika ir Elektrotechnika*, vol. 19, no. 10, pp. 53–57, Dec. 2013. [Online]. Available: https://eejournal.ktu.lt/index.php/elt/article/view/1941

[80] O. B. Fosso, "PyDSAL - Python Distribution System Analysis Library," *2020 IEEE International Conference on Power Systems Technology (POWERCON)*, pp. 1–6, 2020.

Appendix A

RBTS

The RBTS has 5 load busbars (Bus 2 - Bus 6). Three of these system (Bus 2, Bus 5 and Bus 6) are selected based on their distribution network design. In this section, the necessary component parameters for reliability evaluation for all the studied bus systems are presented in the Tables A.1 and A.2. It should be noted that these include the original notation.

Table A.1: Reliability parameters of the components in RBTS [34].

Component	Failure rate, λ [f/yr· km]	Repair time, r [h]	Replacement time, r_p [h]	Switching time, r_s [h]
Line (Section) (11kV)	0.065	5	-	1
Line (Lateral) (0.415kV)	0.065	5	-	1
Transformer (11/0.415 kV)	0.015 f/yr	200	10	1

Table A.2: Feeder type and length for RBTS bus 5 [33].

Feeder type	Length [km]	Feeder section numbers
a) Bus 2		
1	0.60	2, 6, 10, 14, 17, 21, 25, 28, 30, 34
2	0.75	1, 4, 7, 9, 12, 16, 19, 22, 24, 27, 29, 32, 35
3	0.80	3, 5, 8, 11, 13, 15, 18, 20, 23, 26, 31, 33, 36
b) Bus 5		
1	0.50	1, 6, 9, 13, 14, 18, 21, 25, 27, 31, 35, 36, 39, 42
2	0.65	4, 7, 8, 12, 15, 16, 19, 22, 26, 28, 30, 33, 37, 40
3	0.80	2, 3, 5, 10, 11, 17, 20, 23, 24, 29, 32, 34, 38, 41, 43
c) Bus 6		
1	0.60	2, 3, 8, 9, 12, 13,17, 19, 20, 24, 25, 28, 31, 34, 41, 47
2	0.75	1, 5, 6, 7, 10, 14, 15, 22, 23, 26, 27, 30, 33, 43, 61
3	0.80	4, 11, 16, 18, 21, 29, 32, 35, 55
4	0.90	38, 44
5	1.60	37, 39, 42, 49, 54, 62
6	2.50	36, 40, 52, 57, 60
7	2.80	35, 46, 50, 56, 59, 64
8	3.20	45, 51, 53, 58, 63
9	3.50	48

Appendix B

Bus 2 of the RBTS

B.1 Description of Test System

The benchmark system Bus 2 of RBTS is used in this thesis. This section presents all relevant parameters needed to perform reliability analysis of Bus 2. The data is gathered from [34] and modified to fit the notation as illustrated in Figure B.1. Tables B.1 and B.2 gives the parameters for the section and lateral lines, respectively, while the load point parameters of the network can be found in Table B.3.
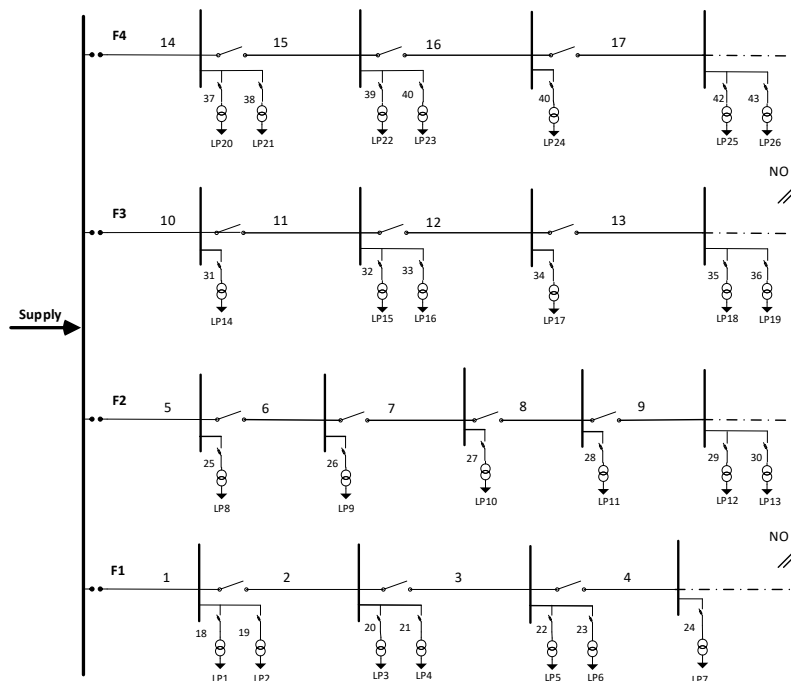
Table B.1: Reliability parameters for sections of Bus 2 of the RBTS.

Section no. (New notation)	Length [km]	Failure rate [f/yr]
1	0.75	0.04875
2	0.75	0.04875
3	0.75	0.04875
4	0.60	0.03900
5	0.75	0.04875
6	0.60	0.03900
7	0.75	0.04875
8	0.80	0.05200
9	0.60	0.03900
10	0.75	0.04875
11	0.80	0.05200
12	0.75	0.04875
13	0.75	0.04875
14	0.60	0.03900
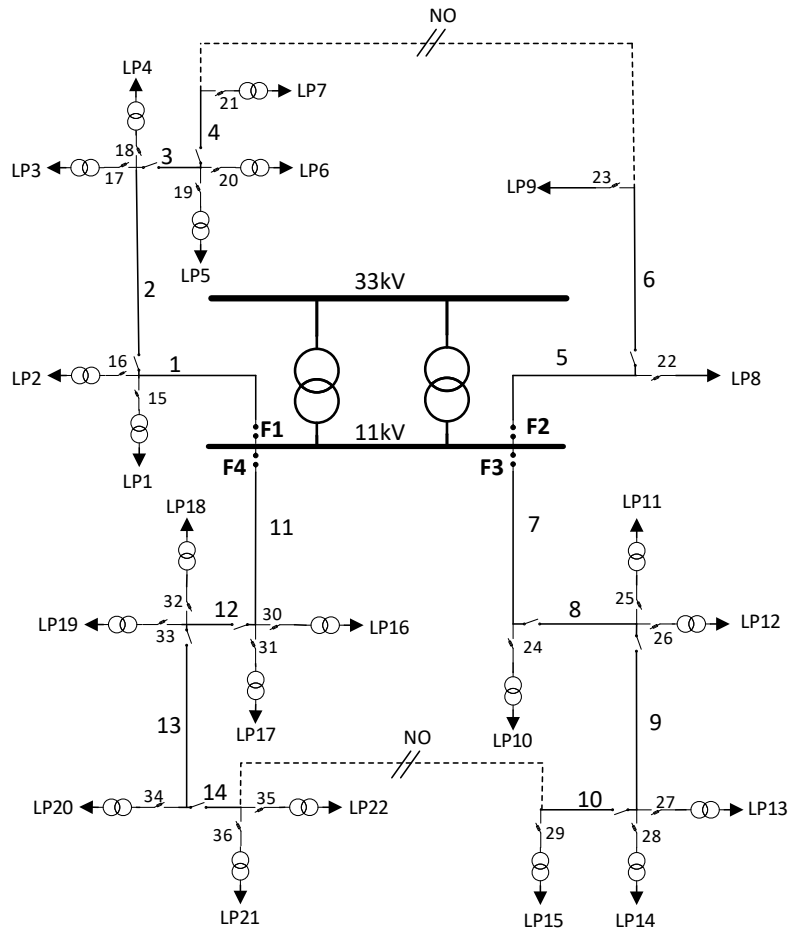
Figure B.1: System configuration of Bus 2 of RBTS, with updated notation.

Table B.2: Reliability parameters for laterals of Bus 2 of the RBTS.

Lateral no. (New notation)	Length [km]	Failure rate [f/yr]
15	0.60	0.03900
16	0.80	0.05200
17	0.80	0.05200
18	0.60	0.03900
19	0.80	0.05200
20	0.75	0.04875
21	0.80	0.05200
22	0.80	0.05200
23	0.80	0.05200
24	0.60	0.03900
25	0.75	0.04875
26	0.80	0.05200
27	0.75	0.04875
28	0.80	0.05200
29	0.60	0.03900
30	0.75	0.04875
31	0.60	0.03900
32	0.60	0.03900
33	0.80	0.05200
34	0.80	0.05200
35	0.75	0.04875
36	0.80	0.05200

Table B.3: Load point parameters of Bus 2 of the RBTS.

Load point no.	Feeder no.	Average load [MW]	Peak load [MW]	No. of customers
1	1	0.5350	0.8668	210
2	1	0.5350	0.8668	210
3	1	0.5350	0.8668	210
4	1	0.5660	0.9167	1
5	1	0.5660	0.9167	1
6	1	0.4540	0.7500	10
7	1	0.4540	0.7500	10
8	2	1.0000	1.6279	1
9	2	1.1500	1.8721	1
10	3	0.5350	0.8668	210
11	3	0.5350	0.8668	210
12	3	0.4500	0.7291	200
13	3	0.5660	0.9167	1
14	3	0.5660	0.9167	1
15	3	0.4540	0.7500	10
16	4	0.4540	0.7500	10
17	4	0.4500	0.7291	200
18	4	0.4500	0.7291	200
19	4	0.4500	0.7291	200
20	4	0.5660	0.9167	1
21	4	0.5660	0.9167	1
22	4	0.4540	0.7500	10

B.2 Reliability Evaluation of Bus 2

The estimated load point reliability indices of Bus 2 from both the analytical approach and the MCS method are presented in Table B.4.

Table B.4: Estimated load point reliability indices of Bus 2 of the RBTS.

Load Point no.	Average failure rate [f/yr]			Average outage duration [h/yr]		
	Analytical	Simulated	Difference [%]	Analytical	Simulated	Difference [%]
1	0.2393	0.2378	0.6061	0.7253	0.7371	-1.6285
2	0.2523	0.2471	2.0548	0.7903	0.7721	2.2918
3	0.2523	0.2503	0.7863	0.7903	0.7909	-0.0830
4	0.2393	0.2369	0.9962	0.7253	0.7209	0.6072
5	0.2523	0.2488	1.3677	0.7903	0.7799	1.3149
6	0.2490	0.2478	0.4819	0.7740	0.7737	0.03658
7	0.2523	0.2519	0.1255	0.7513	0.7696	-2.4411
8	0.1398	0.1424	-1.8962	0.5428	0.5493	-1.2134
9	0.1398	0.1425	-1.9439	0.5038	0.5090	-1.0470
10	0.2425	0.2367	2.4055	0.7285	0.7210	1.0289
11	0.2523	0.2447	3.0063	0.7903	0.7701	2.5486
12	0.2555	0.2511	1.7352	0.8065	0.8072	-0.0805
13	0.2523	0.2479	1.7377	0.7383	0.7284	1.3336
14	0.2555	0.2497	2.2831	0.7545	0.7621	-1.0018
15	0.2425	0.2376	2.0206	0.7285	0.7085	2.7428
16	0.2523	0.2497	1.0241	0.7903	0.8102	-2.5263
17	0.2425	0.2395	1.2234	0.7415	0.7493	-1.0515
18	0.2425	0.2371	2.2405	0.7285	0.7047	3.2712
19	0.2555	0.2476	3.0920	0.7935	0.7917	0.2278
20	0.2555	0.2481	2.8832	0.7935	0.7838	1.2293
21	0.2523	0.2457	2.5834	0.7383	0.7262	1.6296
22	0.2555	0.2503	2.0222	0.7545	0.7546	-0.0165

Appendix C

Bus 5 of the RBTS

C.1   Description of Test System

The benchmark system Bus 5 of RBTS is used in this thesis. This section presents all relevant parameters needed to perform reliability analysis of Bus 5. The data is gathered from [33] which are in this thesis modified to the configured line notation as illustrated in Figure C.1 and listed in the Tables C.1 and C.2 gives the parameters for the section and lateral lines, respectively, while the load point parameters of the network can be found in Table C.3.

Figure C.1: System configuration of Bus 5 with updated notation.

Table C.1: Reliability parameters for sections of Bus 5 of the RBTS.

Section no. (New notation)	Length [km]	Failure rate [f/yr]
1	0.50	0.03250
2	0.65	0.04225
3	0.65	0.04225
4	0.80	0.05200
5	0.65	0.04225
6	0.50	0.03250
7	0.65	0.04225
8	0.50	0.03250
9	0.80	0.05200
10	0.80	0.05200
11	0.50	0.03250
12	0.65	0.04225
13	0.65	0.04225
14	0.65	0.04225
15	0.50	0.03250
16	0.50	0.03250
17	0.80	0.05200

Table C.2: Reliability parameters for laterals of Bus 5 of the RBTS.

Lateral no. (New notation)	Length [km]	Failure rate [f/yr]
18	0.80	0.05200
19	0.80	0.05200
20	0.80	0.05200
21	0.50	0.03900
22	0.65	0.04225
23	0.50	0.03250
24	0.80	0.05200
25	0.50	0.03250
26	0.65	0.04225
27	0.80	0.05200
28	0.65	0.04225
29	0.50	0.03250
30	0.65	0.04225
31	0.80	0.05200
32	0.65	0.04225
33	0.50	0.03250
34	0.80	0.05200
35	0.50	0.03250
36	0.80	0.05200
37	0.80	0.05200
38	0.50	0.03250
39	0.65	0.04225
40	0.80	0.05200
41	0.65	0.04225
42	0.50	0.03250
43	0.80	0.05200

Table C.3: Load point parameters of Bus 5 of the RBTS.

Load point no.	Feeder no.	Average load [MW]	Peak load [MW]	No. of customers
1	1	0.4269	0.7625	210
2	1	0.4269	0.7625	210
3	1	0.6247	1.1100	1
4	1	0.4171	0.7450	240
5	1	0.6247	1.1100	1
6	1	0.4171	0.7450	240
7	1	0.4089	0.7400	15
8	2	0.6247	1.1100	1
9	2	0.3213	0.5740	195
10	2	0.3213	0.5740	195
11	2	0.3213	0.5740	195
12	2	0.3786	0.6167	1
13	2	0.3213	0.5740	195
14	3	0.4089	0.7400	15
15	3	0.4171	0.7450	240
16	3	0.3786	0.6167	1
17	3	0.6247	1.1100	1
18	3	0.4089	0.7400	15
19	3	0.3786	0.6167	1
20	4	0.4269	0.7625	210
21	4	0.4269	0.7625	210
22	4	0.4089	0.7400	15
23	4	0.6247	1.1100	1
24	4	0.4089	0.7400	15
25	4	0.4171	0.7450	240
26	4	0.3213	0.5740	195

C.2 Reliability Evaluation of Bus 5

The result of the reliability evaluation of Bus 5 for the analytical and MCS approach are listed in the Tables C.4 and C.5, presenting the load point reliability indices and the system reliability indices, respectively.

Table C.4: Estimated load point reliability indices of Bus 5 of the RBTS

Load Point no.	Average failure rate [f/yr]			Average outage duration [h/yr]		
	Analytical	Simulated	Difference [%]	Analytical	Simulated	Difference [%]
1	0.2360	0.2363	-0.1130	0.7090	0.6877	3.0091
2	0.2360	0.2373	-0.5650	0.7090	0.6957	1.8690
3	0.2360	0.2347	0.5650	0.7480	0.7262	2.9096
4	0.2165	0.2225	-2.7868	0.6505	0.6664	-2.4433
5	0.2263	0.2295	-1.4217	0.6993	0.7323	-4.7289
6	0.2165	0.2179	-0.6313	0.6505	0.6696	-2.9364
7	0.2360	0.2363	-0.1412	0.7870	0.8034	-2.0834
8	0.2490	0.2444	1.8474	0.6830	0.7092	-3.8307
9	0.2588	0.2523	2.4799	0.6928	0.6940	-0.1764
10	0.2685	0.2629	2.0732	0.7805	0.7815	-0.1231
11	0.2588	0.2519	2.6345	0.6928	0.6791	1.9723
12	0.2490	0.2451	1.5797	0.7220	0.7175	0.6218
13	0.2588	0.2529	2.2738	0.7708	0.7302	5.2553
14	0.2360	0.2325	1.4972	0.7870	0.8107	-3.0052
15	0.2263	0.2259	0.1400	0.6603	0.6465	2.0807
16	0.2165	0.2194	-1.3395	0.6115	0.6039	1.2496
17	0.2360	0.2397	-1.5537	0.7480	0.7513	-0.4351
18	0.2165	0.2173	-0.3849	0.6505	0.6355	2.3106
19	0.2360	0.2415	-2.3446	0.7480	0.7523	-0.5783
20	0.2263	0.2278	-0.6851	0.7383	0.7574	-2.5935
21	0.2068	0.2083	-0.7658	0.6408	0.6659	-3.9178
22	0.2165	0.2155	0.4773	0.6505	0.6605	-1.5296
23	0.2263	0.2211	2.2615	0.6993	0.7293	-4.3032
24	0.2165	0.2134	1.4319	0.6505	0.6260	3.7641
25	0.2068	0.2060	0.3628	0.6798	0.6898	-1.4745
26	0.2263	0.2241	0.9355	0.7773	0.7619	1.9733

Table C.5: Comparison of the system reliability indices for Bus 5 of the RBTS.

Indices	Analytical estimation	Simulated estimation	Difference [%]
SAIFI [int/yr· customer]	0.2325	0.2315	0.4228
SAIDI [h/yr· customer]	0.7012	0.7000	0.1682
CAIDI [h/int· yr]	3.0161	3.0238	-0.2557
EENS [MWh/yr]	7.9534	7.9945	-0.5169

Appendix D

Bus 6 of the RBTS

D.1 Description of Test System

The benchmark system Bus 6 of RBTS is used in this thesis. This section presents all relevant parameters needed to perform reliability analysis of Bus 6. The data is gathered from [33]. The notation from the original system is modified as illustrated in Figure D.1, by changing and divided the numbering of lines with respect to the type (S,sS,L,sL). Tables D.1, D.2, D.3 and D.4 gives the parameters for the section, sub-section, lateral and sub-lateral lines, respectively, while the load point parameters of the network can be found in Table D.5.
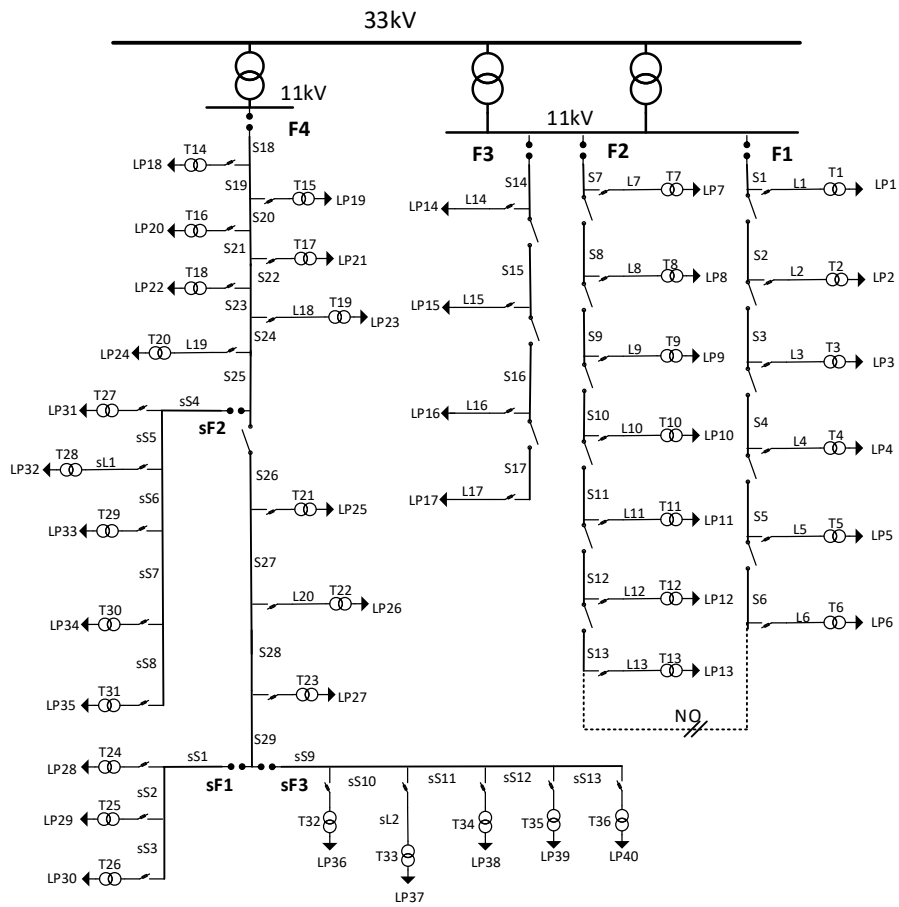
Figure D.1: System configuration of Bus 6 with updated notation.

Table D.1: Reliability parameters for sections of Bus 6 of the RBTS.

Section no. (New notation)	Length [km]	Failure rate [f/yr]
1	0.75	0.04875
2	0.60	0.03900
3	0.75	0.04875
4	0.75	0.04875
5	0.60	0.03900
6	0.80	0.05200
7	0.60	0.03900
8	0.75	0.04875
9	0.60	0.03900
10	0.60	0.03900
11	0.80	0.05200
12	0.75	0.04875
13	0.60	0.03900
14	0.75	0.04875
15	0.80	0.05200
16	0.60	0.03900
17	0.75	0.04875
18	2.80	0.18200
19	2.50	0.16250
20	1.60	0.10400
21	0.90	0.05850
22	1.60	0.10400
23	2.50	0.16250
24	1.60	0.10400
25	0.90	0.05850
26	3.20	0.20800
27	2.80	0.18200
28	3.50	0.22750
29	1.60	0.10400

Table D.2: Reliability parameters for sub-sections of Bus 6 of the RBTS.

Sub-section no. (New notation)	Length [km]	Failure rate [f/yr]
1	2.80	0.18200
2	3.20	0.20800
3	2.50	0.16250
4	3.20	0.20800
5	1.60	0.10400
6	2.80	0.18200
7	2.50	0.16250
8	3.20	0.20800
9	2.80	0.18200
10	2.50	0.16250
11	1.60	0.10400
12	3.20	0.20800
13	2.80	0.18200

Table D.3: Reliability parameters for laterals of Bus 6 of the RBTS.

Lateral no. (New notation)	Length [km]	Failure rate [f/yr]
1	0.60	0.03900
2	0.80	0.05200
3	0.75	0.04875
4	0.60	0.03900
5	0.75	0.04875
6	0.60	0.03900
7	0.75	0.04875
8	0.80	0.05200
9	0.80	0.05200
10	0.60	0.03900
11	0.75	0.04875
12	0.60	0.03900
13	0.75	0.04875
14	0.60	0.03900
15	0.75	0.04875
16	0.80	0.05200
17	0.60	0.03900
18	0.60	0.03900
19	0.75	0.04875
20	0.60	0.03900

Table D.4: Reliability parameters for sub-laterals of Bus 6 of the RBTS.

Sub-lateral no. (New notation)	Length [km]	Failure rate [f/yr]
1	0.80	0.05200
2	0.75	0.04875

Table D.5: Load point parameters of Bus 6 of the RBTS.

Load point no.	Feeder no.	Sub-feeder no.	Average load [MW]	Peak load [MW]	No. of customers
1	2	-	0.1775	0.3171	138
2	2	-	0.1808	0.3229	126
3	2	-	0.1775	0.3171	138
4	2	-	0.1808	0.3229	126
5	2	-	0.2163	0.3864	118
6	2	-	0.2163	0.3864	118
7	1	-	0.1659	0.2964	147
8	1	-	0.1659	0.2964	147
9	1	-	0.1775	0.3171	138
10	1	-	0.1659	0.2964	147
11	1	-	0.1808	0.3229	126
12	1	-	0.2070	0.3698	132
13	1	-	0.2070	0.3698	132
14	3	-	0.4697	0.8500	10
15	3	-	1.6391	1.9670	1
16	3	-	0.9025	1.0830	1
17	3	-	0.4697	0.8500	10
18	4	-	0.1659	0.2964	147
19	4	-	0.1808	0.3229	126
20	4	-	0.2501	0.6517	1
21	4	-	0.2633	0.6860	1
22	4	-	0.2070	0.3698	132
23	4	-	0.1659	0.2964	147
24	4	-	0.3057	0.7965	1
25	4	-	0.1554	0.2776	79
26	4	-	0.2831	0.7375	1
27	4	-	0.1585	0.2831	76
28	4	1	0.1554	0.2776	79
29	4	1	0.1585	0.2831	76
30	4	1	0.2501	0.6517	1
31	4	2	0.1554	0.2776	79
32	4	2	0.1929	0.5025	1
33	4	2	0.1585	0.2831	76
34	4	2	0.2501	0.6517	1
35	4	2	0.2633	0.6860	1
36	4	3	0.1554	0.2776	79
37	4	3	0.1929	0.5025	1
38	4	3	0.2831	0.7375	1
39	4	3	0.1585	0.2831	76
40	4	3	0.3057	0.7965	1

D.2 Reliability Evaluation of Bus 6

The estimated load point reliability indices of Bus 6 from both the analytical approach and the MCS method are presented in Table D.6.

D.3 Modification of Bus 6

To incorporate microgrid to the evaluation, Feeder 4 of Bus 6 is found to be appropriate as a test system in this work. With an aim of creating a realistic and generalised analysis, a modification of the original test system in [33] is presented in D.2. Particularly, the modification consisted of introducing circuit breakers at the beginning of each feeder, disconnectors in each section and fuses in each lateral. Moreover, additional lateral lines are implemented for all load points by defining their length, and the load points are assumed connected to their individual lateral through a low voltage transformer. A transformer is added in-between the busbar and the main feeder, to align the voltage level with the correct reliability parameters from [34] used in [33]. Table D.7 gives the new parameters of the section, sub-section, lateral and sub-laterals, and Table D.8 presents the used load point parameters.
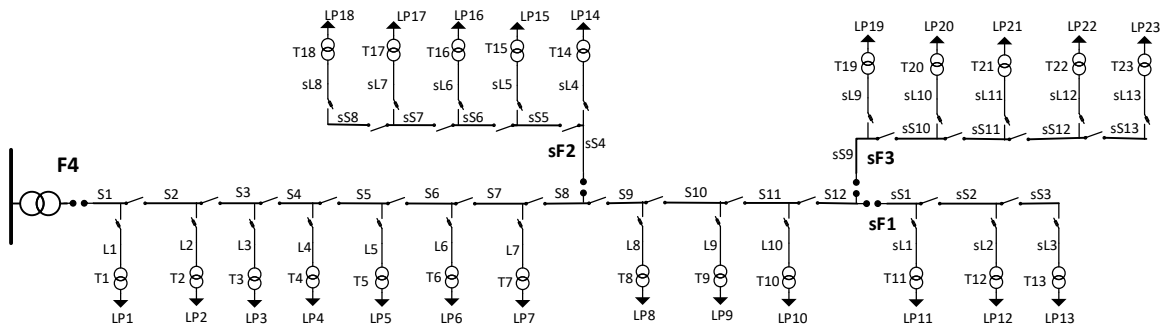
Figure D.2: System configuration of the modified Feeder 4, Bus 6 of the RBTS.

Table D.6: Estimated load point reliability indices of Bus 6 of the RBTS.

Load Point no.	Average failure rate [f/yr]			Average outage duration [h/yr]		
	Analytical	Simulated	Difference [%]	Analytical	Simulated	Difference [%]
1	0.3303	0.3365	-1.9026	0.8163	0.8347	-2.2590
2	0.3433	0.3420	0.3642	0.8423	0.8189	2.7684
3	0.3400	0.3439	-1.1569	0.8650	0.8406	2.8208
4	0.3303	0.3311	-0.2473	0.8163	0.8117	0.5540
5	0.3400	0.3429	-0.8628	0.8260	0.8388	-1.5431
6	0.3303	0.3315	-0.3886	0.8293	0.8302	-0.1114
7	0.3693	0.3739	-1.2683	0.8553	0.8797	-2.8612
8	0.3725	0.3793	-1.8345	0.9105	0.9374	-2.9525
9	0.3725	0.3739	-0.3669	0.8715	0.8486	2.6240
10	0.3595	0.3618	-0.6398	0.8065	0.8160	-1.1782
11	0.3693	0.3725	-0.8711	0.9073	0.8876	2.1699
12	0.3595	0.3630	-1.2146	0.8455	0.8592	-1.6216
13	0.3693	0.3710	-0.4739	0.8553	0.8199	4.1354
14	0.2275	0.2270	0.2198	0.5785	0.5898	-1.9562
15	0.2373	0.2314	2.4658	0.8353	0.8189	1.9608
16	0.2405	0.2392	0.5405	1.0075	0.9987	0.8777
17	0.2275	0.2251	1.0403	1.1375	1.1241	1.1777
18	1.6725	1.6724	0.0060	5.5515	5.5689	-0.3135
19	1.6725	1.6729	-0.0259	5.5515	5.5583	-0.1220
20	1.6725	1.6743	-0.1056	5.5515	5.5741	-0.4064
21	1.6725	1.6722	0.0179	5.5515	5.5400	0.2074
22	1.6725	1.6733	-0.0458	5.5515	5.5553	-0.0680
23	1.7115	1.7141	-0.1500	5.7465	5.7700	-0.4097
24	1.7212	1.7229	-0.0939	5.7953	5.7921	0.0551
25	1.6725	1.6726	-0.0060	8.4375	8.4384	-0.0106
26	1.7115	1.7137	-0.1305	8.6325	8.6485	-0.1858
27	1.6725	1.6717	0.0458	8.4375	8.4321	0.0641
28	2.2250	2.2244	0.0270	11.2000	11.2440	-0.3922
29	2.2250	2.2208	0.1888	11.2000	11.2000	-0.0027
30	2.2250	2.2220	0.1348	11.2000	11.2170	-0.1521
31	2.5370	2.5493	-0.4835	9.8740	9.9528	-0.7985
32	2.5890	2.6045	-0.6000	10.1340	10.2250	-0.8975
33	2.5370	2.5491	-0.4783	9.8740	9.9481	-0.7508
34	2.5370	2.5505	-0.5334	9.8740	9.9774	-1.0472
35	2.5370	2.5502	-0.5203	9.8740	9.9894	-1.1683
36	2.5110	2.5081	0.1142	12.6300	12.6290	0.0088
37	2.5598	2.5579	0.0736	12.8740	12.8730	0.0042
38	2.5110	2.5091	0.0743	12.6300	12.6550	-0.2010
39	2.5110	2.5113	-0.0133	12.6300	12.6820	-0.4107
40	2.5110	2.5094	0.0637	12.6300	12.6450	-0.1172

Table D.7: System data of the modified Feeder 4, Bus 6 of the RBTS.

Sections (S)		Laterals (L)		Sub-sections (sS)		Sub-laterals (sL)	
Number	Length [km]	Number	Length [km]	Number	Length [km]	Number	Length [km]
1	2.80	1	0.60	1	2.80	1	0.80
2	2.50	2	0.75	2	3.20	2	0.80
3	1.60	3	0.60	3	2.50	3	0.80
4	0.90	4	0.60	4	3.20	4	0.80
5	1.60	5	0.60	5	1.60	5	0.80
6	2.50	6	0.60	6	2.80	6	0.80
7	1.60	7	0.60	7	2.50	7	0.80
8	0.90	8	0.60	8	3.20	8	0.80
9	3.20	9	0.60	9	2.80	9	0.80
10	2.80	10	0.60	10	2.50	10	0.75
11	3.50			11	1.60	11	0.80
12	1.60			12	3.20	12	0.80
				13	2.80	13	0.80

Table D.8: Load point parameters of Feeder 4, Bus 6 of the RBTS.

Load Point no.	Average load [74] [MW]	Peak load [33] [MW]	No. of customers
1	0.2115	0.2964	147
2	0.2304	0.3229	126
3	0.4649	0.6517	1
4	0.4894	0.6860	1
5	0.2638	0.3698	132
6	0.2115	0.2964	147
7	0.5683	0.7965	1
8	0.1981	0.2776	79
9	0.5262	0.7375	1
10	0.2020	0.2831	76
11	0.1981	0.2776	79
12	0.2020	0.2831	76
13	0.4649	0.6517	1
14	0.1981	0.2776	79
15	0.3585	0.5025	1
16	0.2020	0.2831	76
17	0.4649	0.6517	1
18	0.4894	0.6860	1
19	0.1981	0.2776	79
20	0.3585	0.5025	1
21	0.5262	0.7375	1
22	0.2020	0.2831	76
23	0.5683	0.7965	1

Appendix E

IEEE Load Data

The variable load data applied in this work are extracted from [74]. The Tables E.1, E.2 and E.3 gives the weekly, daily and hourly peak load weighted factors in percentage, respectively.

Table E.1: Weekly peak load weighted factors in percentage of Annual peak.

Week no.	Peak load [%]	Week no.	Peak load [%]
1	86.2	27	75.5
2	90.0	28	81.6
3	87.8	29	80.1
4	83.4	30	88.0
5	88.0	31	72.2
6	84.1	32	77.6
7	83.2	33	80.0
8	80.6	34	72.9
9	74.0	35	72.6
10	73.7	36	70.5
11	71.5	37	78.0
12	72.7	38	69.5
13	70.4	39	72.4
14	75.0	40	72.4
15	72.1	41	74.3
16	80.0	42	74.4
17	75.4	43	80.0
18	83.7	44	88.1
19	87.0	45	88.5
20	88.0	46	90.9
21	85.6	47	94.0
22	81.1	48	89.0
23	90.0	49	94.2
24	88.7	50	97.0
25	89.6	51	100.0
26	86.1	52	95.2

Table E.2: Daily peak load weighted factors in percentage of Weekly peak.

Day of week	Name of day	Peak load [%]
1	Monday	93
2	Tuesday	100
3	Wednesday	98
4	Thursday	96
5	Friday	94
6	Saturday	77
7	Sunday	75

Table E.3: Hourly peak load weighted factors in percentage of Daily peak.

| Hour of day	Peak Load [%] for Winter Weeks 1-8 & 44-52		Peak Load [%] for Summer Weeks 18-30		Peak Load [%] for Spring/fall Weeks 9-17 & 31-43	
	Wkdy	Wknd	Wkdy	Wknd	Wkdy	Wknd
0-1	67	78	64	74	63	75
1-2	63	72	60	70	62	73
2-3	60	68	58	66	60	69
3-4	59	66	56	65	58	66
4-5	59	64	56	64	59	65
5-6	60	65	58	62	65	65
6-7	74	66	64	62	72	68
7-8	86	70	76	66	85	74
8-9	95	80	87	81	95	83
9-10	96	88	95	86	99	89
10-11	96	90	99	91	100	92
11-12	95	91	100	93	99	94
12-13	95	90	99	93	93	91
13-14	95	88	100	92	92	90
14-15	93	87	100	91	90	90
15-16	94	87	97	91	88	86
16-17	99	91	96	92	90	85
17-18	100	100	96	94	92	88
18-19	100	99	93	95	96	92
19-20	96	97	92	95	98	100
20-21	91	94	92	100	96	97
21-22	83	92	93	93	90	95
22-23	73	87	87	88	80	90
23-24	63	81	72	80	70	85

Appendix F

Results of Case 1

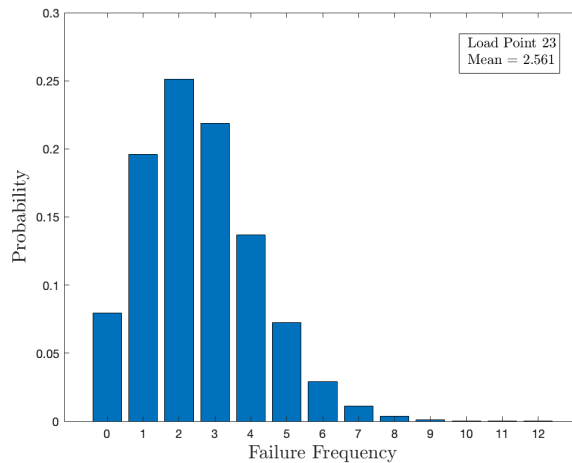## F.1   Probability Distribution of Load Points

The probability distributions of the annual failure frequency and duration for each load point in the distribution system have been evaluated, along with the distribution of the annual EENS. Figures F.1a, F.1b and F.1c present the histograms of the failure frequency for Load Point 1, 14 and 23, respectively. The probability distribution of the failure frequency clearly shows the probability of having a different number of load point failures in each year for each load point. Figures F.2a, F.2b and F.2c present the histograms of the outage duration for Load Point 1, 14 and 23, respectively. Further, Figures F.3a, F.3b and F.3c present the histograms of the EENS for the same load points.
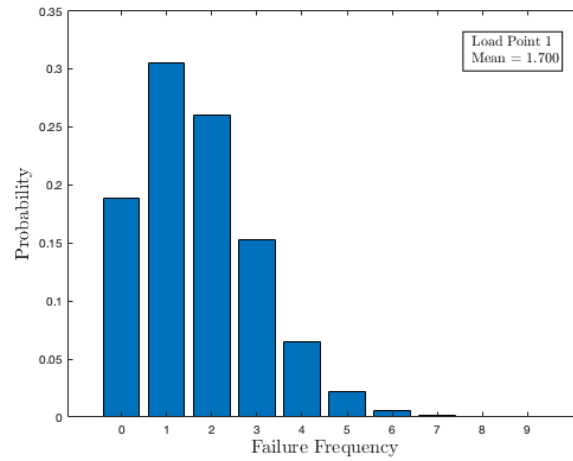
(a) Failure frequency histogram, Load Point 1.
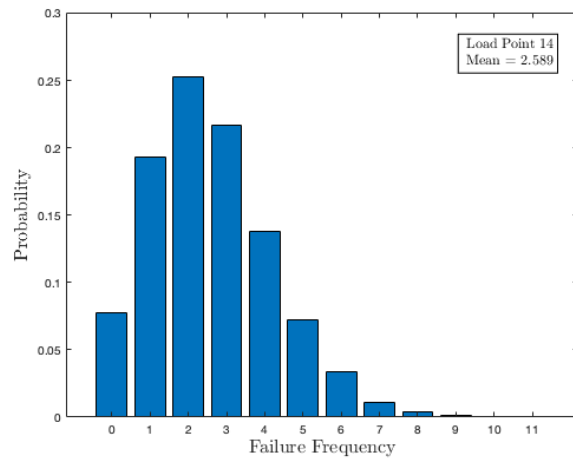
(b) Failure frequency histogram, Load Point 14
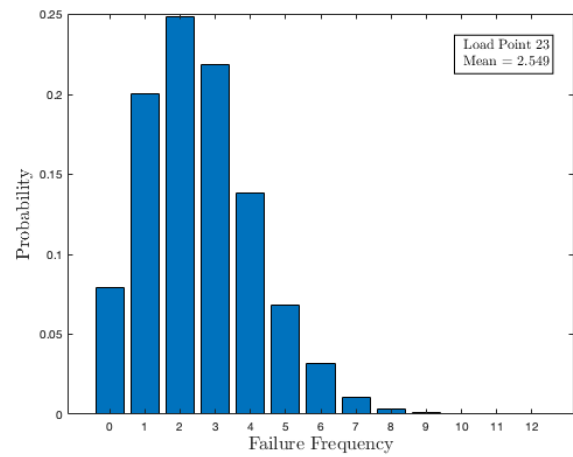
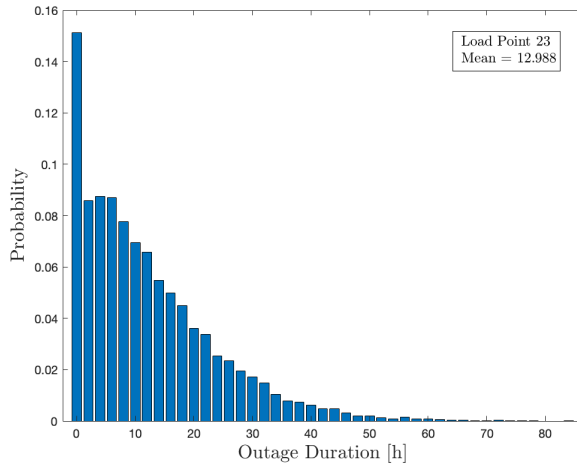(c) Failure frequency histogram, Load Point 23.

Figure F.1: Case 1: Probability distribution of failure rate for selected load points.
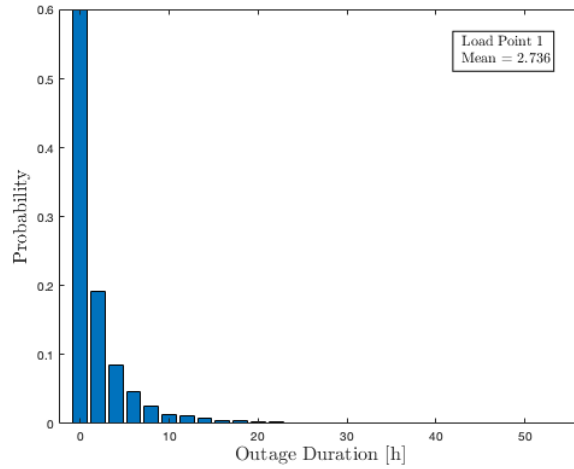
(a) Outage duration histogram, Load Point 1.
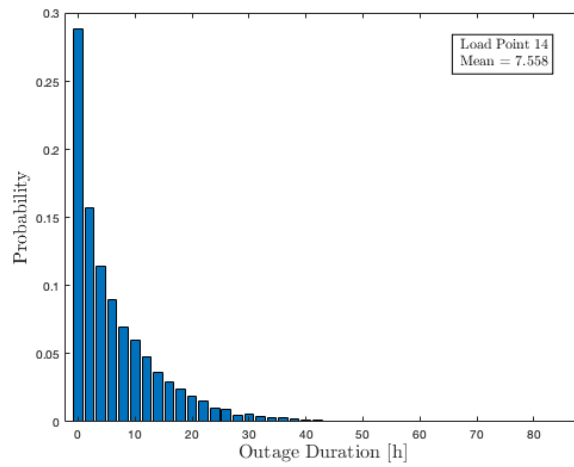


(b) Outage duration histogram, Load Point 14.
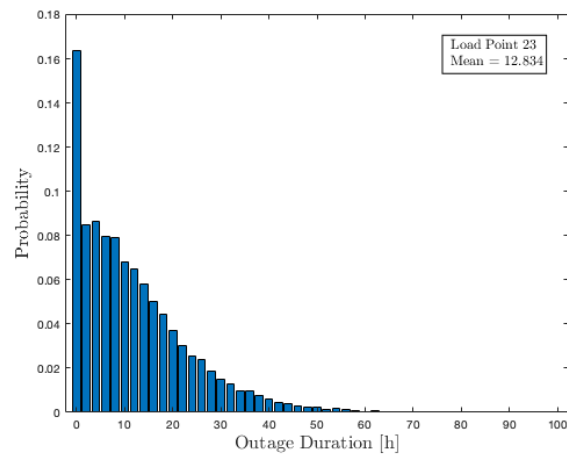
(c) Outage duration histogram, Load Point 23.

Figure F.2: Case 1: Probability distribution of outage duration for selected load points.
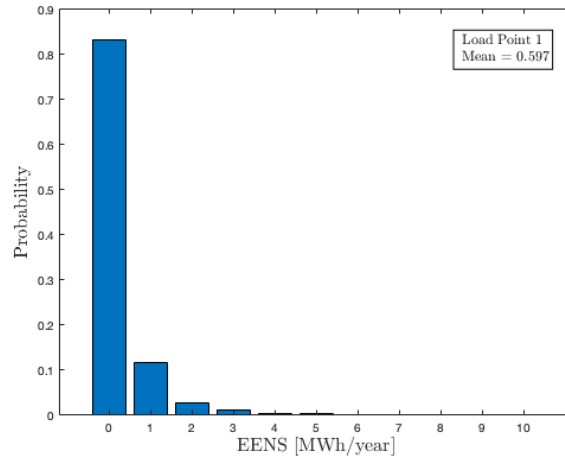
(a) Histogram of EENS, Load Point 1.
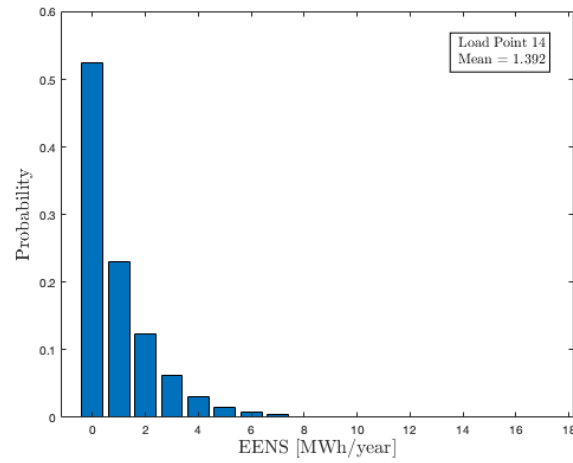
(b) Histogram of EENS, Load Point 14.
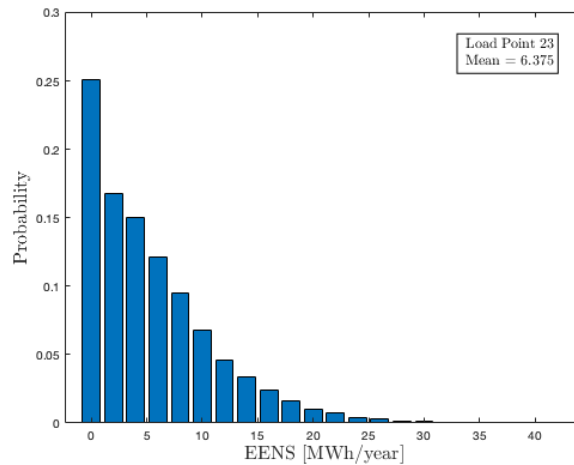
(c) Histogram of EENS, Load Point 23.

Figure F.3: Case 1: Probability distribution of the index EENS for selected load points.

F.2   Probability Distribution of Distribution System Indices

The probability distribution of the system reliability indices SAIFI, SAIDI, CAIDI and EENS are presented in the Figures F.4a, F.4b, F.4c and F.4d, respectively.
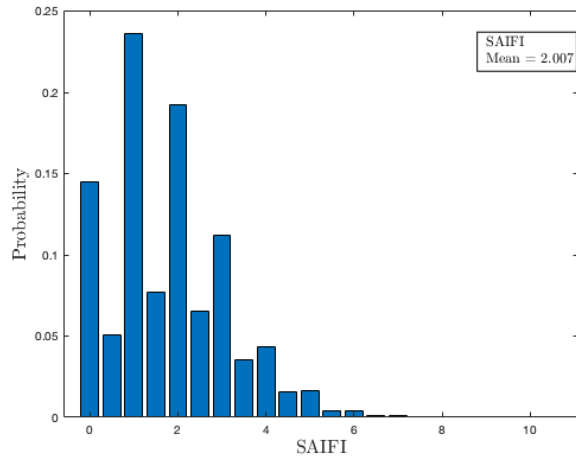
(a) Histogram of SAIFI.
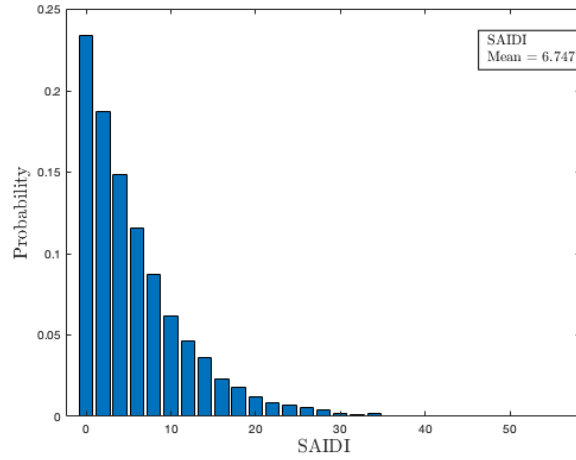
(b) Histogram of SAIDI.
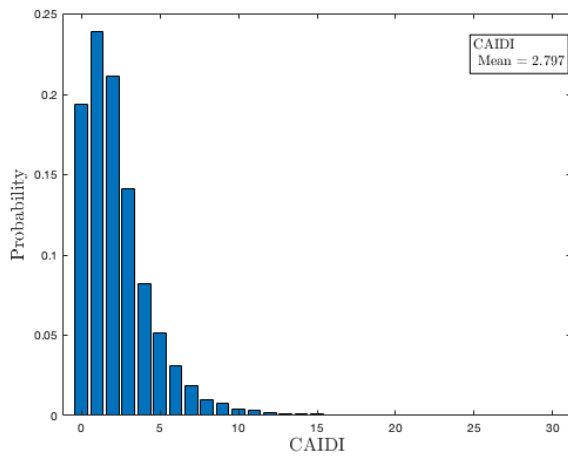
(c) Histogram of CAIDI.
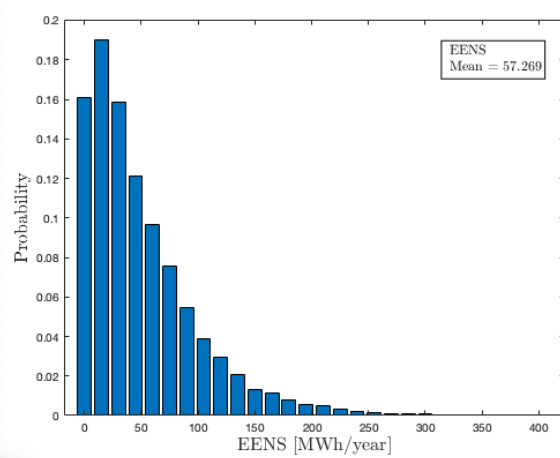
(d) Histogram of EENS.

Figure F.4: Probability distribution of system reliability indices.

F.3 Probability Distribution of Microgrid System Indices

The probability distribution of the microgrid system reliability indices MAIFI, MAIDI, MCAIDI and EENS are presented in the Figures F.5a, F.5b, F.5c and F.5d, respectively.
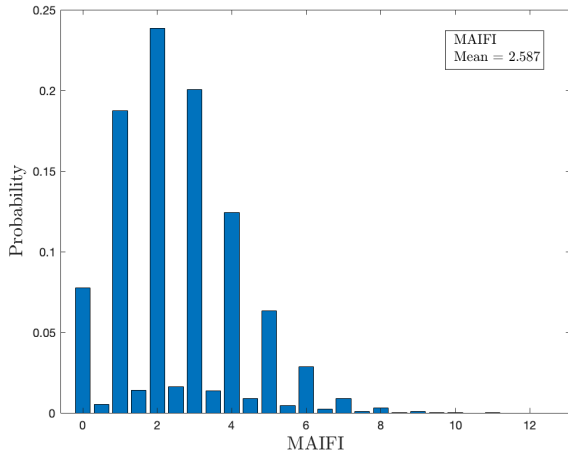
(a) Histogram of MAIFI.
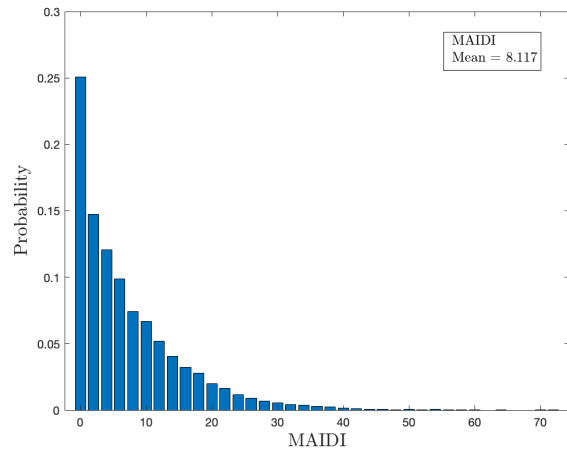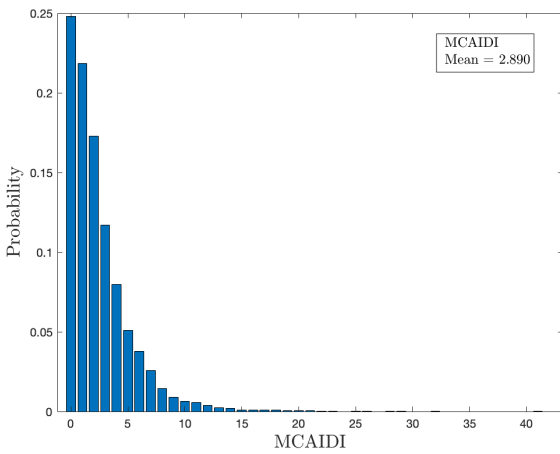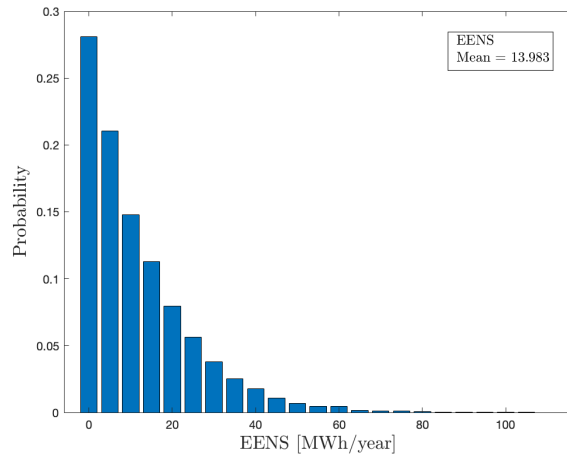
(b) Histogram of MAIDI.

(c) Histogram of MCAIDI.

(d) Histogram of EENS (for the micorgrid).

Figure F.5: Probability distribution of microgrid system reliability indices.

Appendix G

Results of Case 2

G.1   Probability Distribution of Load Points

The probability distributions of the annual failure frequency and duration for each load point in the distribution system have been evaluated, along with the distribution of the annual EENS. Figures G.1a, G.1b and G.1c present the histograms of the failure frequency for Load Point 1, 14 and 23, respectively. The probability distribution of the failure frequency clearly shows the probability of having a different number of load point failures in each year for each load point. Figures G.2a, G.2b and G.2c present the histograms of the outage duration for Load Point 1, 14 and 23, respectively. Further, Figures G.3a, G.3b and G.3c present the histograms of the EENS for the same load points.
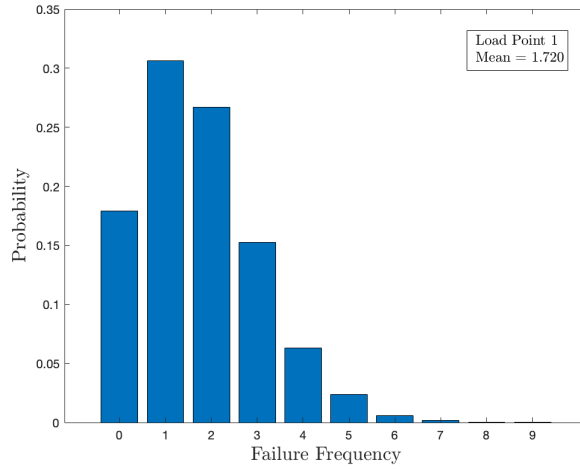
(a) Failure frequency histogram, Load Point 1.
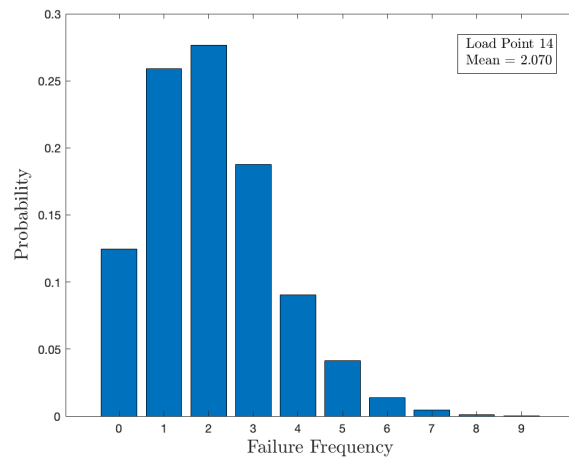
(b) Failure frequency histogram, Load Point 14
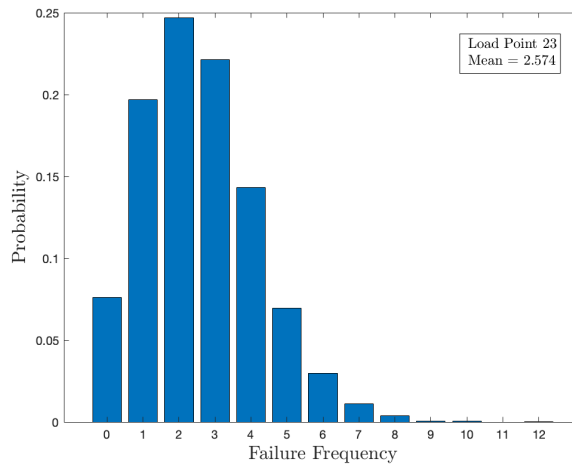
(c) Failure frequency histogram, Load Point 23.

Figure G.1: Case 2: Probability distribution of failure rate for selected load points.
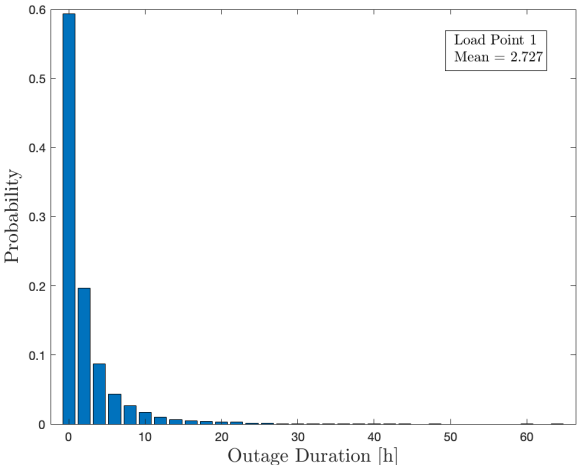
(a) Outage duration histogram, Load Point 1.
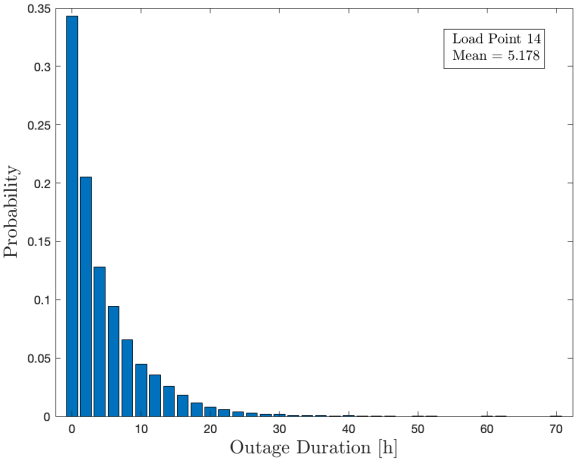
(b) Outage duration histogram, Load Point 14.
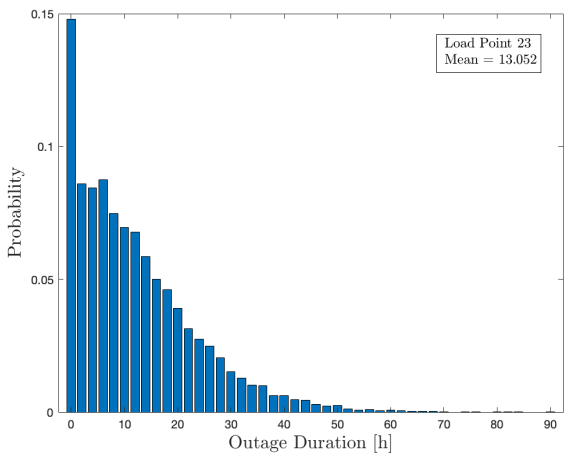
(c) Outage duration histogram, Load Point 23.

Figure G.2: Case 2: Probability distribution of outage duration for selected load points.
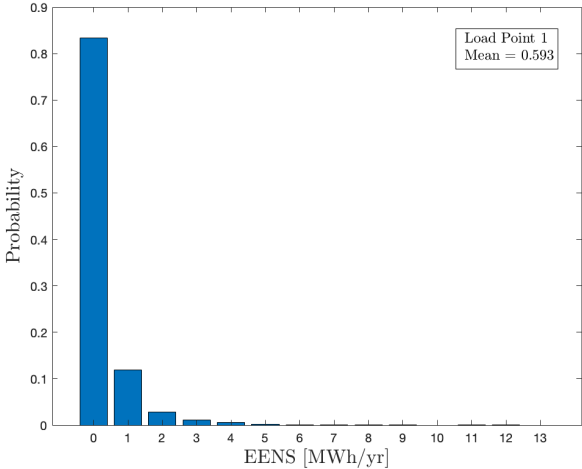
(a) Histogram of EENS, Load Point 1.
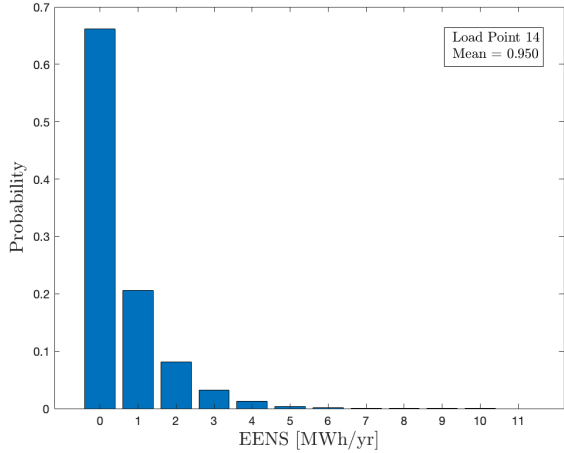
(b) Histogram of EENS, Load Point 14.
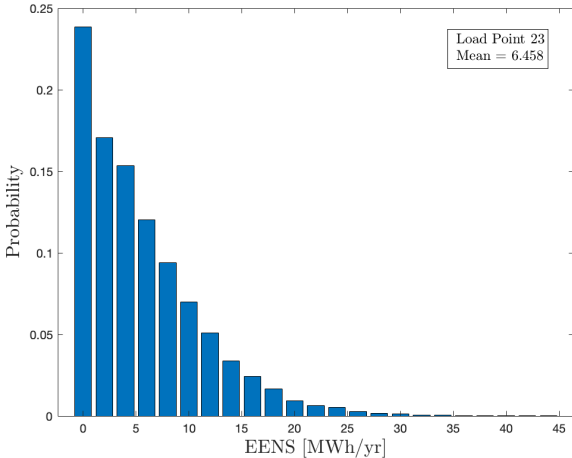
(c) Histogram of EENS, Load Point 23.

Figure G.3: Case 2: Probability distribution of the index EENS for selected load points.

G.2 Probability Distribution of Distribution System Indices

The probability distribution of the system reliability indices SAIFI, SAIDI, CAIDI and EENS are presented in the Figures G.4a, G.4b, G.4c and G.4d, respectively.
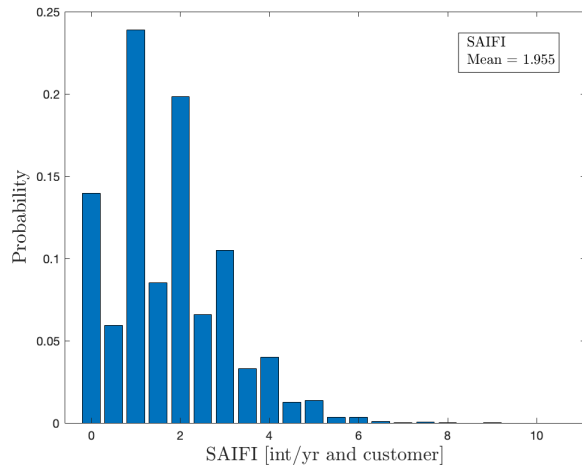
(a) Histogram of SAIFI.
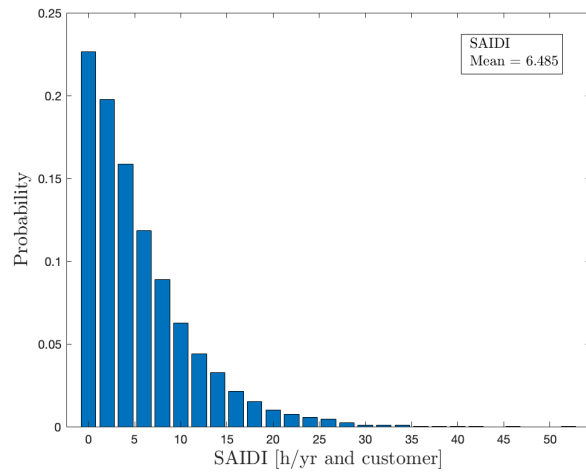
(b) Histogram of SAIDI.
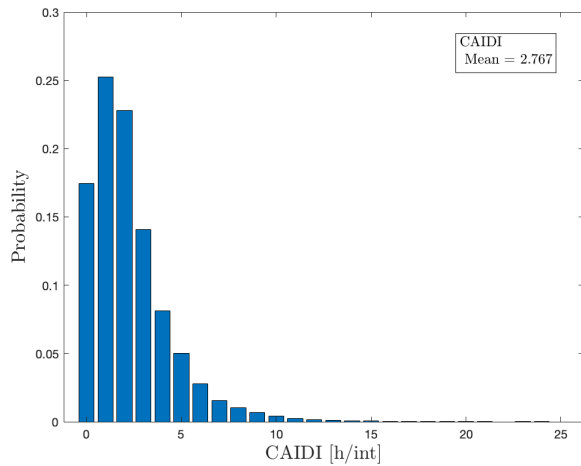
(c) Histogram of CAIDI.
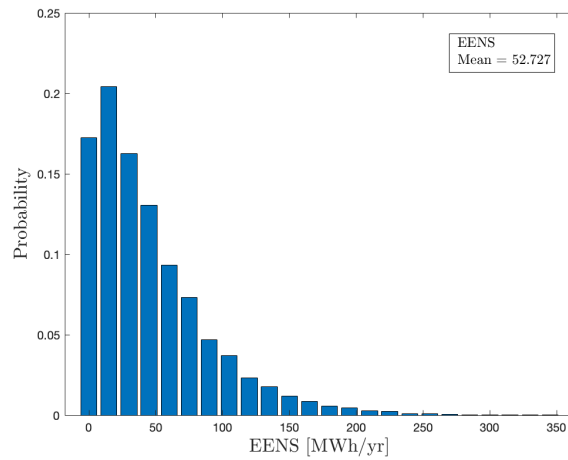
(d) Histogram of EENS.

Figure G.4: Probability distribution of system reliability indices.
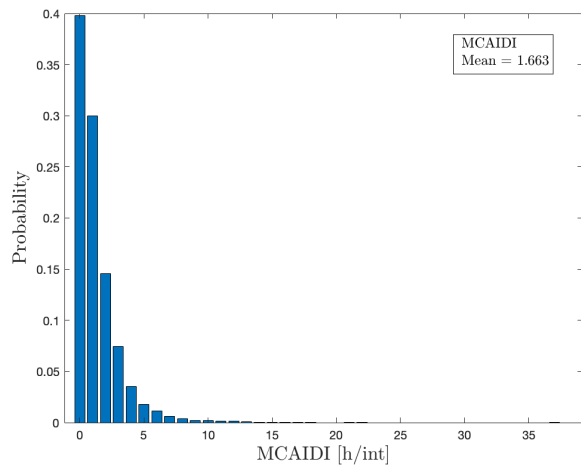
G.3 Probability Distribution of Microgrid System Indices

The probability distribution of the microgrid system reliability indices MAIFI, MAIDI, MCAIDI and EENS are presented in the Figures G.5a, G.5b, G.5c and G.5d, respectively.
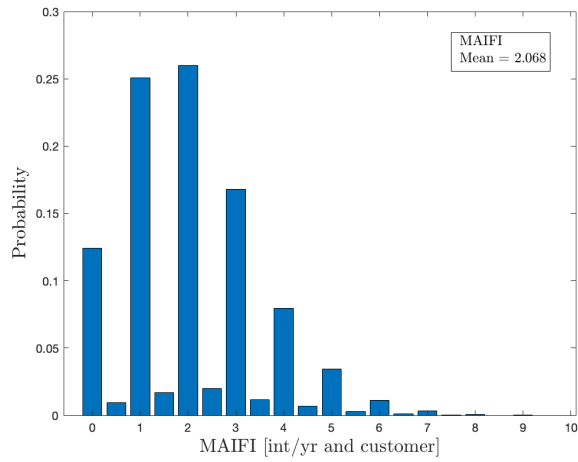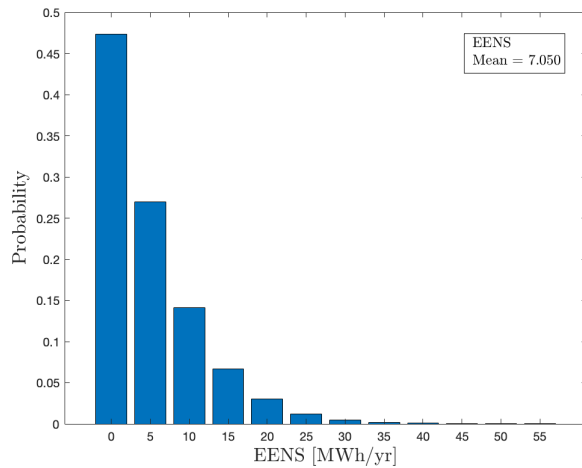

(a) Histogram of MAIFI.
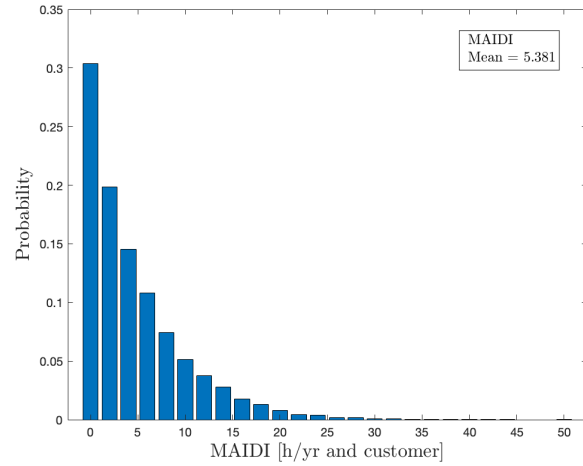
(b) Histogram of MAIDI.
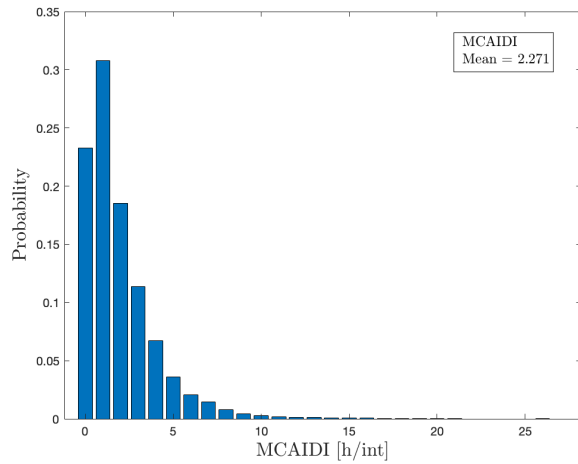
(c) Histogram of MCAIDI.
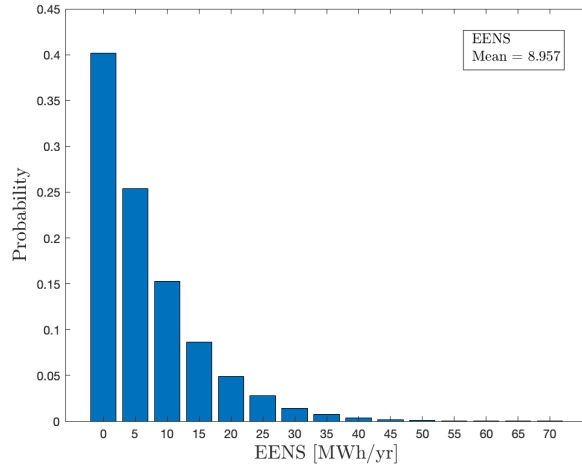
(d) Histogram of EENS (for the micorgrid).
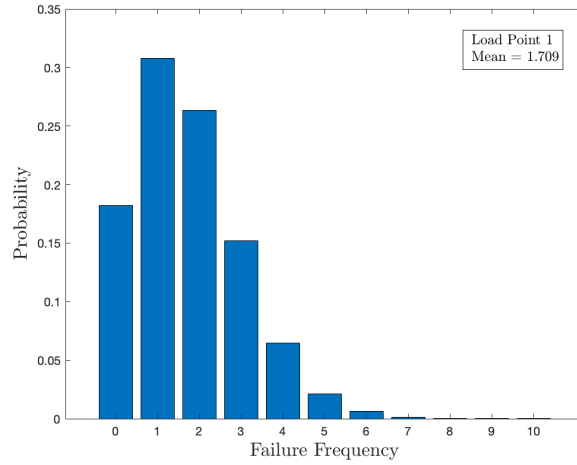
Figure G.5: Probability distribution of microgrid system reliability indices.

Appendix H

Results of Case 3

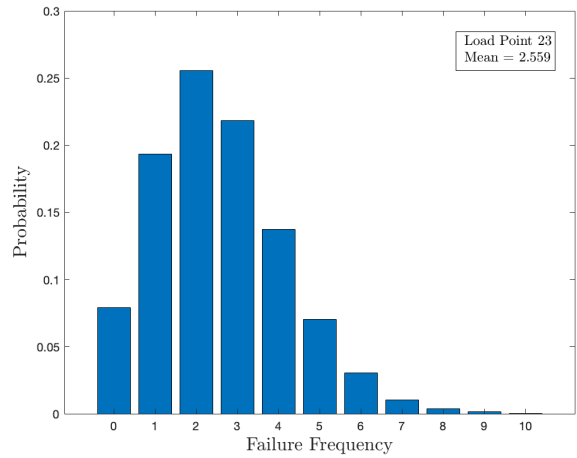## H.1 Probability Distribution of Load Points

The probability distributions of the annual failure frequency and duration for each load point in the distribution system have been evaluated, along with the distribution of the annual EENS. Figures H.1a, H.1b and H.1c present the histograms of the failure frequency for Load Point 1, 14 and 23, respectively. The probability distribution of the failure frequency clearly shows the probability of having a different number of load point failures in each year for each load point. Figures H.2a, H.2b and H.2c present the histograms of the outage duration for Load Point 1, 14 and 23, respectively. Further, Figures H.3a, H.3b and H.3c present the histograms of the EENS for the same load points.
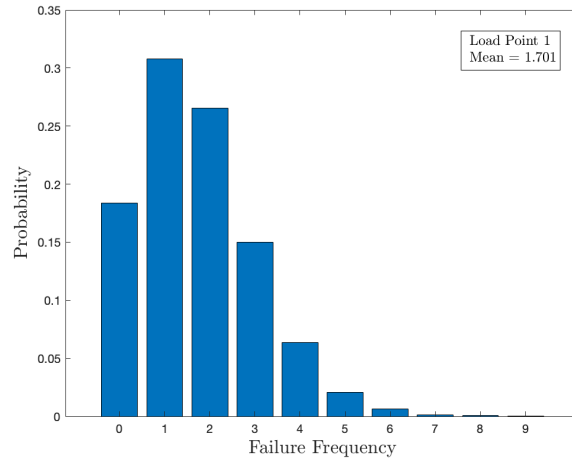
(a) Failure frequency histogram, Load Point 1.
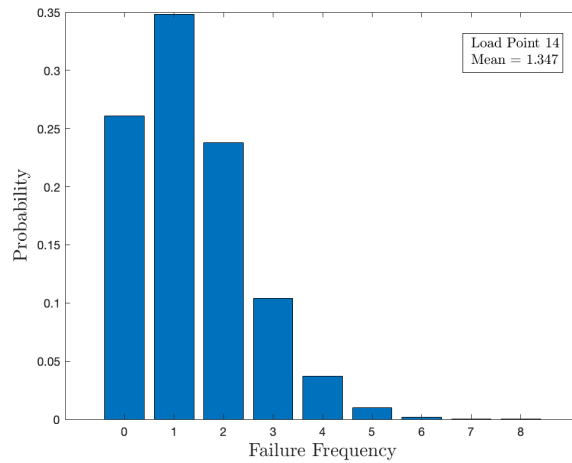
(b) Failure frequency histogram, Load Point 14

(c) Failure frequency histogram, Load Point 23.

Figure H.1: Case 3: Probability distribution of failure rate for selected load points.
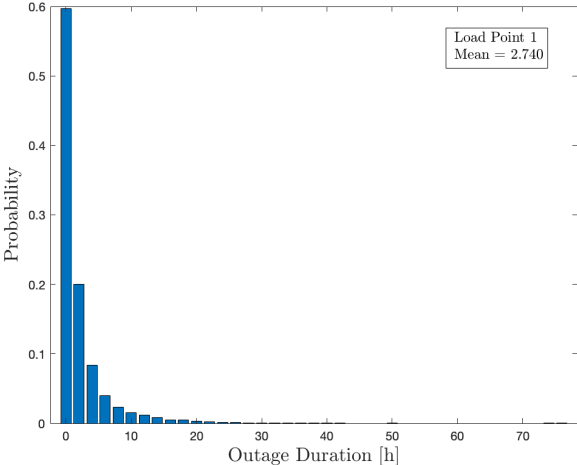
(a) Outage duration histogram, Load Point 1.
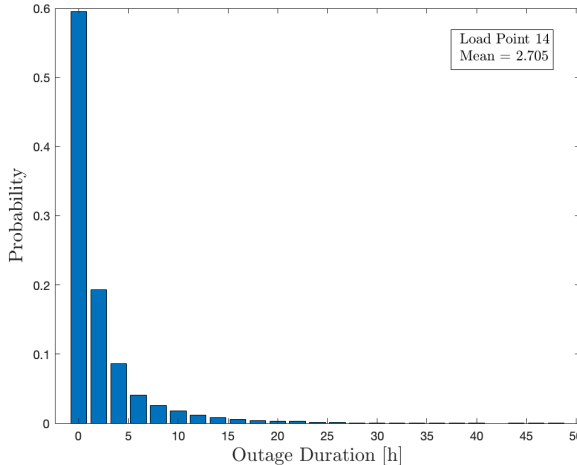
(b) Outage duration histogram, Load Point 14.
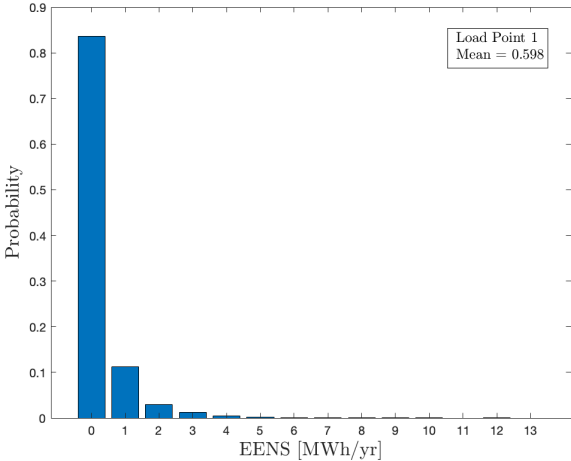

(c) Outage duration histogram, Load Point 23.

Figure H.2: Case 3: Probability distribution of outage duration for selected load points.
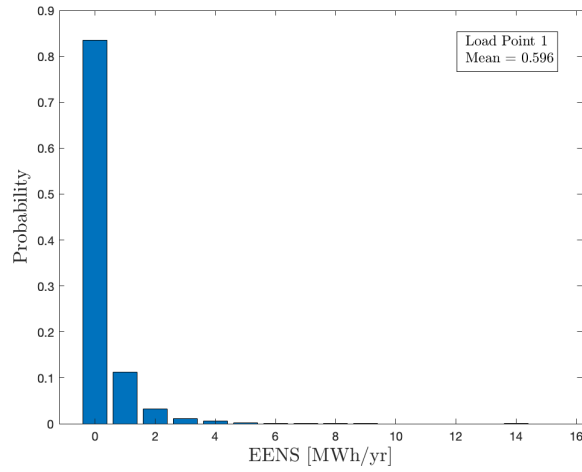
(a) Histogram of EENS, Load Point 1.
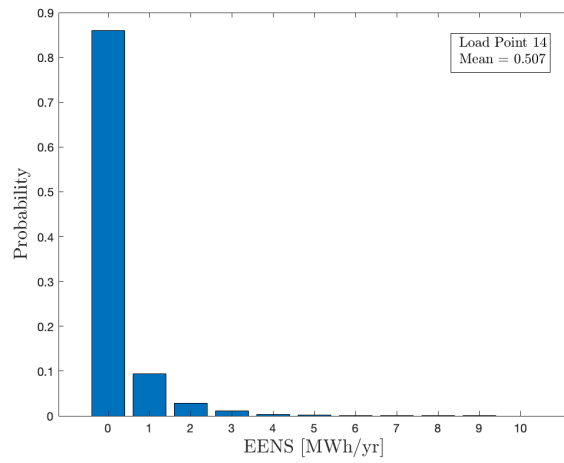
(b) Histogram of EENS, Load Point 14.
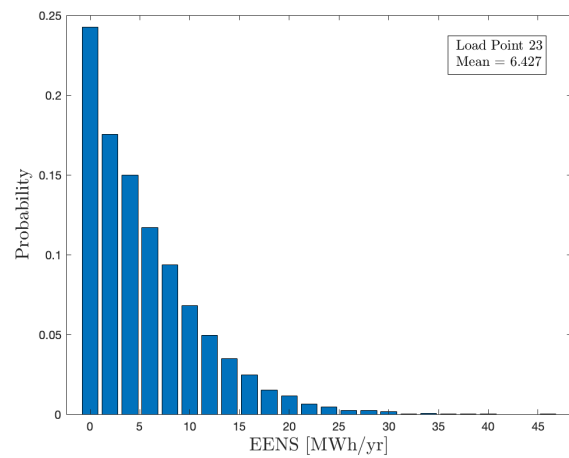
(c) Histogram of EENS, Load Point 23.

Figure H.3: Case 3: Probability distribution of the index EENS for selected load points.

H.2   Probability Distribution of Distribution System Indices

The probability distribution of the system reliability indices SAIFI, SAIDI, CAIDI and EENS are presented in the Figures H.4a, H.4b, H.4c and H.4d, respectively.
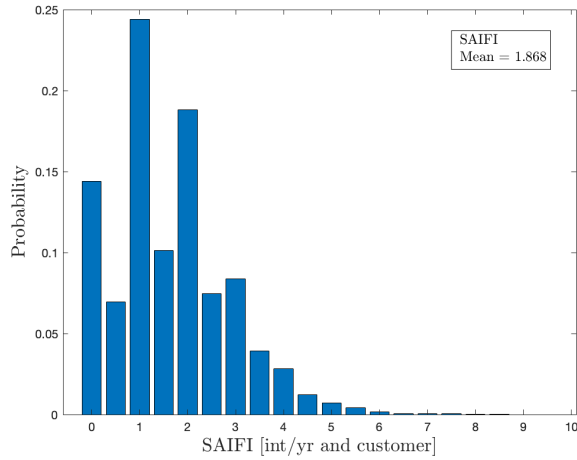
(a) Histogram of SAIFI.
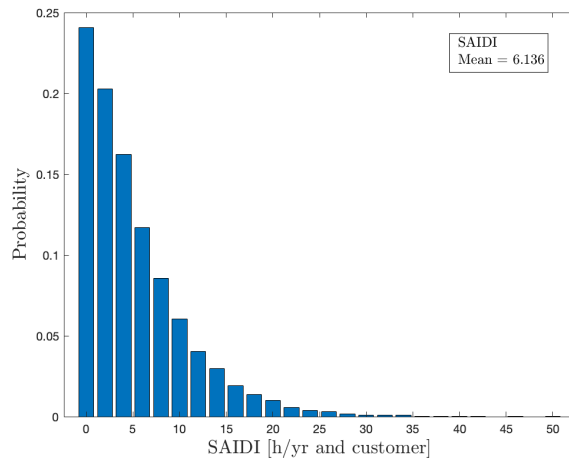
(b) Histogram of SAIDI.
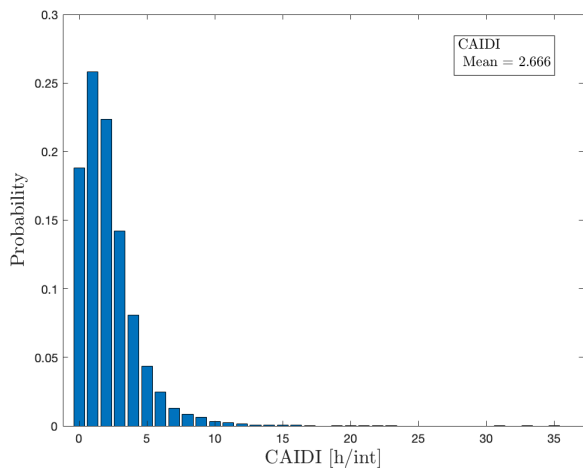
(c) Histogram of CAIDI.
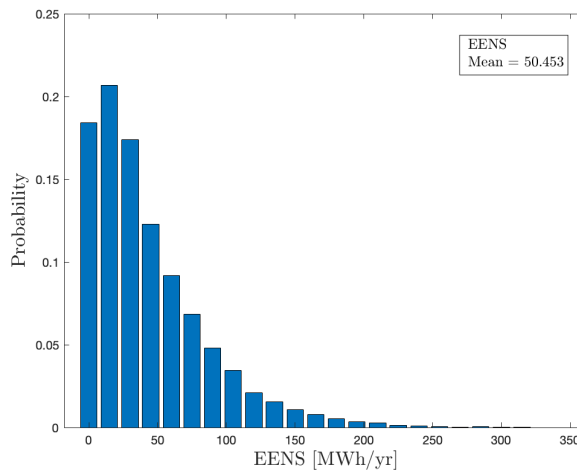
(d) Histogram of EENS.

Figure H.4: Probability distribution of system reliability indices.

H.3   Probability Distribution of Microgrid System Indices

The probability distribution of the microgrid system reliability indices MAIFI, MAIDI, MCAIDI and EENS are presented in the Figures H.5a, H.5b, H.5c and H.5d, respectively.
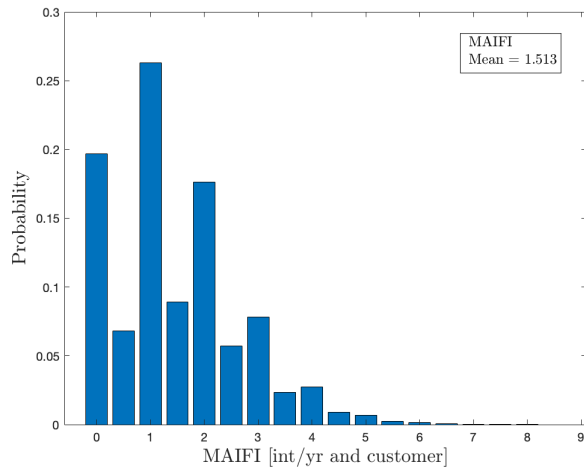
(a) Histogram of MAIFI.
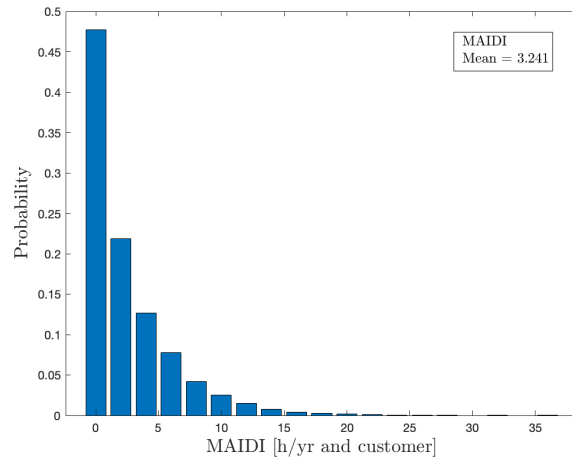
(b) Histogram of MAIDI.

(c) Histogram of MCAIDI.

(d) Histogram of EENS (for the micorgrid).

Figure H.5: Probability distribution of microgrid system reliability indices.

Appendix I

Results of Case 4

I.1   Probability Distribution of Load Points

The probability distributions of the annual failure frequency and duration for each load point in the distribution system have been evaluated, along with the distribution of the annual EENS. Figures I.1a, I.1b and I.1c present the histograms of the failure frequency for Load Point 1, 14 and 23, respectively. The probability distribution of the failure frequency clearly shows the probability of having a different number of load point failures in each year for each load point. Figures I.2a, I.2b and I.2c present the histograms of the outage duration for Load Point 1, 14 and 23, respectively. Further, Figures I.3a, I.3b and I.3c present the histograms of the EENS for the same load points.

(a) Failure frequency histogram, Load Point 1.
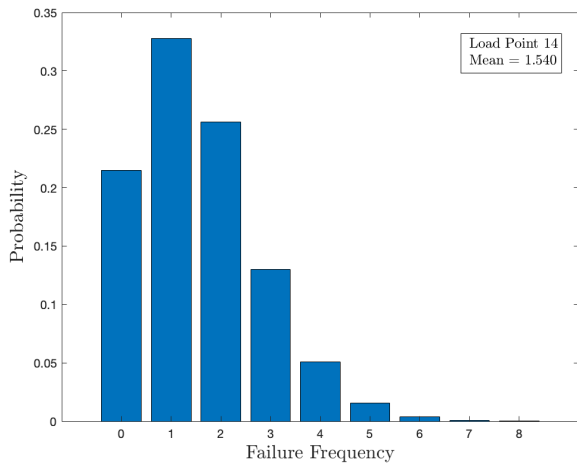
(b) Failure frequency histogram, Load Point 14

(c) Failure frequency histogram, Load Point 23.

Figure I.1: Case 4: Probability distribution of failure rate for selected load points.
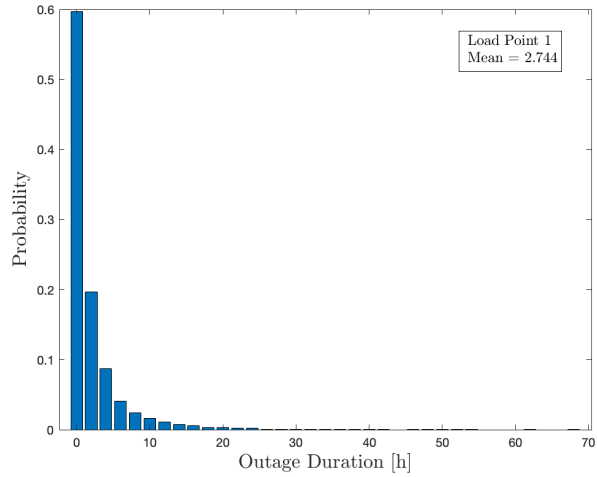
(a) Outage duration histogram, Load Point 1.
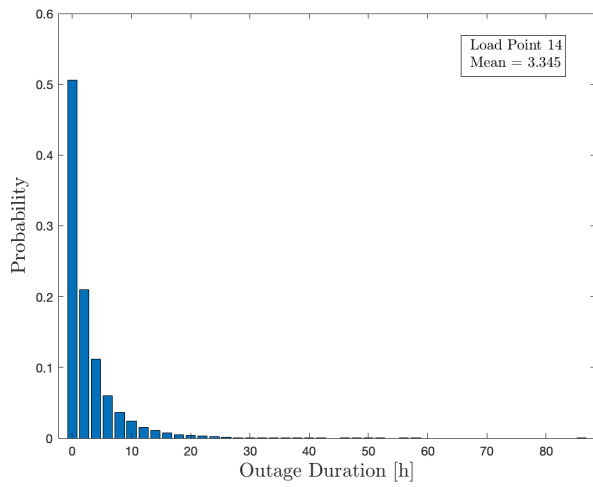
(b) Outage duration histogram, Load Point 14.
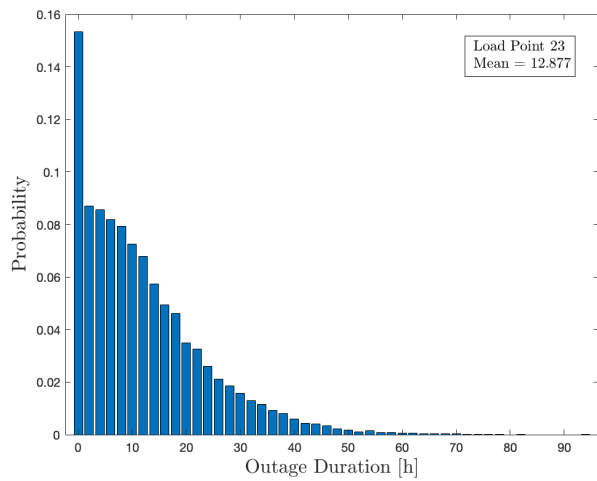
(c) Outage duration histogram, Load Point 23.

Figure I.2: Case 4: Probability distribution of outage duration for selected load points.

(a) Histogram of EENS, Load Point 1.
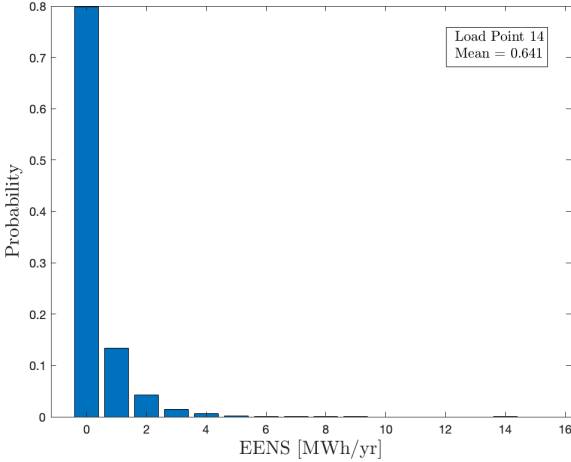
(b) Histogram of EENS, Load Point 14.
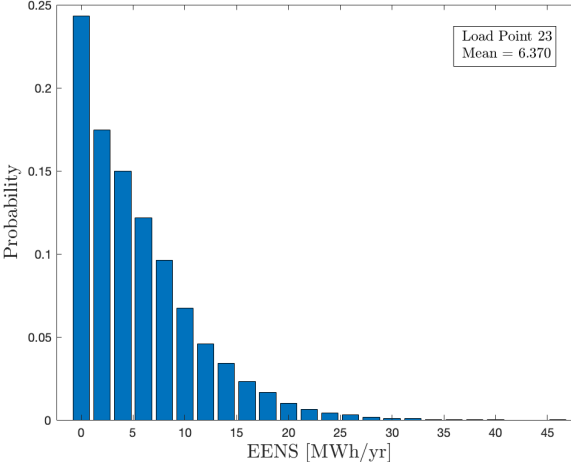
(c) Histogram of EENS, Load Point 23.

Figure I.3: Case 4: Probability distribution of the index EENS for selected load points.

I.2 Probability Distribution of Distribution System Indices

The probability distribution of the system reliability indices SAIFI, SAIDI, CAIDI and EENS are presented in the Figures I.4a, I.4b, I.4c and I.4d, respectively.
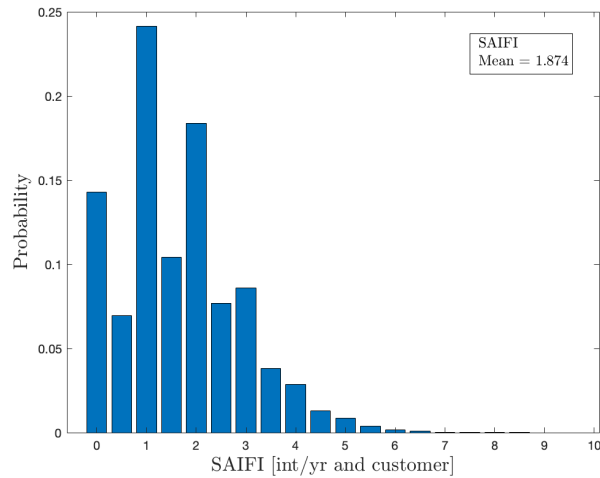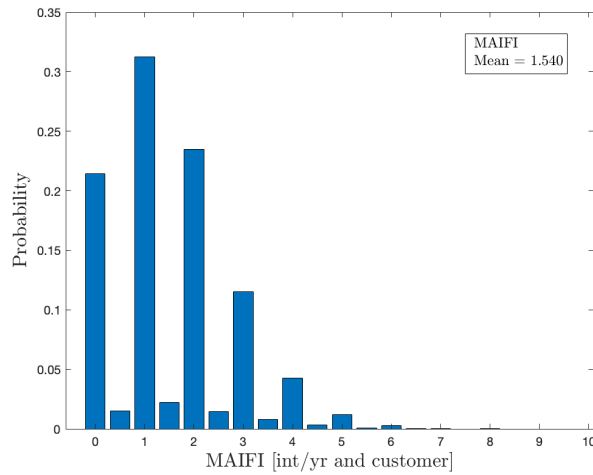

(a) Histogram of SAIFI.
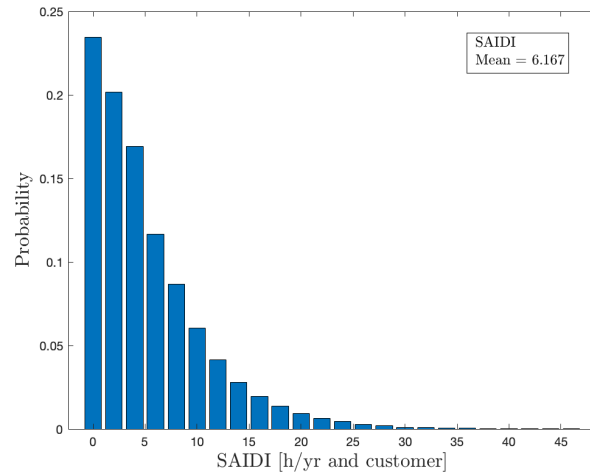
(b) Histogram of SAIDI.
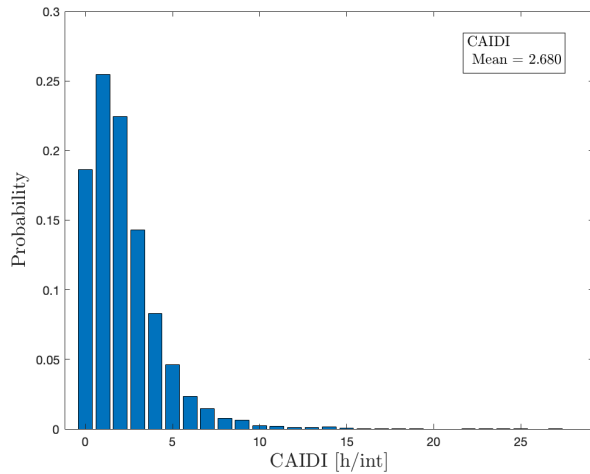
(c) Histogram of CAIDI.
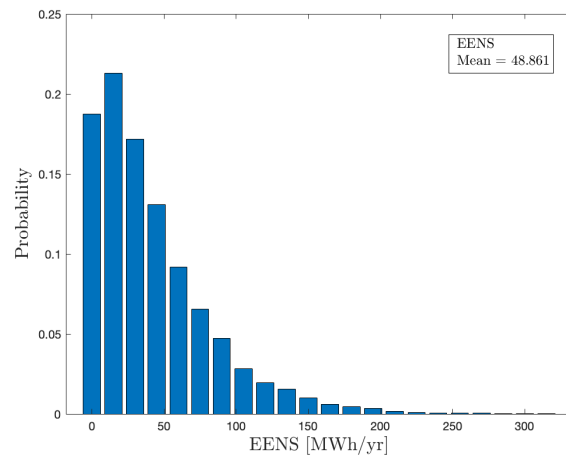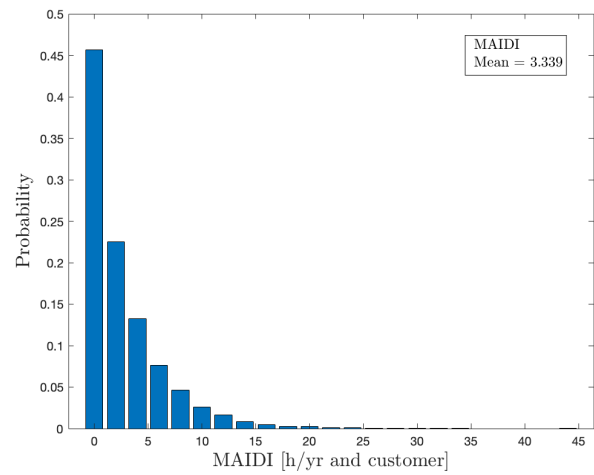
(d) Histogram of EENS.

Figure I.4: Probability distribution of system reliability indices.

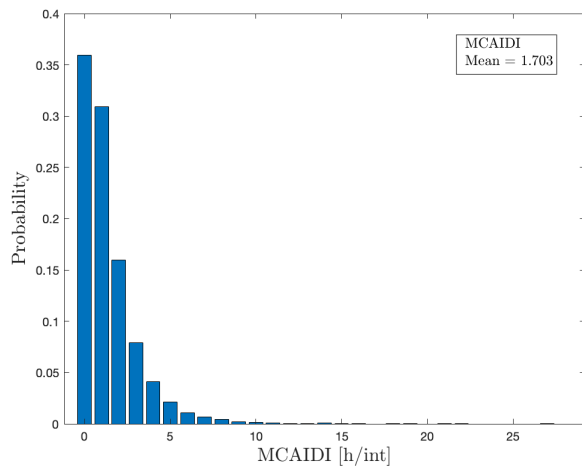# I.3 Probability Distribution of Microgrid System Indices

The probability distribution of the microgrid system reliability indices MAIFI, MAIDI, MCAIDI and EENS are presented in the Figures I.5a, I.5b, I.5c and I.5d, respectively.
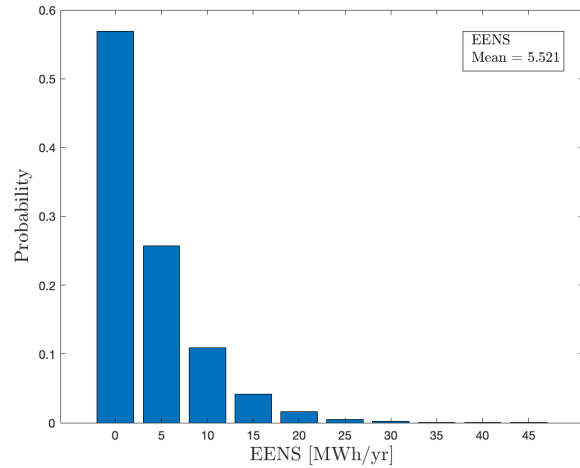

(a) Histogram of MAIFI.

(b) Histogram of MAIDI.

(c) Histogram of MCAIDI.

(d) Histogram of EENS (for the micorgrid).

Figure I.5: Probability distribution of microgrid system reliability indices.

Appendix J

Software Codes

(Restricted Public Access)

NTNU

Norwegian University of
Science and Technology